

Feasibility of Cracking Resistance on Self-compacting Concrete using Expansive Agent
&
Three-dimensional Composite Model of Expansive Concrete

Ming-Hung Hsieh

Graduate School of Engineering

Kochi University of Technology

A dissertation submitted to
Kochi University of Technology
in partial fulfillment of the requirements for the degree of

Doctor of Engineering

Kochi, Japan
March 2005

Feasibility of Cracking Resistance on Self-compacting Concrete using Expansive Agent
&
Three-dimensional Composite Model of Expansive Concrete

Ming-Hung Hsieh

Graduate School of Engineering

Kochi University of Technology

A dissertation submitted to
Kochi University of Technology
in partial fulfillment of the requirements for the degree of

Doctor of Engineering

Kochi, Japan
March 2005

© Copyright by Ming-Hung Hsieh 2005
All rights reserved

Feasibility of Cracking Resistance on Self-compacting Concrete using Expansive Agent
&
Three-dimensional Composite Model of Expansive Concrete

by

Ming-Hung Hsieh

B.Eng. (Tamkang University, Taiwan) 1994
M. Eng. (National Taiwan University, Taiwan) 1999

A dissertation submitted to
Kochi University of Technology
in partial fulfillment of the requirements for the degree of

Doctor of Engineering

Advisor: Associate Professor, Dr. Masahiro Ouchi

Examination Committees: Associate Professor, Dr. Masahiro Ouchi
Professor, Dr. Hajime Okamura
Professor, Dr. Hiroshi Shima
Professor, Dr. Nobumitsu Fujisawa
Professor, Dr. Seigo Nasu

Abstract

Feasibility of Cracking Resistance on Self-compacting Concrete using Expansive Agent & Three-dimensional Composite Model of Expansive Concrete

Crack due to the shrinkage in concrete is widely acknowledged as one of the fundamental defects for reinforced concrete structure, it leads to premature deterioration and shortening the service life. The shrinkage together with the weak tensile strength may result in the injurious crack. Therefore, expansive agent has been employed to enhance the cracking resistance of concrete. With regard to self-compacting concrete (SCC), due to the low water-to-cement ratio and the high paste volume, the volume change at the hardening and drying process cannot be neglected. Most of the past researches on the application of expansive agent until now have been carried out for conventional concrete under water curing. The purpose of this research is to verify the feasibility of cracking resistance of SCC by using expansive agent under practical construction site environment.

From the experimental result, the maximum expansion strain of SCC using expansive agent was less than that of conventional concrete with high water-to-cement ratio for the same dosage of expansive agent. And the insufficient expansion resulted in crack after the specimen was dried. It seemed that the efficiency of expansive agent was reduced on the application of SCC, due to the very low water-to-cement ratio. It was also found that the expansion characteristics greatly differ depending on curing method and then the influence of curing method on SCC using expansive agent was studied. From experimental result, the difference in the influence on expansion under water- and sealed-curing was very clear. On the other hand, the influence of the drying-curing on the expansion was not so clear compared with the sealed curing. It was revealed that the necessity for water in SCC using expansive agent was higher than the conventional concrete. Besides, the dosage of expansive agent for SCC under sealed curing condition had to be increased in order to achieve the enough expansion to prevent crack.

As the influence of the variation of coarse aggregate, when same amount of expansive agent was employed, the expansion strain reduced as the amount of coarse aggregate decreased, though coarse aggregate was regarded as the resistant force to

expansion. It was explained by the decrease of the ratio of expansive agent to total powder ($E/(C+E)$). Since the dispersion density of expansive agent in paste reduced when the amount of coarse aggregate reduced, therefore, the expansion reduced. That is to say that the efficiency of expansive agent reduced on the application of SCC.

Limestone powder was employed to be the countermeasure to enhance the efficiency of expansive agent. From the experimental result, replacing cement with limestone powder was proved to be contributive to the compensation for the shrinkage and crack was not occurred, although the drying shrinkage might be increased. In the case of the utilization of limestone powder, the expansion strain for the same dosage of expansive agent was increased due to the increase of the dispersion density of expansive agent in paste. And the dosage of expansive agent to achieve the same expansion with the conventional concrete was reduced as well. That is to say that the shortage of water in SCC using expansive agent can be solved by the employment of limestone powder. On the other hand, the compressive strength was reduced as the replacement ratio of limestone powder increased.

The expansive characteristics of SCC using expansive agent under multi-axial restraint were experimentally investigated. The mutual effect of restraint and expansion in perpendicular directions was clarified. Not only the axial expansion but also the expansion in the other two directions was reduced when the restraint was installed in the axial direction. In another word, the expansion was reduced in all the directions; even the restraint was only installed in one direction. The friction occurred between coarse aggregate and mortar was set to be the hypothesis to explain the mechanism and proved by mortar and paste experiment. Moreover, the friction concept was reflected to the friction between expansion and compression elements in three-dimension composite model. And the friction coefficient, the ratio of the friction to normal stress on the interface of expansion and compression elements, was decided by the experimental results.

Three-dimensional composite model of expansive concrete was proposed to estimate the expansion of expansive concrete based on the existing one-dimensional composite model by taking the mix proportions, curing methods and degree of the restraints into accounted. In the three-dimensional composite model, concrete was regarded as a composite material of three types of elements: expansion element, tension element and compression element. The concrete was divided into eight elements and the restraint of steel was expressed as the external restraint. By using the multi-axial restraint experimental result and the friction concept, one-dimensional

composite model was extended to three-dimensional one. And the friction between the expansion and the tension elements was calculated by the multiplication of friction coefficient and the normal stress. The friction coefficient was defined as the character of the interface of expansion and compression elements and assumed to be constant. In addition, based on the volume distribution concept of each component material from mix proportion, new determination method for the length of expansion element was proposed. And the potential expansion was assumed as the character of expansive agent under the specific curing method and divided into two parts related to the type of expansive agent and curing method respectively. By using the parameters decided above, the potential expansion could be estimated from the one-axial restraint experimental result. And then friction coefficient could be estimated by the multi-axial restraint experimental result. By the input of the parameters decided above: friction coefficient, the potential expansion, the length of expansion element, restraint steel ratio, Young's modulus and creep coefficient, the expansion with the same expansive agent for the different mix proportion under multi-axial restraint condition could be predicted.

膨張材による自己充填コンクリートのひび割れ防止の可能性と 膨張コンクリートの三次元複合モデル

ひび割れは鉄筋コンクリート構造物の代表的な欠陥であり、耐久性を損ね寿命を縮める原因となる。コンクリートの収縮はその低い引張強度により致命的なひび割れを生じさせ得る。自己充填コンクリートはその低い水セメント比および高いペースト容積と相まって、硬化および乾燥過程における体積変化は無視できないものとなっている。

本研究では、ひび割れの防止や低減を目的としてコンクリートに用いられてきた膨張材を、自己充填コンクリートに適用するための研究である。実施工での養生条件を念頭に置き、膨張材の自己充填コンクリートのひび割れ防止への有効性を検証した。

最初に低熱ポルトランドセメントを使用した汎用の自己充填コンクリートに膨張材を添加し、その膨張量を測定した。その結果、普通コンクリートと比較して十分な膨張量を得ることが出来ず、供試体の乾燥開始後にひび割れが生じた。これは普通コンクリートと異なり極めて低い水セメント比により膨張材が十分な効果を発揮できなかったものと思われる。

また、養生方法が自己充填コンクリートにおける膨張量の効果に極めて大きな影響を及ぼすことが分かった。封緘養生と気中養生とでは膨張量にあまり差が見られなかったが、封緘養生と水中養生との差は大きかった。膨張材を使用した自己充填コンクリートでは、実際の養生では水和反応に必要な水分の供給が行われない可能性があることを示した。

粗骨材の影響として、膨張材の添加量が同じである場合、粗骨材量の増加に伴い、拘束が大きくなるにもかかわらず膨張ひずみも増加した。この現象は合計のセメント・結合材量に対する膨張材量の比率で説明できた。粗骨材量が大きくなるとこの比率も同時に大きくなった。

実施工では水中養生が期待できないことが多い現状に鑑み、自己充填コンクリートにおける膨張量を確保するため、低熱ポルトランドセメントの一部を石灰石微粉末に置換して膨張量を測定した。その結果、石灰石微粉末への置換率の増加に伴い乾燥収縮量が大きくなるにも関わらず、膨張ひずみは増加した。

乾燥開始後にもひび割れは生じなかった。石灰石微粉末置換の有効性が確認された。ただし、石灰石微粉末の使用によりコンクリートの強度が低下することが確認された。

次に、多軸拘束下での自己充填コンクリートの膨張挙動を明らかにするための実験を行った。拘束の影響はその軸方向のみならず直角方向にも及び、膨張量が減少することを確認した。粗骨材とモルタルとの間に生じる摩擦を、このメカニズムを説明する仮設とし、モルタルとペーストによる同種の実験により証明した。さらに、この摩擦のコンセプトを三次元複合要素モデルの膨張と圧縮要素に反映した。この膨張量の減少を膨張コンクリートの複合モデルにおける膨張要素と圧縮要素との摩擦力に起因するものと仮定した。そして、この摩擦力と直応力との比率を摩擦係数として定義し、実験結果から求めた。

以上の実験から得られた知見を元に、膨張コンクリートの三次元複合モデルを提案した。本モデルは既存の一次元複合モデルを三次元に拡張し、配合、養生方法および拘束度を考慮に入れたものである。本モデルではコンクリート部材を膨張要素、引張要素および圧縮要素の三種類の要素に区分し、合計 8 要素に分割した。鉄筋による拘束は外部拘束として表現した。一次元から三次元に拡張するために、膨張要素と圧縮要素との摩擦力を直角方向の拘束の影響によるものと仮定した。この摩擦係数は一定と仮定し、三次元の実験結果から決定した。

さらに、本モデルに使用する膨張要素の一辺の長さを、膨張材が配合に占める容積割合から求める方法を提案した。潜在膨張量は特定の養生方法で決定される膨張材の特性値として決定する方法も提案した。以上の方法により求めた値を用いることにより、1 回の実験結果から潜在膨張量を予測することが可能となった。摩擦係数、潜在膨張量、膨張要素長、拘束鉄筋比、ヤング係数およびクリープ係数を入力データとすることにより、異なる配合での三次元の膨張量を予測することが可能となった。

Acknowledgement

In this age, no one can carry out research work alone. Therefore, I would like to extend my appreciation to many people who ever assisted directly or indirectly with this study.

First, I would like to give thanks to my supervisor Dr. Masahiro Ouchi who helped with this work and gave continuing encouragement to me. Especially, profound gratitude was extended to Prof. Hajime Okamura. Without his constructive comments and valuable suggestions, this research would not be possible.

It's my great honor to have Prof. Hajime Okamura, Prof. Hiroshi Shima, Prof. Nobumitsu Fujisawa and Prof. Seigo Nasu and as my research examination members. I did enjoy the discussion with them and thank for their useful advices and information.

Research is not the only thing for foreign students. I really appreciated Mr. Miyaji and Ms. Okabayasi for her enthusiastic support and concern. They encouraged me when I felt frustrated and advised me when I felt confused, like my Japanese father and mother. Their concern let me feel that I was not alone in Japan.

Sincere thanks are also extended to Mr. Hamada and Ms. Kataoka at IRC for their kind assistance and help in taking care of dormitory and many affairs throughout my study in KUT.

Furthermore, I would like to acknowledge the scholarship from Heiwa Nakajima Foundation. With their help, I could concentrate on my research.

Last but not least, I especially want to give thanks to my family (my parents, my wife and Tsung-Yeh) for their support and encouragement throughout my study period. Ending is another beginning. I will continue to learn and accept another challenge.

LIST OF CONTENTS

Abstract	
Acknowledgement	
List of Contents	vii
List of Figures	xi
List of Tables	xv
List of Photos	xvi
CHAPTER 1 INTRODUCTION	1
1.1 Research Background	1
1.1.1 Definition and Requirements for Self-Compacting Concrete (SCC)	1
1.1.2 Development of Expansive Concrete in Japan	3
1.2 Previous Research on Application of Expansive Agent	4
1.2.1 Classification of Expansive Agent	4
1.2.2 Concept of Expansion Strain and Chemical Prestrain about Expansive Concrete	5
1.3 Expansion Estimation Method of Expansive Concrete	6
1.3.1 Expansion Energy Method	7
1.3.2 1-Dimensional Composite Model for Expansive Concrete	8
1.4 Purpose of this Research	10
1.5 Research Program	11
CHAPTER 2 EXPANSIVE CHARACTERISTICS OF SELF-COMPACTING CONCRETE USING EXPANSIVE AGENT	14
2.1 Introduction	14
2.2 Experimental Procedures	14
2.2.1 Materials and Mix Proportions	14
2.2.2 Measurement and Curing	16
2.3 Experimental Results and Discussion	16
2.3.1 Low Water-to-cement Ratio and Autogeneous Shrinkage	21
2.3.2 Insufficient Water Supply under Sealed Curing	22
2.4 Summary	23
CHAPTER 3 INFLUENCE OF CURING ON SELF-COMPACTING CONCRETE USING EXPANSIVE AGENT	24

3.1 Introduction	24
3.2 Experimental Procedures	24
3.2.1 Materials and Mix Proportions	24
3.2.2 Measurement and Curing	26
3.3 Experimental Results and Discussion	26
3.3.1 Curing Effect on Expansion Strain of Different Dosage of Expansive Agent	26
3.3.2 Cracking Occurrence Mechanism	33
3.4 Summary	35
CHAPTER 4 INFLUENCE OF COARSE AGGREGATE ON SELF-COMPACTING CONCRETE USING EXPANSIVE AGENT	37
4.1 Introduction	37
4.2 Experimental Procedures	37
4.2.1 Materials and Mix Proportions	37
4.2.2 Measurement and Curing	39
4.3 Experimental Results and Discussion	39
4.4 Summary	43
CHAPTER 5 EXPANSIVE CHARACTERISTICS OF SELF-COMPACTING CONCRETE USING LIMESTONE POWDER	44
5.1 Introduction	44
5.2 Experiment Procedures	44
5.2.1 Materials and Mix Proportions	44
5.2.2 Measurement and Curing	46
5.3 Experimental Results and Discussion	46
5.3.1 Influence of Replacement of Limestone Powder on Expansion Strain	46
5.3.2 Influence of Replacement of Limestone Powder on Compressive Strength	50
5.4 Summary	51
CHAPTER 6 EXPANSIVE CHARACTERISTICS OF SELF-COMPACTING CONCRETE USING EXPANSIVE AGENT UNDER MULTI-AXIAL RESTRAINT	52

6.1 Introduction	52
6.2 Experimental Procedures	52
6.2.1 Materials and Mix Proportions	52
6.2.2 Measurement and Curing	53
6.3 Experimental Results and Discussion	54
6.3.1 Mutual influence of the restraint and the expansion in the perpendicular direction	54
6.3.2 Mechanism of the Lateral Restraint Effect on the Axial Expansion Strain	62
6.3.3 Mortar Experiment to prove the Mechanism of the Lateral Restraint Effect on the Axial Expansion	64
6.4 Summary	67
CHAPTER 7 THREE-DIMENSIONAL COMPOSITE MODEL OF EXPANSIVE CONCRETE	71
7.1 Introduction	71
7.2 Three-Dimensional Composite Model	71
7.2.1 Geometric Shape of 3-Dimensional Composite Model	71
7.2.2 Friction between Expansion Element and Compression Element	73
7.2.3 Determination of Friction Coefficient	73
7.2.4 Determination of Normal Stress	74
7.2.5 New Proposal to Determine the Length of Expansion Element “ l ”	74
7.2.6 Potential Expansion of Expansion Element “ e_o ”	76
7.2.7 Young’s Modulus	76
7.2.8 Creep Coefficient	77
7.3 Calculation of Three-Dimensional Composite Model	81
7.3.1 Equations of the Increment of Apparent Expansion	81
7.3.2 Calculation Method of Apparent Expansion	82
7.3.3 Calculation Flow Chart of 3-dimensional Composite Model	84
7.4 Comparison of Estimation by Three-dimensional Composite Model and Experimental Result	85
7.5 Evaluation of Three-dimensional Composite Model	86
7.6 Summary	87
CHAPTER 8 CONCLUSIONS	95
8.1 Summary and Conclusions	95
8.2 Recommendations for the Future Work	97

LIST OF FIGURES

Fig.-1.1 Definition of Self-compacting high performance concrete	1
Fig.-1.2 Effect of utilizing expansive agent	6
Fig.-1.3 One-dimensional composite model of expansive concrete	8
Fig.-1.4 Equivalent one-dimensional composite model of expansive concrete	9
Fig.-1.5 Research framework	13
Fig.-2.1 Outline of specimen	16
Fig.-2.2 Relationship between expansion strain and different dosage of expansive agent at $p=0\%$ (Sealed Curing)	17
Fig.-2.3 Relationship between expansion strain and different dosage of expansive agent at $p=1.27\%$ (Sealed Curing)	18
Fig.-2.4 Relationship between expansion strain and different dosage of expansive agent at $p=2.25\%$ (Sealed Curing)	18
Fig.-2.5 Relationship between expansion strain and different restraint steel ratio for EX40 (Sealed Curing)	19
Fig.-2.6 Relationship between expansion strain and different dosage of expansive agent at $p=0.95\%$ (Sealed Curing)	19
Fig.-2.7 Cracking mechanism of expansive concrete due to insufficient expansion	21
Fig.-2.8 Relationship between autogenous shrinkage and drying shrinkage	22
Fig.-2.9 Water supply under water and sealed curing	22
Fig.-3.1 Outline of specimen	25
Fig.-3.2 Relationship between expansion strain and different restraint steel ratio for EX66 (Sealed Curing)	28
Fig.-3.3 Relationship between expansion strain and different restraint steel ratio for EX66 (Drying Curing)	28
Fig.-3.4 Relationship between expansion strain measured from contact chips and strain gauge on deformed bar for EX66 at $p=2.25\%$ (Sealed Curing)	29
Fig.-3.5 Relationship between expansion strain and different dosage of expansive agent at $p=1.27\%$ (Water Curing)	29
Fig.-3.6 Relationship between expansion strain and different dosage of expansive agent at $p=0\%$ (Water Curing)	30
Fig.-3.7 Relationship between expansion strain and different restraint steel ratio for EX20 (Water Curing)	30
Fig.-3.8 Relationship between expansion strain and different restraint steel ratio for EX40 (Water Curing)	31
Fig.-3.9 Relationship between expansion strain and different curing method for EX40	

(p=1.27%)	31
Fig.-3.10 Relationship between expansion strain and different curing method for EX40 (p=0%)	32
Fig.-3.11 Relationship between expansion strain and different dosage of expansive agent at p=0.95% (Water Curing)	32
Fig.-3.12 Relationship between expansion strain and dosage of expansive agent under different curing methods	33
Fig.-3.13 Mechanism of cracking occurrence and appropriate dosage of expansive agent for SCC	34
Fig.-3.14 Hydration speed of expansive agent and cement	35
Fig.-4.1 Outline of specimen	38
Fig.-4.2 The role of coarse aggregate in expansive concrete	39
Fig.-4.3 Influence of coarse aggregate on expansion strain	40
Fig.-4.4 Relationship of expansion strain and age for different amount of coarse aggregate (EX40)	41
Fig.-4.5 Relationship of expansion strain and the amount of coarse aggregate	42
Fig.-4.6 Relationship of expansion strain and the amount of total aggregate	43
Fig.-5.1 Outline of specimen	46
Fig.-5.2 Relationship between expansion strain and age for different replacement ratio of limestone powder at p-1.27% (Sealed Curing)	47
Fig.-5.3 Relationship of expansion strain between EX20LS0% and EX20LS20% at p=1.27% (Sealed Curing)	47
Fig.-5.4 Relationship of expansion strain between EX20LS0% and EX20LS40% at p=1.27% (Sealed Curing)	48
Fig.-5.5 Relationship between expansion strain and different replacement ratio of limestone powder at p=0.95%	48
Fig.-5.6 Effect of utilization of limestone powder	49
Fig.-5.7 Relationship between the variation of autogeneous and drying shrinkage as the replacement of limestone powder increased	49
Fig.-5.8 Variation of expansion strain and compressive strength with the replacement of limestone powder	50
Fig.-5.9 Relationship between compressive strength and different replacement ratio of limestone powder at the different age	51
Fig.-6.1 Outline of specimen (the first part)	53
Fig.-6.2 Outline of specimen (the second part)	54
Fig.-6.3 Relationship between expansion strain and age under different restraint in axial (X) direction (EX40-Sealed Curing-150 × 150 × 400 mm)	56
Fig.-6.4 Relationship between expansion strain and age under different restraint in	

lateral (Y) direction (EX40-Sealed Curing-150 × 150 × 400 mm)	56
Fig.-6.5 Variation of expansion strain in the X direction between Specimen r0 and Specimen r2 (EX40-Sealed Curing-150 × 150 × 400 mm)	57
Fig.-6.6 Variation of expansion strain in the X direction between Specimen r1 and Specimen r3 (EX40-Sealed Curing-150 × 150 × 400 mm)	57
Fig.-6.7 Variation of expansion strain in the Y direction between Specimen r0 and Specimen r1 (EX40-Sealed Curing-150 × 150 × 400 mm)	58
Fig.-6.8 Variation of expansion strain in the Y direction between Specimen r2 and Specimen r3 (EX40-Sealed Curing-150 × 150 × 400 mm)	58
Fig.-6.9 Relationship between expansion strain and age under different restraint (EX40-Water Curing-150 × 400 × 400 mm)	59
Fig.-6.10 Relationship between expansion strain and age under different restraint (EX40-Sealed Curing-150 × 400 × 400 mm)	59
Fig.-6.11 Relationship between expansion strain and age under different restraint (EX20-Water Curing-150 × 400 × 400 mm)	60
Fig.-6.12 Relationship between expansion strain and age under different restraint (EX20-Sealed Curing-150 × 400 × 400 mm)	60
Fig.-6.13 Variation of expansion strain in the X direction between Specimen R1 and Specimen R2 (EX40-Water Curing-150 × 400 × 400 mm)	61
Fig.-6.14 Variation of expansion strain in the Y direction between Specimen R0 and Specimen R1 (EX40-Water Curing-150 × 400 × 400 mm)	61
Fig.-6.15 Mechanism of the lateral restraint effect on the axial expansion strain-1	62
Fig.-6.16 Mechanism of the lateral restraint effect on the axial expansion strain-2	63
Fig.-6.17 Friction between expansion and tension element in three-dimensional composite model	63
Fig.-6.18 Outline of specimen	65
Fig.-6.19 Relationship between expansion strain and age under different restraint (Mortar experiment)	65
Fig.-6.20 Relationship between expansion strain and age under different restraint (Paste experiment)	66
Fig.-6.21 Influence of lateral restraint on axial expansion from concrete, mortar and paste experiment	67
Fig.-7.1 Geometric shape of three-dimensional composite model	72
Fig.-7.2 Friction between expansion and compression element	73
Fig.-7.3 New proposal to determine the length of expansion element “ ”	75
Fig.-7.4 Calculation of apparent expansion in X direction	84
Fig.-7.5 Calculation flowchart of 3-dimensional Composite Model	85
Fig.-7.6 Estimated potential expansion of EX40 under sealed and water curing	89

Fig.-7.7 Input Young's Modulus of EX40	89
Fig.-7.8 Input creep coefficient of EX40 under water curing	90
Fig.-7.9 Input creep coefficient of EX40 under sealed curing	90
Fig.-7.10 One-axial restraint estimation result of EX40 under water and sealed curing	91
Fig.-7.11 Comparison of estimation and experimental result of EX40 under water curing	91
Fig.-7.12 Comparison of estimation and experimental result of EX40 under sealed curing	92
Fig.-7.13 Comparison of estimation and experimental result of different mix proportion with the variation of coarse aggregate	92
Fig.-7.14 Normal stress of EX40 in Lateral direction (Y direction)	93
Fig.-7.15 Two-axial restraint estimation result of EX40 under water and sealed curing	93
Fig.-7.16 Comparison of 3-D estimation and experimental result of EX40 under sealed curing	94

LIST OF TABLES

Table-1.1 Physical properties and chemical composition of expansive agent	4
Table-1.2 Chemical reaction of expansive agent	4
Table-2.1 Materials used in experiment	15
Table-2.2 Mix proportions of experiment	15
Table-2.3 Result of flowability test	15
Table-2.4 List of specimen	16
Table-2.5 Guideline of design and construction of expansive concrete (JSCE)	20
Table-3.1 Mix proportions of experiment	24
Table-3.2 List of the specimen and curing condition	26
Table-4.1 Materials used in experiment	38
Table-4.2 Mix proportions of experiment	38
Table-5.1 Materials used in experiment	45
Table-5.2 Mix proportions of experiment	45
Table-5.3 Result of flowability test	45
Table-6.1 List of the specimen and curing condition	54
Table-6.2 Materials used in experiment	64
Table-6.3 Mix proportions of experiment	64
Table-7.1 Ambient humidity coefficient (λ)	79

LIST OF PHOTOS

Photo-3.1 Crack occurred on the surface of drying-curing specimen due over-expansion (EX66)	36
Photo-3.2 Crack occurred on the surface of sealed-curing specimen due over-expansion (EX66)	36
Photo-6.1 Paste specimen R1-E/(C+E) =6.5% (before mold removed)	69
Photo-6.2 Paste specimen R2-E/(C+E) =6.5% (before mold removed)	69
Photo-6.3 Paste specimen R1-E/(C+E) =6.5% (after mold removed)	70
Photo-6.4 Paste specimen R2-E/(C+E) =6.5% (after mold removed)	70

CHAPTER 1

INTRODUCTION

1.1 Research Background

1.1.1 Definition and Requirements for Self-Compacting Concrete (SCC)

Self-compacting concrete (SCC), which originated at the University of Tokyo, is a type of concrete specially proportioned to self-compact so that without any additional, external vibration or compaction, SCC is able to flow on its own through reinforcement without any segregation or blockage in the formwork. [1]

The full original name of SCC was *Self-compacting high performance concrete*. This was included in Okamura's definition (1995), which was shown in **Fig.-1.1**. This focused not only on self-compacting properties during construction, but also on the resistance to defects at early ages and long term durability in service.

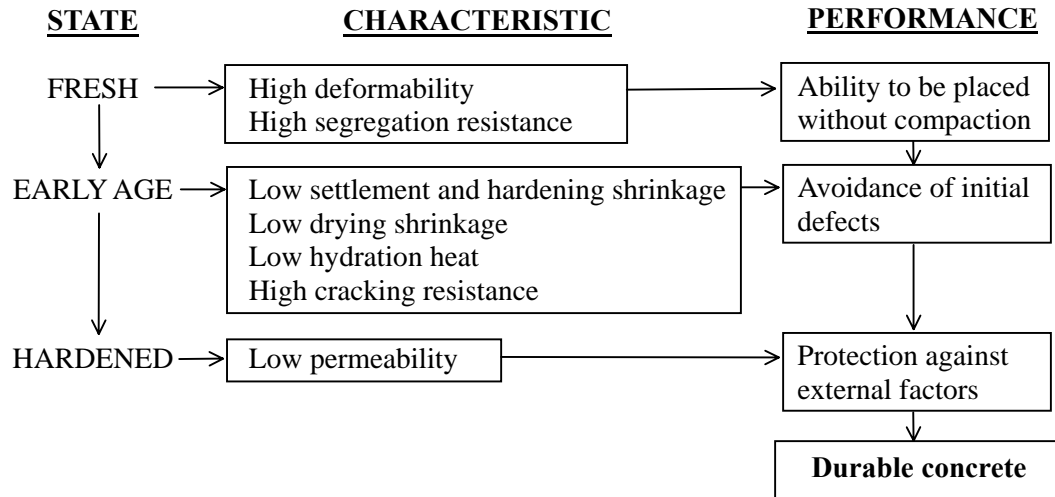


Fig.-1.1 Definition of Self-compacting high performance concrete

The development of Self-compacting concrete was started in 1988 in Japan in order to achieve durable concrete structures. Defects such as honeycombing and segregation caused by poor skill in construction work, particularly insufficient or over-vibration, are major causes of this. Poor structural design detail is another cause, often resulting from imperfect communication between the designers and the

construction engineers. In cases where heavy reinforcement is required and the shape of the cross section is complicated, it is difficult to place concrete without defects with the normal level of labor skill. Therefore, Okamura proposed two alternative practical solutions for these problems.

1. To establish a durability design method by comprehensive evaluation of materials design and construction methods.
2. To develop a new vibration-free concrete, with which durable and reliable structures can be easily constructed. This was the motivation for developing Self-compacting concrete.

The features of Self-compacting concrete are summarized as follows: [2]

1. It is possible to improve durability and reliability of concrete structure. (Improvement of the quality of structures)
2. Due to free of compaction using vibrations, non-vibratile and non-noise environment can be realized. (Improvement of the environment of construction site)
3. New construction systems to shorten construction period and to increase safety can be realized by the labor saving in concrete construction (rationalization of construction works)
4. New type of structure (sandwich structure, etc.) can be achieved. (Increase of the degree of freedom in design)
5. It can be applied to the portions of a structure where compaction work is difficult to be performed.

The development of Self-compacting concrete during the first ten years was summarized as follows:

September 1986: initiated by Okamura in his paper “Waiting for Innovation in Concrete Materials” [Okamura (1986)] (in Japanese)

August 1988: Prototype No.1 of Self-compacting concrete produced by Ozawa, Okamura’s research student

July 1989: Demonstration to the construction industry at the University of Tokyo

July 1989: First publication by Okamura, Maekawa, and Ozawa

1990 onwards: Applications by construction industry

1995 onwards: spreading to the world: research studies on Self-compacting concrete

have been carried out in the UK, France, Sweden, Canada, Holland, Thailand, Korea, China and Taiwan.

1.1.2 Development of Expansive Concrete in Japan

The beginnings of the fundamental thinking of expansive concrete can be seen far back in history in the practical use of joint mortar for aqueduct bridges of approximately 2,000 years ago, but expansive concrete in its present form was started in the 1930's. In Japan, an expansive agent began to be marketed from 1965. Since then, basic researches were initiated and practical application was carried out. [3]

Different with U.S.A and U.S.S.R where expansive cement has been used, in Japan, expansive agent was used alone and added at the time while concrete was mixed where quantity can be varied depending on the purpose of use. This is one reason that expansive concrete has been actively utilized in Japan with wide range especially for chemical prestress.

Until 1979, "Draft of Design and Construction Guideline of Expansive Concrete" was drawn up in the Journal of Concrete Library No.45. And in 1980, quality specification of expansive agent was drawn up by JIS A 6202, the standard experiment of Japanese Standards Association. Since then, the application of expansive concrete was increased. With the construction application increased, there was the necessity to update and add the new information on the draft. Therefore, in 1990, concrete committee of JSCE was entrusted from Expansive Agent Association and expansive concrete chapter of high performance concrete committee was organized to revise the "Draft of Design and Construction Guideline of Expansive Concrete". Then, "Design and Construction Guideline of Expansive Concrete" was published in 1993.

In the past ten years, expansive concrete has been utilized in practical construction to solve the cracking problems, such as bridge's plate and pier, box culvert, tunnel and buildings. And most of the construction cases, expansive concrete revealed the superior anti-cracking performance.

1.2 Previous Research on Application of Expansive Agent

1.2.1 Classification of Expansive Agent

Expansive agent is one kind of material that can cause concrete volume increase during hardened process. However, there is huge variety of chemical reaction and product of expansive agents. According to the main products, expansive agents can be classified into CSA system (also known as ettringite system, $3\text{CaO} \cdot \text{Al}_2\text{O}_3 \cdot 3\text{CaSO}_4 \cdot 32\text{H}_2\text{O}$) and lime system ($\text{Ca}(\text{OH})_2$). Physical properties and chemical composition of various expansive agents were shown in **Table-1.1**. From chemical reaction equations shown in **Table-1.2**, it is clear that A, B and D is CSA system and C and F are lime system. Then, E can be regarded as the combination of two systems.

Table-1.1 Physical properties and chemical composition of expansive agent

	Specific gravity	Specific surface cm^2/g	Chemical composition %							
			LOI	SiO_2	Al_2O_3	Fe_2O_3	CaO	MgO	SO_3	Total
A	2.91	2500	0.8	4.0	10.0	1.0	51.2	0.6	31.9	99.5
B	3.00	3200	1.2	3.1	6.3	0.4	58.0	0.3	29.6	98.9
C	3.14	3500	0.4	9.6	2.5	1.3	67.3	0.4	18.0	99.5
D	3.01	2800	1.0	1.5	13.0	0.5	51.2	1.5	29.3	99.5
E	3.10	2800	1.1	1.7	5.5	2.6	70.3	0.5	18.2	99.9
F	3.18	3010	1.6	4.2	1.1	1.0	74.0	0.5	16.5	99.9

Table-1.2 Chemical reaction of expansive agent

	Chemical reaction
A,D	$3\text{CaO} \cdot 3\text{Al}_2\text{O}_3 \cdot \text{CaSO}_4 + 6\text{CaO} + 8\text{CaSO}_4 + 96\text{H}_2\text{O} \rightarrow 3(3\text{CaO} \cdot \text{Al}_2\text{O}_3 \cdot 3\text{CaSO}_4 \cdot 32\text{H}_2\text{O})$
B	$3\text{CaO} \cdot \text{Al}_2\text{O}_3 + 3\text{CaSO}_4 + 32\text{H}_2\text{O} \rightarrow 3\text{CaO} \cdot \text{Al}_2\text{O}_3 \cdot 3\text{CaSO}_4 \cdot 32\text{H}_2\text{O}$
C,F	$\text{CaO} + \text{H}_2\text{O} \rightarrow \text{Ca}(\text{OH})_2$
E	$3\text{CaO} \cdot 3\text{Al}_2\text{O}_3 \cdot \text{CaSO}_4 + 6\text{CaO} + 8\text{CaSO}_4 + 96\text{H}_2\text{O} \rightarrow 3(3\text{CaO} \cdot \text{Al}_2\text{O}_3 \cdot 3\text{CaSO}_4 \cdot 32\text{H}_2\text{O})$ $\text{CaO} + \text{H}_2\text{O} \rightarrow \text{Ca}(\text{OH})_2$

Main composition; Product

New type of expansive agent was developed recently. In comparison with the past expansive agents, without sacrificing the expansive performance, the unit dosage can be reduced effectively. Besides, by adjusting the composition and fineness of clinker, early strength type of expansive agent can be achieved. Regarding precast concrete product which early strength was required, early strength cement and steam curing were usually used in order to shorten the formwork removing and curing time and reduce the maximum curing temperature. In the case of box culvert, maximum curing temperature was increased in order to achieve required strength to remove formwork. However, it resulted in the occurrence of restraint crack during the temperature-decreasing period after formwork was removed. By using the early strength type of expansive agent, not only the maximum curing temperature can be reduced but also the restraint-cracking problem can be prevented effectively due to the induced chemical prestress. It was revealed there was the space to develop expansive agent that can serve special demands of construction. [4]

1.2.2 Concept of Expansive Strain and Chemical Prestrain about Expansive Concrete

The terminologies about expansive concrete defined in “Guideline of Design and Construction of Expansive Concrete” were stated as follows.

Chemical prestrain: The induced initial strain on expansive concrete when concrete expanded under the restraint.

Chemical prestress: The induced compressive stress on expansive concrete when concrete expanded under the restraint.

Maximum expansion strain: Before specimen was dried, the maximum expansion strain on expansive concrete when concrete expanded under the restraint. The shrinkage strain was included in the maximum expansion strain before achieving the maximum expansion strain.

Induced shrinkage strain of expansive concrete: When expansive concrete was under the restraint, the strain difference between maximum expansion strain and the strain after specimen was dried.

Effective chemical prestrain: When expansive concrete was under the restraint, the strain difference between expansive concrete and concrete without adding expansive

agent. It was regarded as the effect of adding expansive agent.

The effect of utilizing expansive agent was shown from the viewpoint of strain behavior in **Fig.-1.2**. [5]

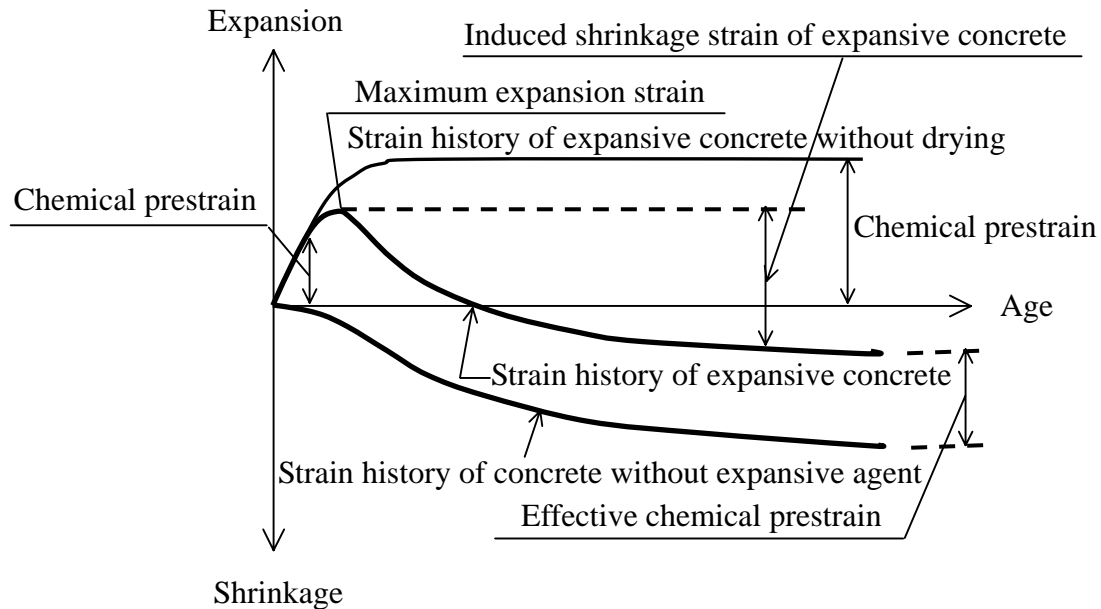


Fig.-1.2 Effect of utilizing expansive agent

1.3 Expansion Estimation Method of Expansive Concrete

The influence factors on the performance of expansive concrete were generalized as follows. [6]

1. Concrete mix proportions:
Type and amount of expansive agent, type and quality of cement, water-to-cement ratio, type and quantity of aggregate, type and quantity of admixture
2. Curing environment:
Temperature and humidity of environment
3. Restraint situation:
Steel restraint ratio and steel arrangement condition

Since an experimental result can be only applied to a case under the same condition, therefore, to estimate the expansion strain of expansive concrete in an

actual member is indispensable for utilizing expansive concrete. Up to now, there are two estimation methods proposed which are introduced in the following sections.

1.3.1 Expansion Energy Method

In order to estimate the expansion of expansive concrete under different steel restraint ratio, Tsuji etc. proposed the expansion energy method. [7] In this method, hypothesis was set up that “the expansion energy of concrete is constant if mix proportion and curing method are identical”. For practical purposes, this hypothesis is equal to the hypothesis that “the quantity of work performed by expansive concrete on restraining steel is constant”.

The expansion energy U can be calculated by one standard experimental result. In the standard experiment, the steel strain ε_s was measured. Then, the expansion energy U was calculated as follows.

Basic mechanism:

$$U = \sigma_c \cdot \varepsilon_c / 2 = \text{const.}$$

Force Balance in cross-section:

$$\sigma_c \cdot A_c = \sigma_s \cdot A_s$$

$$\sigma_c = (A_s / A_c) \cdot \sigma_s = p \cdot \sigma_s$$

Strain compatibility:

$$\varepsilon_c = \varepsilon_s$$

Stress-Strain relation:

$$\sigma_s = E_s \cdot \varepsilon_s$$

Expansion energy was calculated from the measured restraint steel strain:

$$U = \sigma_c \cdot \varepsilon_c / 2 = (p \cdot \sigma_s) \cdot \varepsilon_c / 2 = p \cdot (E_s \cdot \varepsilon_s) \cdot \varepsilon_c / 2 = p \cdot E_s \cdot \varepsilon_s^2 / 2$$

$$U = p \cdot E_s \cdot \varepsilon_s^2 / 2$$

Then, the expansion and chemical prestress of different steel restraint ratio p' could be estimated by following equations.

$$\varepsilon_s' = \sqrt{[2U / (p' \cdot E_s)]}$$

$$\sigma_c' = \sqrt{(2U \cdot p' \cdot E_s)}$$

U : Expansion energy of unit volume of expansive concrete under restraint

σ_c' : Compressive stress of expansive concrete (Chemical prestress)

- ϵ_c : Expansion strain of expansive concrete
- σ_s : Stress of restraint steel
- ϵ_s : Strain of restraint steel
- A_c : Cross-section area of concrete
- A_s : Cross-section area of restraint steel
- p : Restraint steel ratio
- E_s : Young's modulus of steel

1.3.2 1-Dimensional Composite Model for Expansive Concrete

In 1976, Okamura proposed one-dimensional composite model of expansive concrete. [8] In this model, it was composed of three types of elements: expansion element, tension element and compression element, and the restraint of steel was expressed as the external restraint (**Fig.-1.3**). In accordance with the compatibility of strain and force equilibrium, the expansion strain of composite model could be calculated.

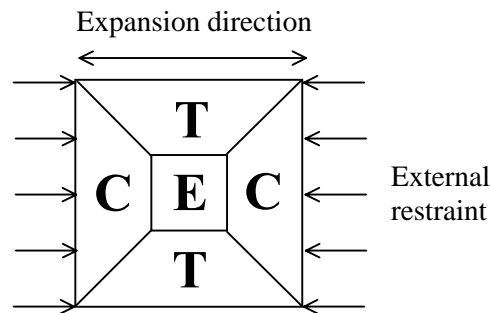


Fig.-1.3 One-dimensional composite model of expansive concrete

“Potential Expansion” and “Apparent Expansion”

The strain of expansion element (ϵ_c) was divided into the chemical expansion (ϵ_{eo}) from the hydration reaction of expansive agent and the strain due to the restraint of compression element (ϵ_{ec}). The chemical expansion was the strain of expansion element without any restraint. Accordingly, if the mix proportion, curing method (temperature, water supply) was fixed, the chemical expansion should be constant. Actually, it was the expansive origin and impossible to measure. Therefore, it was called as “Potential Expansion”. Comparatively, the whole strain of expansive concrete observed from the appearance was called “Apparent Expansion”. And it could be measured from the specimen. [9]

Equations of the Increment of Apparent Expansion

The length and volume of each element was expressed by **Eq.1.1~1.6**. Expansion element (expansion source) was attached with “e” as the suffix. Tension element (sustained by tension force) and compression element (sustained by compression force) was attached with “t” and “c” as the suffix respectively. Moreover, the model and expansion element were cubes with side length as 1 and . Therefore, the average cross-section area in expansion direction was expressed as **Eq.1.7~1.9**. And the equivalent model was shown in **Fig.-1.4**.

$$V_e = \alpha^3 \quad (\text{Eq.1.1})$$

$$V_t = 2 \cdot (1 - \alpha^3) / 3 \quad (\text{Eq.1.2})$$

$$V_c = (1 - \alpha^3) / 3 \quad (\text{Eq.1.3})$$

$$l_e = \alpha \quad (\text{Eq.1.4})$$

$$l_t = 1 \quad (\text{Eq.1.5})$$

$$l_c = 1 - \alpha \quad (\text{Eq.1.6})$$

$$A_e = V_e / l_e \quad (\text{Eq.1.7})$$

$$A_t = V_t / l_t \quad (\text{Eq.1.8})$$

$$A_c = V_c / l_c \quad (\text{Eq.1.9})$$

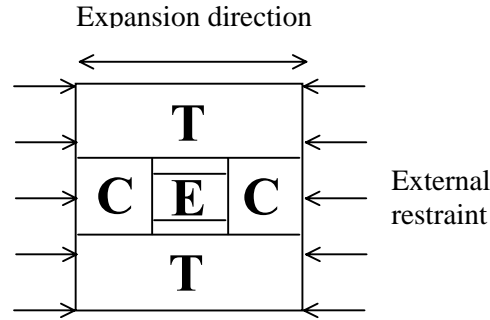


Fig.-1.4 Equivalent one-dimensional composite model of expansive concrete

In a finite period , the apparent expansion was occurred due to the increment of potential expansion ϵ_{e0} . The following equations (**Eq.1.10~1.12**) were set up based on the compatible conditions.

$$\Delta \epsilon_e = \Delta \epsilon_{e0} + \Delta \epsilon_{ee} \quad (\text{Eq.1.10})$$

$$\Delta \epsilon \cdot l = \Delta \epsilon_t \cdot l_t \quad (l = 1) \quad (\text{Eq.1.11})$$

$$\Delta \epsilon \cdot l = \Delta \epsilon_e \cdot l_e + \Delta \epsilon_c \cdot l_c \quad (l = 1) \quad (\text{Eq.1.12})$$

Here, ϵ_t and ϵ_c are the average strain increment of tension and compression

element.

Concerning the force equilibrium, **Eq.1.13** and **Eq.1.14** were set up.

$$\begin{aligned} & \Delta\varepsilon_t \cdot E_t \cdot A_t / A_{concrete} + \Delta\varepsilon_c \cdot E_c \cdot A_c / A_{concrete} \\ & = \Delta\varepsilon_t \cdot E_t \cdot A_t + \Delta\varepsilon_c \cdot E_c \cdot A_c \end{aligned} \quad (\text{Eq.1.13})$$

$$= -\Delta\varepsilon \cdot p \cdot E_s \quad (A_{concrete} = 1)(p = A_{steel} / A_{concrete})$$

$$\Delta\varepsilon_{ee} \cdot E_e \cdot A_e = \Delta\varepsilon_c \cdot E_c \cdot A_c \quad (\text{Eq.1.14})$$

Here, E_e , E_t , E_c and E_s are the Young's modulus of three elements and restraint steel. p is the restraint steel ratio defined as the ratio of steel area to the concrete cross-section area.

The relation of the increment of potential expansion and apparent expansion was expressed as **Eq.1.15** derived from **Eq.1.10** to **Eq.1.14**.

$$\Delta\varepsilon = \Delta\varepsilon_{e0} \cdot l_e / (l + K) = \Delta\varepsilon_{e0} \cdot l_e / (1 + K) \quad (l = 1) \quad (\text{Eq.1.15})$$

$$\text{Here, } K = (K_t + p \cdot E_s) \times (1/K_e + 1/K_c) \quad (\text{Eq.1.16})$$

$$K_e = (E_e \cdot A_e) / (l_e \cdot A_{concrete}) = (E_e \cdot A_e) / l_e \quad (A_{concrete} = 1) \quad (\text{Eq.1.17})$$

$$K_t = (E_t \cdot A_t \cdot l) / (l_t \cdot A_{concrete}) = (E_t \cdot A_t) / l_t \quad (l = 1; A_{concrete} = 1) \quad (\text{Eq.1.18})$$

$$K_c = (E_c \cdot A_c) / (l_c \cdot A_{concrete}) = (E_c \cdot A_c) / l_c \quad (A_{concrete} = 1) \quad (\text{Eq.1.19})$$

1.4 Purpose of this Research

Crack due to the shrinkage in concrete is widely acknowledged as one of the fundamental defects for reinforced concrete structure, it leads to premature deterioration and shortening the service life. The shrinkage together with the weak tensile strength may result in the injurious crack. Therefore, expansive agent has been employed to enhance the cracking resistance of concrete. With regard to self-compacting concrete (SCC), due to the low water-to-cement ratio and the high paste volume, the volume change at the hardening and drying process cannot be neglected. Most of the past researches on the application of expansive agent until now have been carried out for the conventional concrete under water curing. The purpose of this research is to verify the feasibility of cracking resistance of SCC by using expansive agent under practical construction site environment.

In addition, the expansive characteristics of expansive concrete differ greatly depending on mix proportions, curing methods and degree of the restraints. Therefore, an experimental result can be applied only to a case under same condition. In this research, three-dimensional composite model of expansive concrete will be proposed to estimate the expansion of expansive concrete based on the existing one-dimensional composite model by taking the mix proportions, curing methods and degree of the restraints into account.

1.5 Research Program

At first, in Chapter 2, Chapter 3 and Chapter 4, experiments of SCC using expansive agent were carried out under different curing methods. Different dosage of expansive agent and different restraint steel ratio were set up to be the parameters. Then, specimens were put in the temperature-controlled room to observe cracking occurrence. From the experiment, the basic characteristics of SCC using expansive agent was verified. And the appropriate dosage of expansive agent for SCC was suggested. In addition, the experimental results were used to be the database for 3-dimensional composite model.

From the experimental result of previous chapters, the efficiency of expansive agent was reduced on the application of SCC due to the low water-to-cement ratio character of SCC. In Chapter 5, limestone powder was employed to be the countermeasure to enhance the efficiency of expansive agent. Different replacement ratio of limestone powder in volume was employed and crack was observed as well.

In Chapter 6, the expansive characteristics of SCC using expansive agent under multi-axial restraint were experimentally investigated. The mutual effect of restraint and expansion in perpendicular directions was revealed from the experimental results. The friction occurred between coarse aggregate and mortar was set to be the hypothesis to explain the mechanism and proved by mortar and paste experiment. Moreover, the friction concept was reflected to the friction between expansion and compression elements in 3-dimension composite model. And the experimental results were employed to decide the friction coefficient, the ratio of the friction to normal stress on the interface of expansion and compression elements.

Finally, the 3-dimensional composite model of expansive concrete was proposed to estimate the expansion of expansive concrete based on the existing 1-dimensional

composite model by taking the mix proportions, curing methods and degree of the restraints into account. The one-axial restraint experimental results in Chapter 2, Chapter 3 and Chapter 4 were employed to decide the potential expansion of expansion element and the multi-axial restraint experimental result in Chapter 6 was employed to decide the friction coefficient. With the determination of above two parameters, 3-dimensional composite model was achieved. And estimation was made to compare with the other experimental result.

The framework of this research was shown in **Fig.-1.5**.

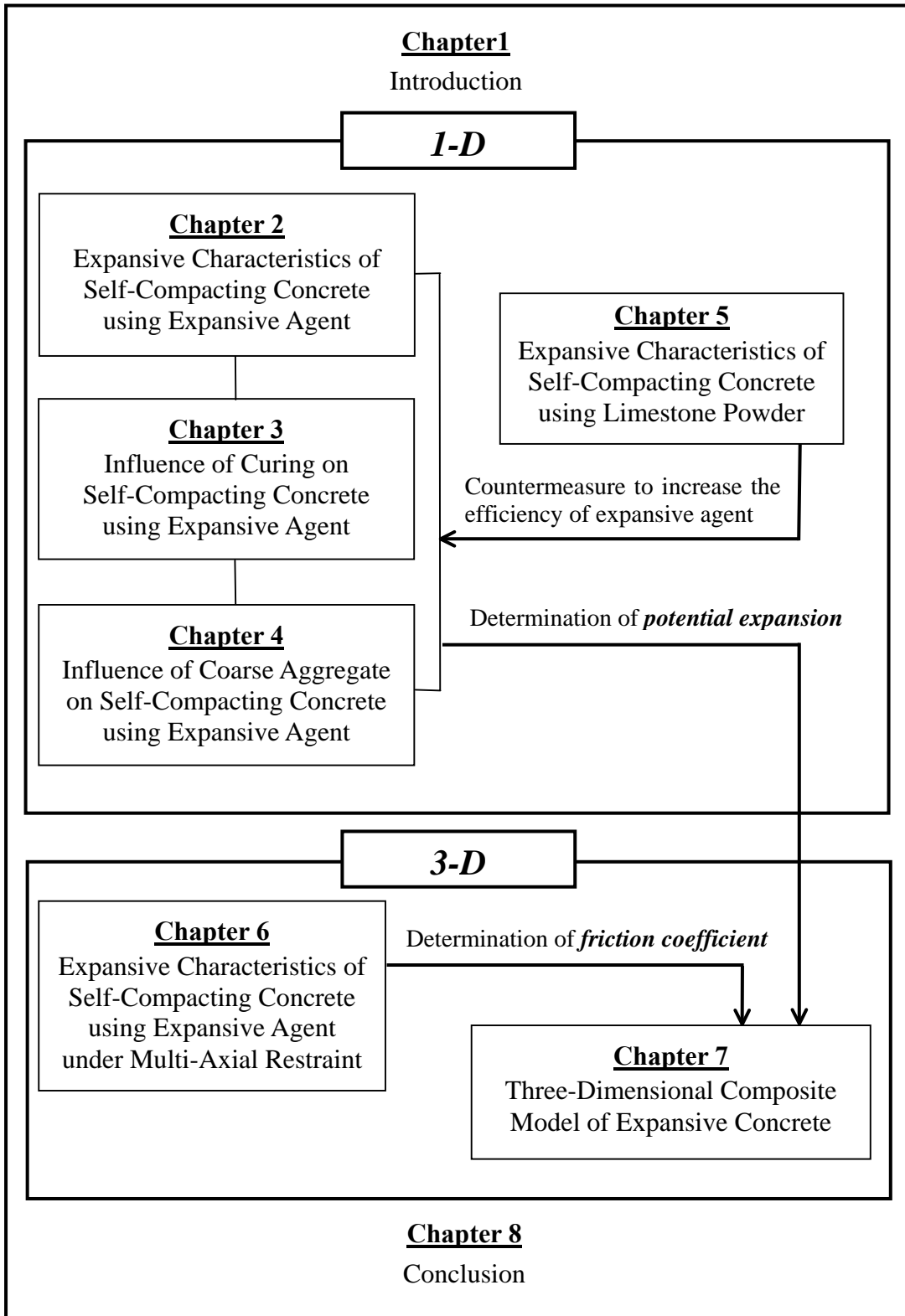


Fig.-1.5 Research framework

CHAPTER 2

EXPANSIVE CHARACTERISTICS OF SELF-COMPACTING CONCRETE USING EXPANSIVE AGENT

2.1 Introduction

From the past research, it was proved that the addition of expansive agent was an effective way to compensate for the shrinkage of concrete. [10] And expansion was increased as the dosage of expansive agent increased. Most of the past researches on the application of expansive agent until now have been carried out for conventional concrete under water curing. As stated in Chapter 1, shrinkage compensation effect of expansive agent greatly depends on mix proportion and curing method. Therefore, the expansive characteristics of SCC using expansive agent in practical environment were studied.

In this chapter, different dosage of expansive agent and different restraint steel ratio were set up to be the parameters and experiment was carried out under sealed curing to simulate the practical curing situation in the construction site.

2.2 Experimental Procedures

2.2.1 Materials and Mix Proportions

The materials in use and the mix proportions were shown in **Table-2.1** and **Table-2.2**. The requirement of the mix proportions is that all mix proportions have to possess good workability. The result of flowability test was shown in **Table-2.3** and all mix proportions showed the good workability.

Table-2.1 Materials used in experiment

Cement	C	Low Heat Cement: Specific gravity: 3.24
Expansive agent	E	CSA System: Specific gravity: 3.20
Admixture	SP	SP-S: Polycarboxylic acid-based AE HWRA
Fine aggregate	S	Crushed sand (C.S.): Specific gravity: 2.60 Sea sand (S.S.): Specific gravity: 2.59
Gravel	G	Specific gravity: 2.68
Steel		Es: 210 kN/mm ²

Table-2.2 Mix proportions of experiment

No.	W/P%	W/(C+E)%	W	C	E	S	G	SP
			Unit: kg/m ³					
EX0	30.0	30.0	184	614	0	793	780	7.982
EX20	30.0	30.0	184	594	20	793	780	7.982
EX40	30.0	30.0	184	574	40	793	780	7.982

Table-2.3 Result of flowability test

	Slumpflow	V-funnel	Box
EX0	685*695 mm	12.5 sec	325 mm
EX20	655*655 mm	12.7 sec	325 mm
EX40	670*675 mm	12.0 sec	320 mm

As showed in **Fig.-2.1**, one-axial restraint experiment of SCC using different dosage of expansive agent was carried out. And two types of deformed bar, D19 and D25, were installed in the cross-section center. The restraint steel ratio was 1.27% and 2.25% respectively. In addition, pure concrete specimen was prepared to compare with the restraint specimens as well. The list of specimen was shown in **Table-2.4**.

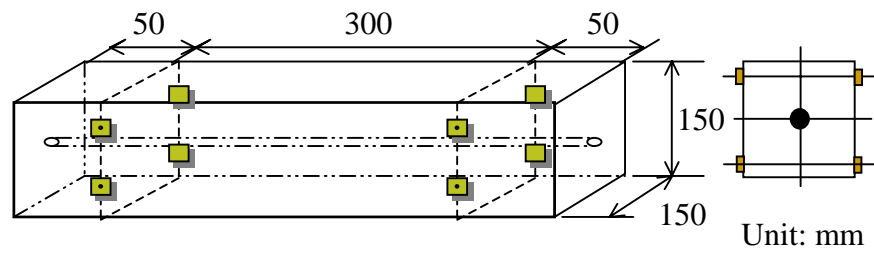


Fig.-2.1 Outline of specimen

Table-2.4 List of specimen

	p=0%	p=1.27%	p=2.25%
EX0			
EX20			
EX40			

2.2.2 Measurement and Curing

The mold was removed at the age of 1 day. Then, the specimens were sealed with double layers of polyethylene. In the meantime, contact chips were attached at 50 mm away from the edge of the member. All sealed specimens were placed in the temperature-controlled room at 20°C and RH = 60% and measured from the spacing of contact chips regularly until the age of 28 day. Then seal was removed and all specimens were put in the same environment to observe the crack.

2.3 Experimental Results and Discussion

The experimental results were shown from **Fig.-2.2** to **Fig.-2.5**. Each point on the figure was the average value from four measured values of each specimen. Due to the addition of expansive agent, the stain behavior changed from shrinkage to expansion. In addition, the expansion strain increased as the dosage of expansive agent increased.

According to “Design and Construction Guideline of Expansive Concrete” from

JSCE (Table-2.5), expansive concrete was classified into shrinkage-compensation concrete and chemically prestressed concrete based on expansion strain. The dosage of expansive agent of shrinkage-compensation concrete was 30kg/m^3 and the expansion strain was $150\sim 250\ \mu$. For chemically prestressed concrete, it was divided into two cases. For the expansive concrete casting on the construction site, the dosage of expansive agent was $35\sim 45\text{kg/m}^3$ and the expansion strain was $200\sim 700\ \mu$. For precast expansive concrete, the dosage of expansive agent was $30\sim 65\text{kg/m}^3$ and the expansion strain was $200\sim 1000\ \mu$. The regulation was based on the experiment of JIS A 6202, the standard experiment of Japanese Standards Association (JIS). In the standard experiment, the expansion strain was stipulated as the measured expansion strain at 7 day and the restraint steel ratio was 0.95%. Besides, the specimen was cured in the water until 7 day. The minimum expansion strain for shrinkage compensation is $150\ \mu$. [11]

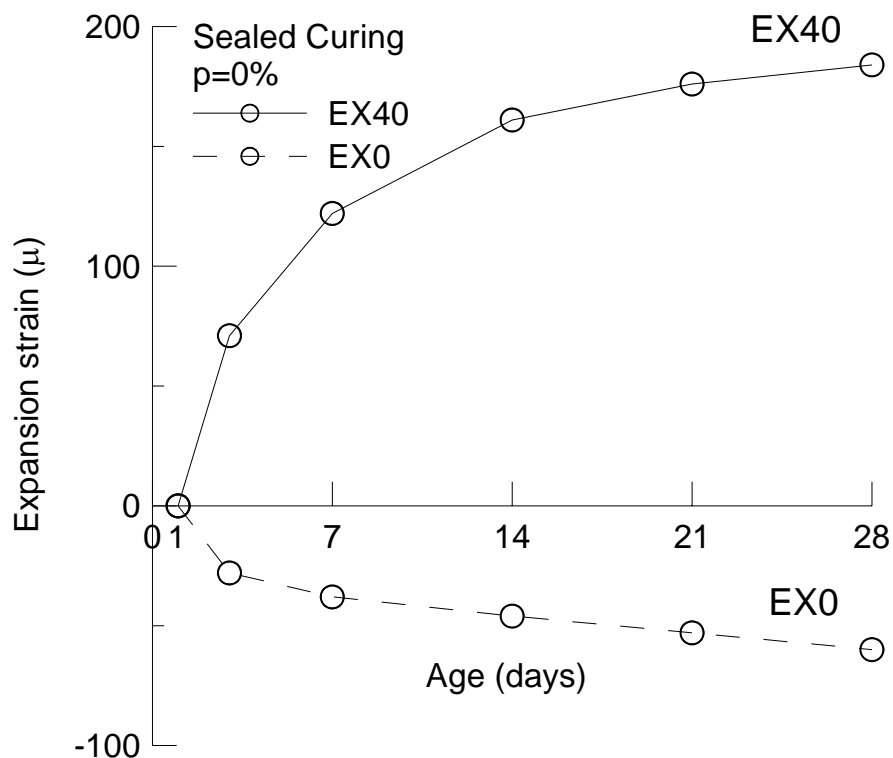


Fig.-2.2 Relationship between expansion strain and different dosage of expansive agent at $p=0\%$ (Sealed Curing)

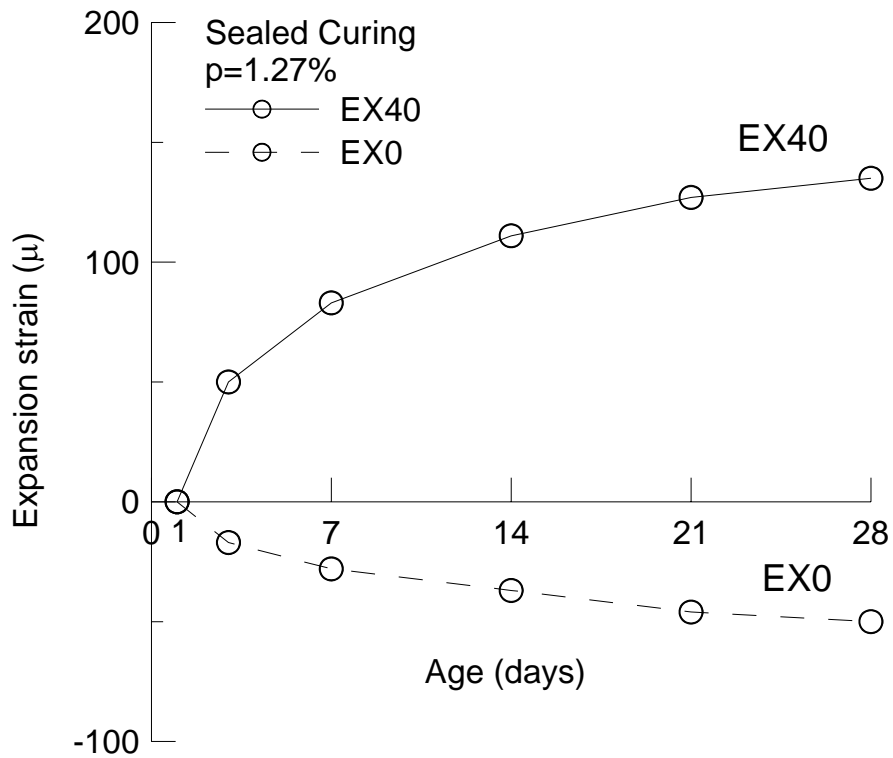


Fig.-2.3 Relationship between expansion strain and different dosage of expansive agent at p=1.27% (Sealed Curing)

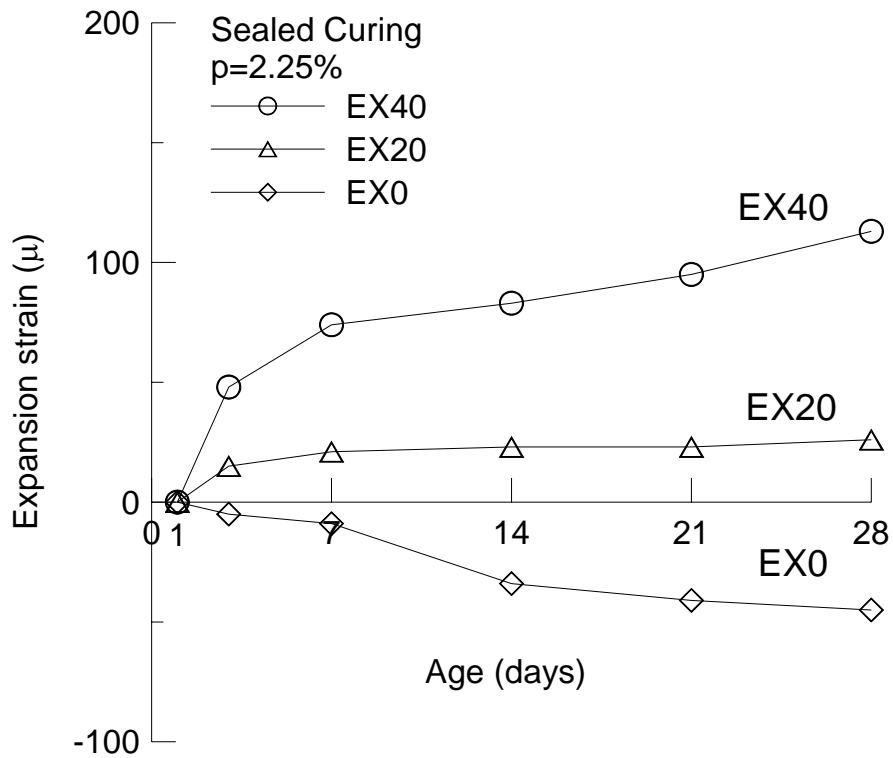


Fig.-2.4 Relationship between expansion strain and different dosage of expansive agent at p=2.25% (Sealed Curing)

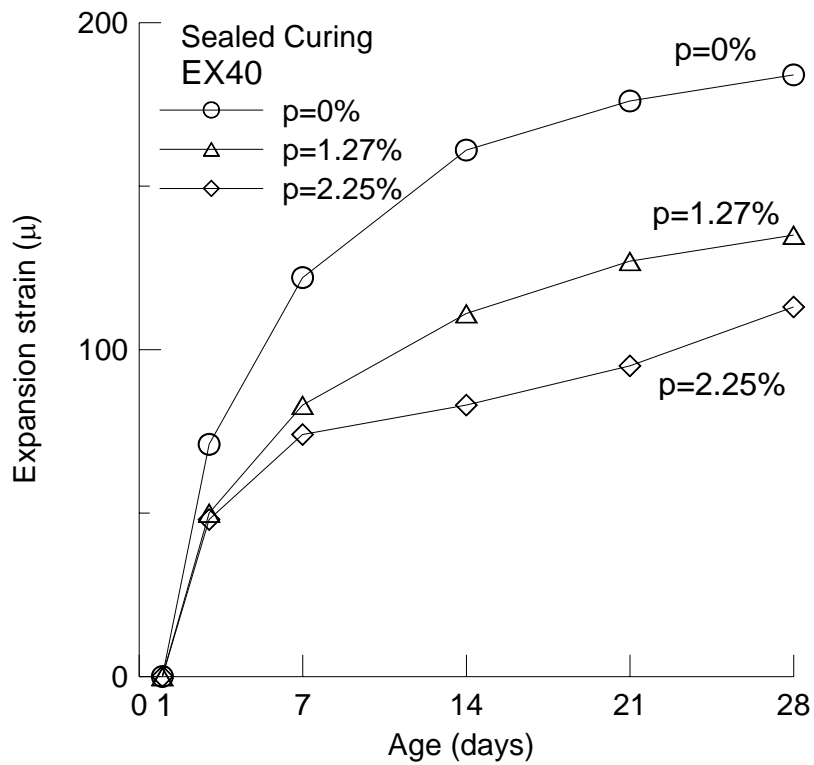


Fig.-2.5 Relationship between expansion strain and different restraint steel ratio for EX40 (Sealed Curing)

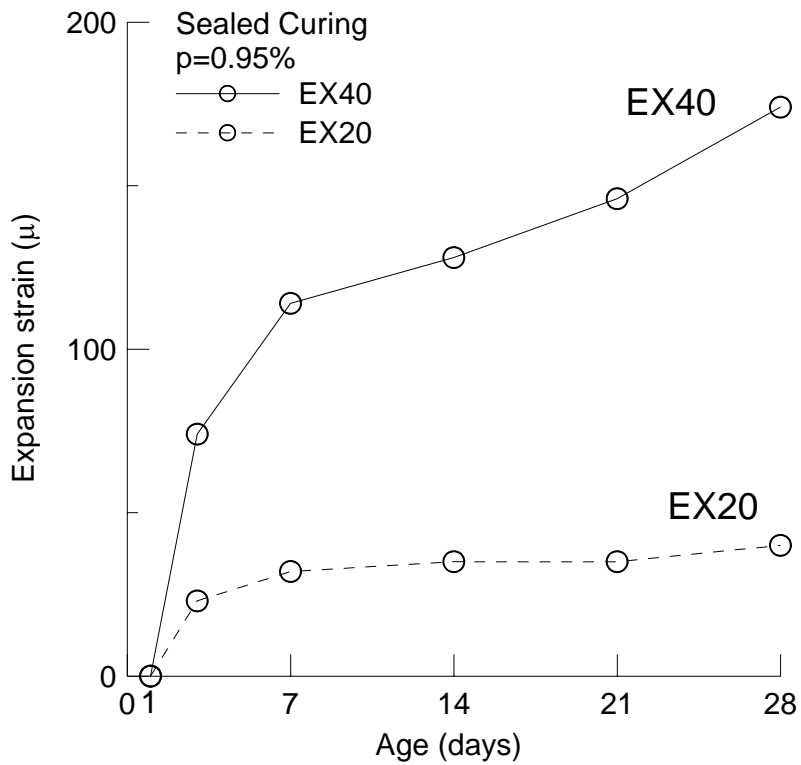


Fig.-2.6 Relationship between expansion strain and different dosage of expansive agent at p=0.95% (Sealed Curing)

Table-2.5 Guideline of design and construction of expansive concrete (JSCE) [11]

	Shrinkage compensation	Chemical prestress	
		Construction site	Precast product
Dosage	30kg/m ³	30~45kg/m ³	30~65kg/m ³
Expansion strain*	150~250 μ	200~700 μ	200~1000 μ

(*: Expansion strain at 7 day according to the standard experiment of JIS A 6202)

As shown in **Fig.-2.4**, the expansion strain of EX20 and EX40 specimen at 7 day were only about 20 μ and 75 μ that were much smaller than the regulation of JSCE. Even at the age of 28 day, the expansion strain were still only about 25 μ and 110 μ, though the restraint steel ratio was 2.25% which was larger than 0.95% in the standard experiment. In **Fig.-2.5**, the expansion strain of EX40 at 7 day was 80 μ and 120 μ when restraint steel ration was 1.27% and 0%. Therefore, the expansion strain at p=0.95% could be estimated reasonably to be in the range of 80 μ and 120 μ which was still below 150 μ, the minimum expansion strain of regulation.

In order to compare the experimental results with the regulation, expansion energy method was adopted to calculate the equivalent expansion strain at p=0.95% and the results were shown in **Fig.-2.6**. The calculation expansion strain of EX20 and EX40 at 7 day was 30 μ and 115 μ respectively. Both of the expansion strains were still less than the minimum value of regulation.

The insufficient expansion stain represented the shrinkage compensation of expansive concrete was not enough. In the view of stress, chemical prestress was induced into the concrete due to the steel restraint in the curing stage. After the specimen was dried, the stress status of concrete became tensile stress as the drying shrinkage increased. If the expansion strain was not enough in the curing period, crack may occur once the tensile stress of concrete overpasses tensile strength. On the contrary, if the expansion strain was enough in the curing period, the possibility of crack could be reduced greatly. (**Fig.-2.7**)

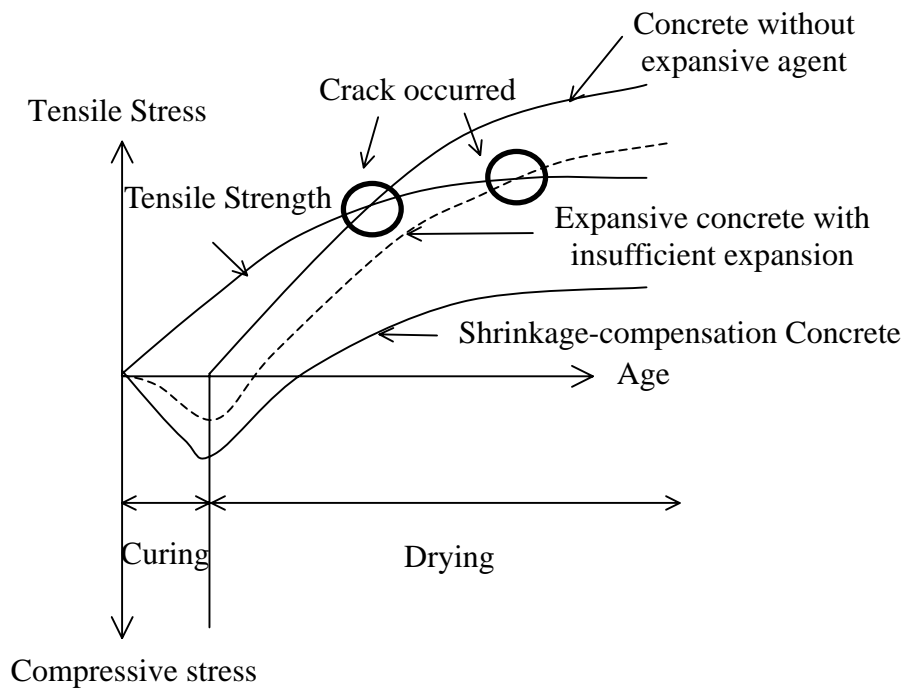


Fig.-2.7 Cracking mechanism of expansive concrete due to insufficient expansion

From the experimental result, the both expansion strain of EX20 and EX40 under sealed curing was not achieved the regulation of JSCE. In another words, crack may occur after drying started due to the drying shrinkage. As a matter of fact, although no crack occurred in measurement period, fine cracks were observed on the surface of EX20 specimens after seal was removed. In the case of EX40, although the expansion strain was less than 150μ at 7 day, before the specimen was dried, the expansion strain was more than 150μ . Therefore, crack was not occurred after the specimen was dried.

2.3.1 Low Water-to-cement Ratio and Autogeneous Shrinkage

Viscosity was the key for the flowability of SCC. In order to keep sufficient viscosity of SCC, a large amount of cement was employed in SCC. Therefore, most of the mix proportions of SCC were low water-to-cement ratio and high paste volume. In the case of conventional concrete, water-to-cement was high and autogeneous shrinkage was small enough to be neglected. However, as the water-to-cement ratio reduced, the percentage of autogeneous shrinkage to total shrinkage was increased rapidly. In the case of 30% of water-to-cement ratio, about 50% of shrinkage was

from autogenous shrinkage. Furthermore, if water-to-cement ratio was less than 20 %, almost all shrinkage came from autogenous shrinkage. [12] (Fig.-2.8) As mentioned above, due to the necessity for large amount of cement, most of the water-to-cement ratio of SCC was about 30% or less than 30%. Therefore, in comparison with the high water-to-cement conventional concrete, the maximum expansion strain of SCC with the same dosage of expansive agent was reduced due to the autogenous shrinkage.

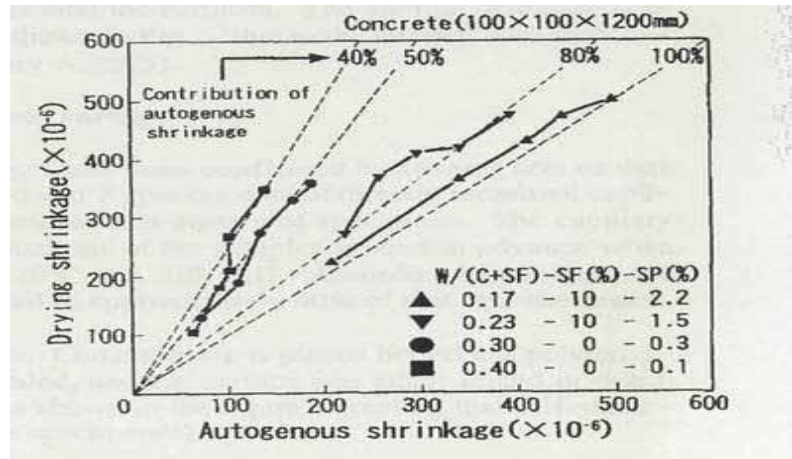


Fig.-2.8 Relationship between autogenous shrinkage and drying shrinkage

2.3.2 Insufficient Water Supply under Sealed Curing

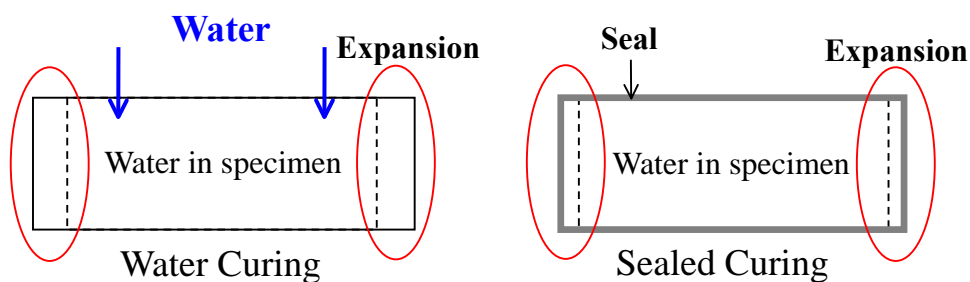


Fig.-2.9 Water supply under water and sealed curing

The standard experiment in the regulation of JSCE was carried out under water curing. Thus water could be supplied from outside. Considering the actual curing condition, water curing was difficult to be carried out in construction site for 7 days.

On the contrary, seal curing in this experiment was closer to the practical curing condition. In this case, the water in the specimen became the only source for the hydration of expansive agent. From the experimental result, it was clear that the water existed in the specimen was not enough to provide the water for the hydration of expansive agent. In another words, the expansion strain cannot compensate the drying shrinkage after the specimen was dried.

2.4 Summary

From the experimental results, the characteristics of SCC using expansive agent were revealed and generalized as follows.

- ♦ Due to the necessity of large amount of cement, the water-to-cement ratio of SCC was much smaller than conventional concrete. And the very low water-to-cement character of SCC resulted in the increase of autogenous shrinkage. Therefore, in comparison with the high water-to-cement conventional concrete, the maximum expansion strain of SCC was less than conventional concrete with the same dosage of expansive agent. That is to say that the efficiency of expansive agent was reduced on the application of SCC under sealed curing.
- ♦ The regulation of JSCE was set up for conventional concrete using expansive agent. And the recommended expansion value was from the standard experiment carried out under water curing for 7 days. Comparing with the recommended expansion value, it was revealed for SCC using expansive agent that the minimum expansive strain couldn't be achieved under sealed curing condition. Therefore, the dosage of expansive agent for SCC under sealed curing condition had to be increased in order to achieve the enough expansion to prevent crack.

CHAPTER 3

INFLUENCE OF CURING ON SELF-COMPACTING CONCRETE USING EXPANSIVE AGENT

3.1 Introduction

From the experimental result of Chapter 2, the maximum expansion strain of SCC using expansive agent was less than that of conventional concrete with high water-to-cement ratio for the same dosage of expansive agent. And the insufficient expansion resulted in crack after the specimen was dried. It seemed that the efficiency of expansive agent was reduced on the application of SCC, due to the very low water-to-cement ratio. It was also found that the expansive characteristics greatly differ depending on curing method. In this chapter, the influence of curing method on SCC using expansive agent was studied by experimental method.

3.2 Experimental Procedures

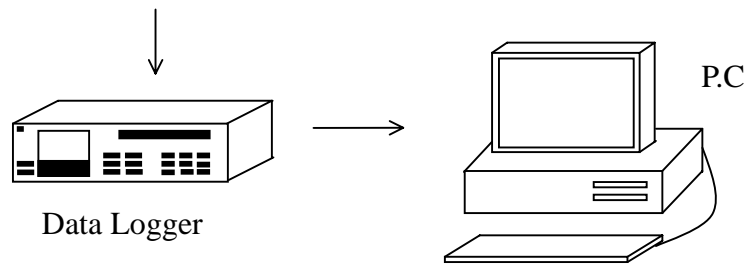
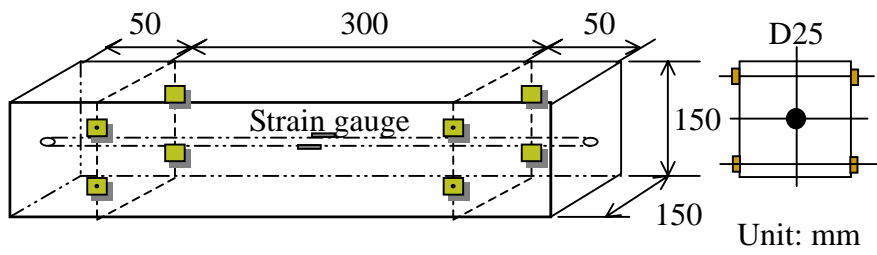
3.2.1 Materials and Mix Proportions

The materials in use were as same as the used materials in Chapter 2 (**Table-2.1**). And the mix proportions were shown in **Table-3.1**. (EX20 and EX40 were as same as the mix proportions in Chapter 2.) One-axial restraint specimen was prepared and deformed bar was installed in the center of the cross-section. In addition, pure concrete specimen was prepared as well. However, since contact chip could drop when the specimen was cured in water, stain gauge was attached on the middle of deformed bar to measure the expansion strain. The outline of specimen was shown in **Fig.-3.1**.

Table-3.1 Mix proportions of experiment

No.	W/P%	W/(C+E)%	W	C	E	S	G	SP
			Unit: kg/m ³					
EX20	30.0	30.0	184	594	20	793	780	7.982
EX40	30.0	30.0	184	574	40	793	780	7.982
EX66	30.0	30.0	184	548	66	793	780	7.982

Drying-curing and Sealed-curing specimen



Water-curing specimen

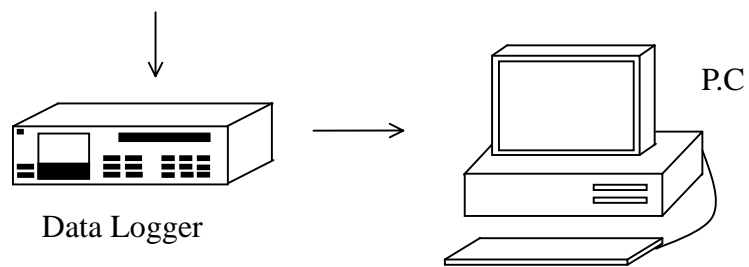
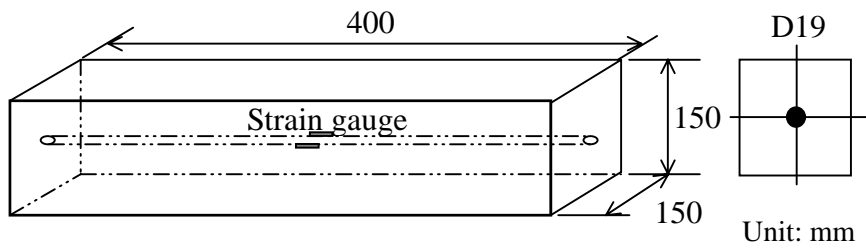


Fig.-3.1 Outline of specimen

Table-3.2 List of the specimen and curing condition

	Drying curing	Sealed curing (3 days)	Water curing (7 days)
EX20			p=0% & 1.27%
EX40	p=0% & 2.25%	p=0% & 2.25%	p=0% & 1.27%
EX66	p=0% & 2.25%	p=0% & 2.25%	

3.2.2 Measurement and Curing

The influence of curing method on SCC using expansive agent was studied. In this experiment, three types of curing methods were employed: drying curing, sealed curing and water curing. (**Table-3.2**)

The mold was removed at the age of 1 day for all specimens. For the drying- and sealed-curing specimen, contact chips were attached at 50 mm away from the edge of the member and the strain gauge was attached on the center of deformed bar. Sealed-curing specimens were sealed with double layers of polyethylene. All sealed-curing specimens were placed in the temperature-controlled room at 20 °C and RH = 60%. The seal was removed at the age of 4 day and then all specimens were put in the same environment to observe the crack. With regard to the drying-curing specimen, it was explored to the atmosphere in temperature-controlled room after mold was removed. The expansion strain of drying- and sealed- specimen was measured from the spacing of contact chips and the strain gauge on deformed bar from data logger. (**Fig.-3.1**)

In the case of water curing, after the mold was removed at 1 day, the specimen was cured in the water until the age of 7 day. During this time, the expansion strain was measured from data logger connected to the strain gauge on the center of deformed bar. Then the specimen was moved out of water and put in the temperature-controlled room to observe the crack.

3.3 Experimental Results and Discussion

3.3.1 Curing Effect on Expansion Strain of Different Dosage of Expansive Agent

The experimental results of EX66 measured from contact chips were shown in **Fig.-3.2** and **Fig.-3.3**. The expansion strain before the seal was removed was about

1000 μ and 1500 μ for the restraint and unrestraint specimen respectively. Even for the drying-curing specimen, expansion strain was about 500 μ and 1000 μ for the restraint and unrestraint specimen respectively. The excessive expansion could be observed by the difference of expansion strain measured from contact chips and strain gauge on the deformed bar. (**Fig.-3.4**) After seal was removed one day, the expansion strain measured from contact chips and strain gauge was about 700 μ and 100 μ respectively. The great difference of expansion strain was revealed that the restraint of deformed bar could not cover the whole concrete cross-section due to the great dosage of expansive agent. Therefore, the excessive expansion was occurred on the concrete surface and resulted in the crack in the early age. For the drying-curing specimen, the same phenomenon was observed and crack was occurred in three days. (**Photo-3.1** and **Photo-3.2**) In addition, there was no clear decrease of expansion strain after the seal was removed since the crack already occurred before the seal was removed. With regard to EX40, there was no difference of the expansion strain measured from contact chips and strain gauge.

The experimental results of EX20 and EX40 under water curing were shown in **Fig.-3.5**. In the case of EX40, the expansion strain at 7 day was about 160 μ which was more than the minimum value of regulation of JSCE, though the restraint steel ratio was 1.27% which is higher than 0.95%. However, in the case of EX20, the expansion strain at 7 day was only 75 μ when restraint steel ratio is 1.27%. Even without steel's restraint, the expansion strain of unrestrained specimen was only about 100 μ . (**Fig.-3.6**) In addition, for EX20, the influence of restraint steel was not clear due to the insufficient expansive agent. (**Fig.-3.7**) As to EX40, the effect of restraint steel was very clear. (**Fig.-3.8**) In **Fig.-3.9** and **Fig.-3.10**, the expansion strain of EX40 under water curing was compared with the experimental result under sealed curing in Chapter 2. It was clear that the expansion stain was increased substantially due to the sufficient supplement of water from outside.

The equivalent expansion strain at $p=0.95\%$ was calculated by expansion energy method and the results were shown in **Fig.-3.11**. The calculation expansion strain of EX20 and EX40 at 7 day was about 90 μ and 190 μ respectively. In the case of EX20, after the specimens were dried, crack occurred on not only the restrained specimen ($p=1.27\%$) but also unrestrained specimen ($p=0\%$) since the insufficient expansion strain of both specimens. It was found that 20kg/m^3 of expansive agent was not enough for SCC to prevent crack. On the other hand, crack was not occurred on both specimens of EX40.

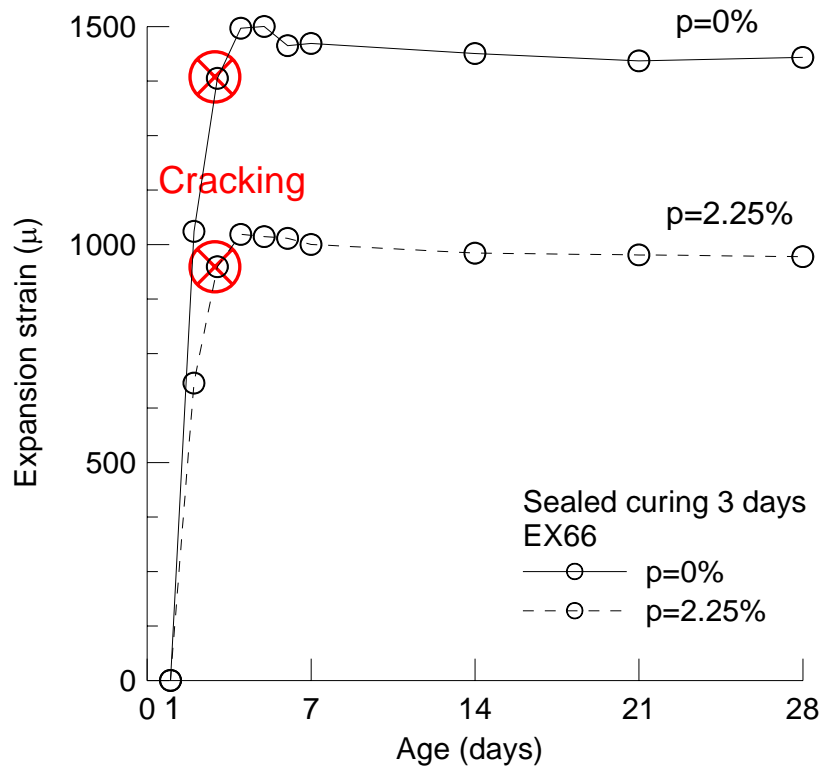


Fig.-3.2 Relationship between expansion strain and different restraint steel ratio for EX66 (Sealed Curing)

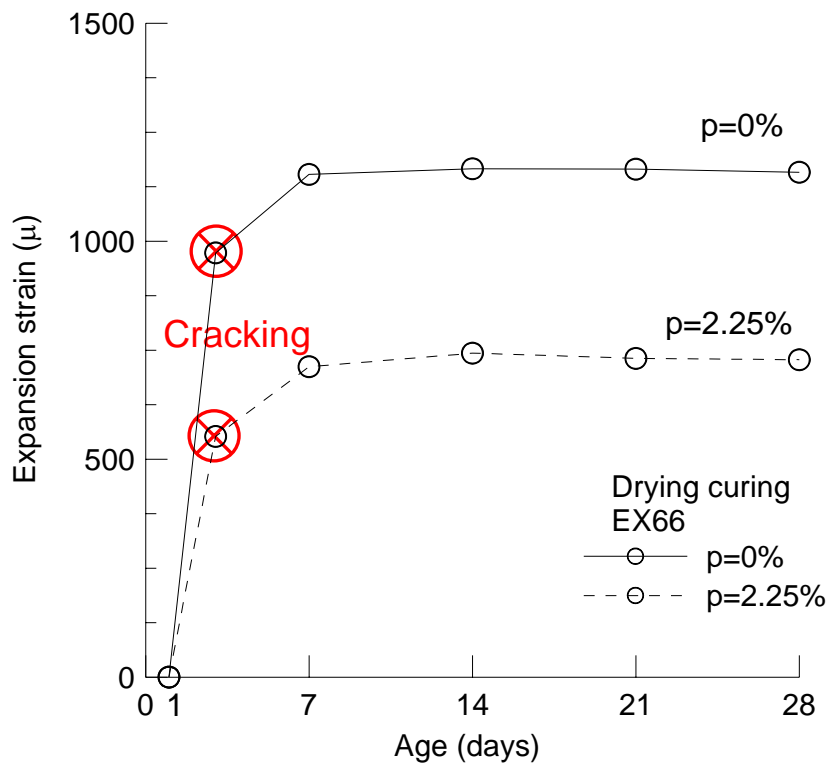


Fig.-3.3 Relationship between expansion strain and different restraint steel ratio for EX66 (Drying Curing)

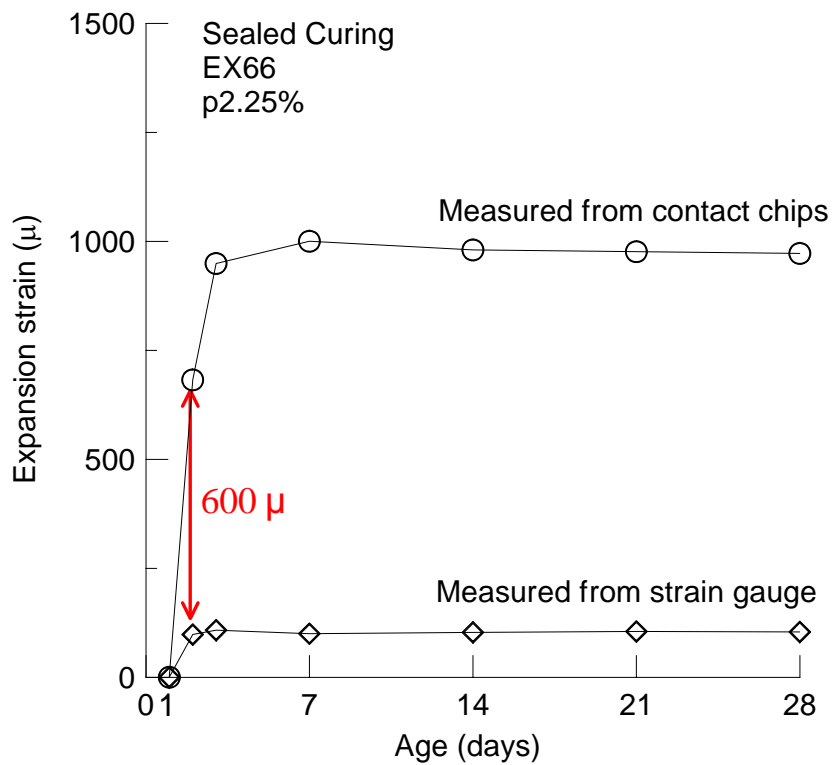


Fig.-3.4 Relationship between expansion strain measured from contact chips and strain gauge on deformed bar for EX66 at p=2.25% (Sealed Curing)

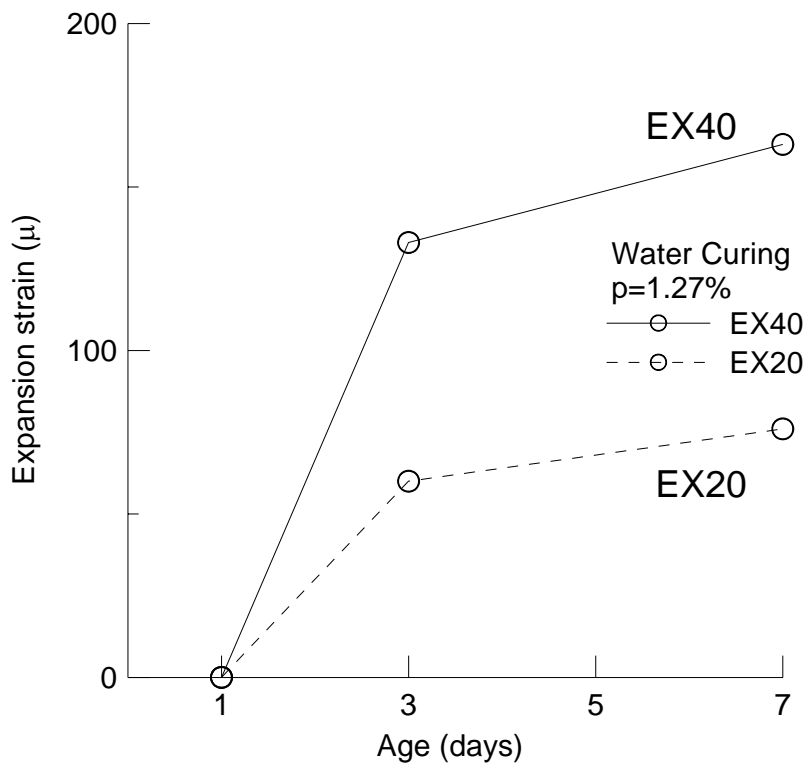


Fig.-3.5 Relationship between expansion strain and different dosage of expansive agent at p=1.27% (Water Curing)

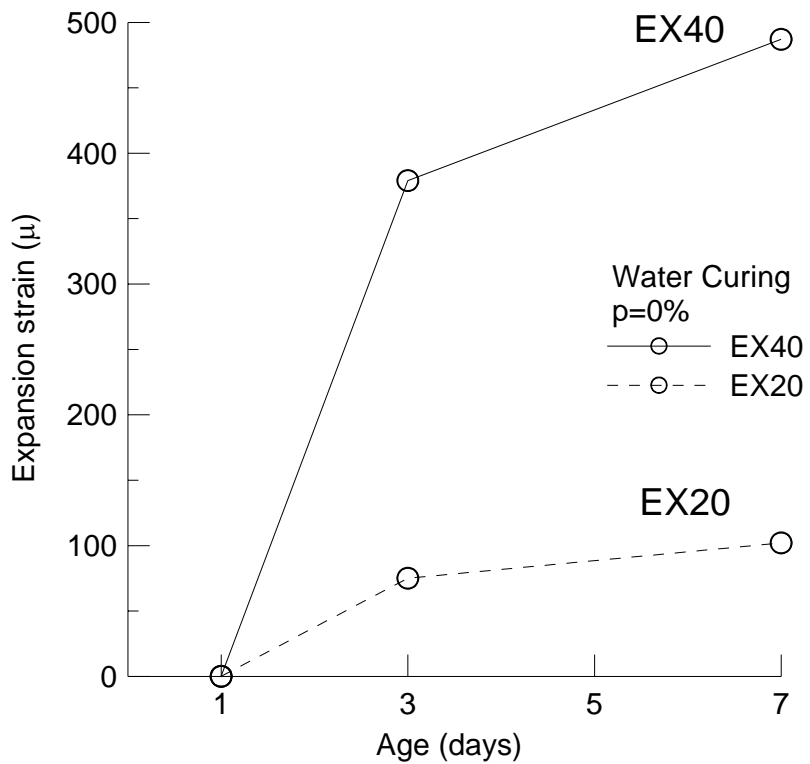


Fig.-3.6 Relationship between expansion strain and different dosage of expansive agent at p=0% (Water Curing)

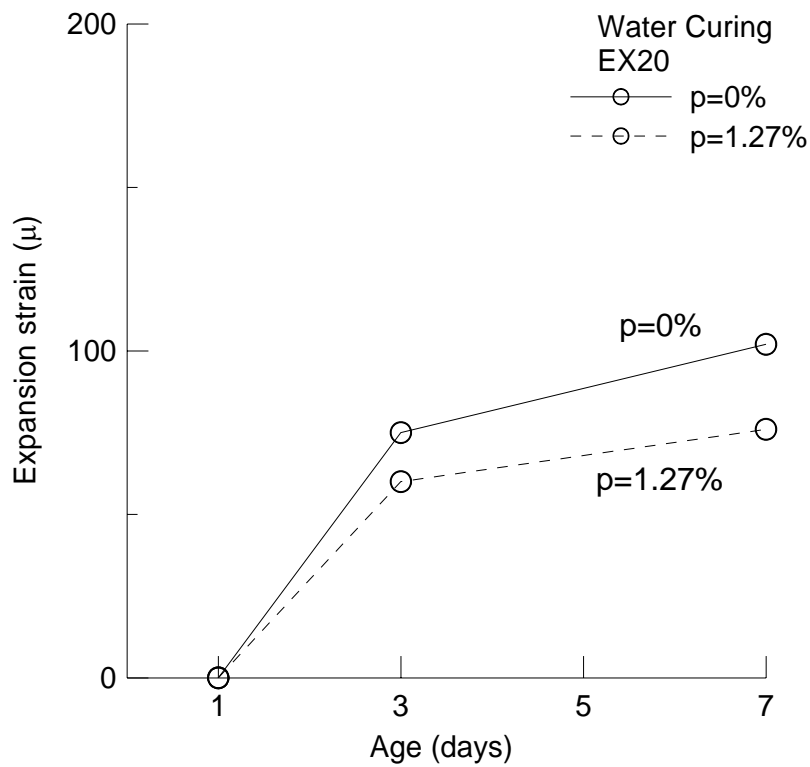


Fig.-3.7 Relationship between expansion strain and different restraint steel ratio for EX20 (Water Curing)

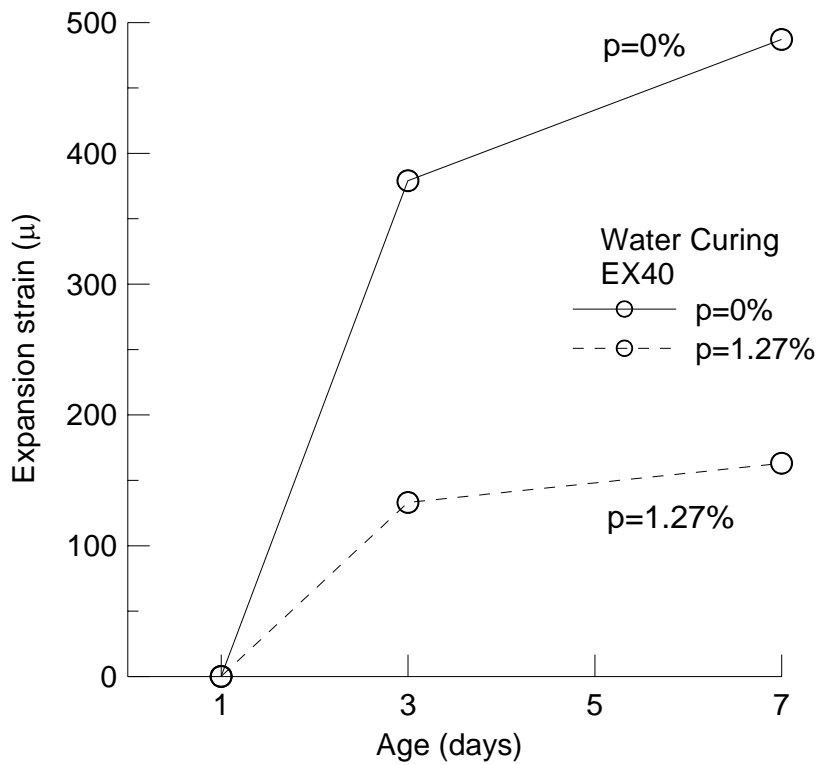


Fig.-3.8 Relationship between expansion strain and different restraint steel ratio for EX40 (Water Curing)

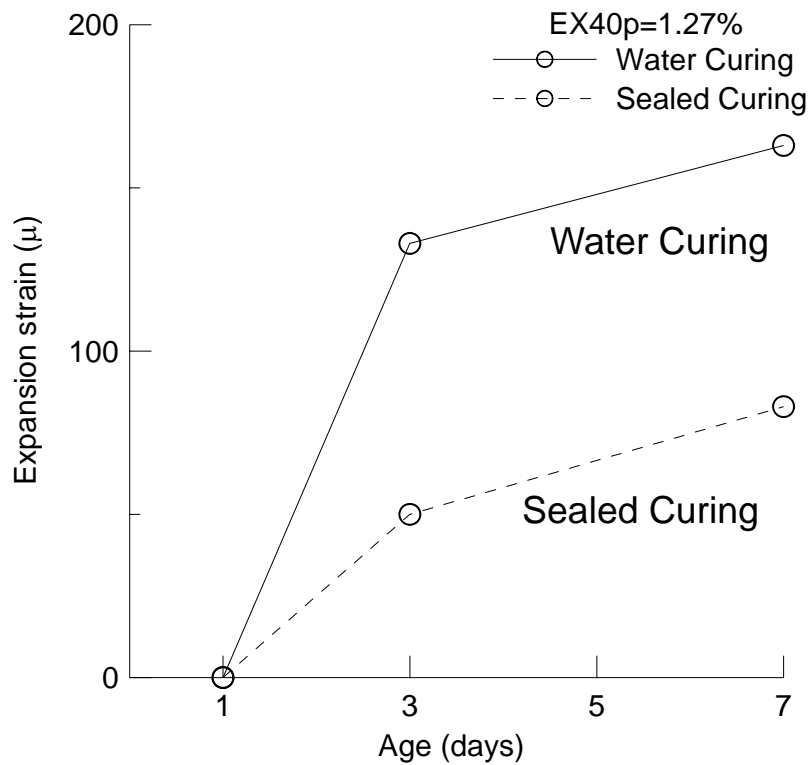


Fig.-3.9 Relationship between expansion strain and different curing method for EX40 (p=1.27%)

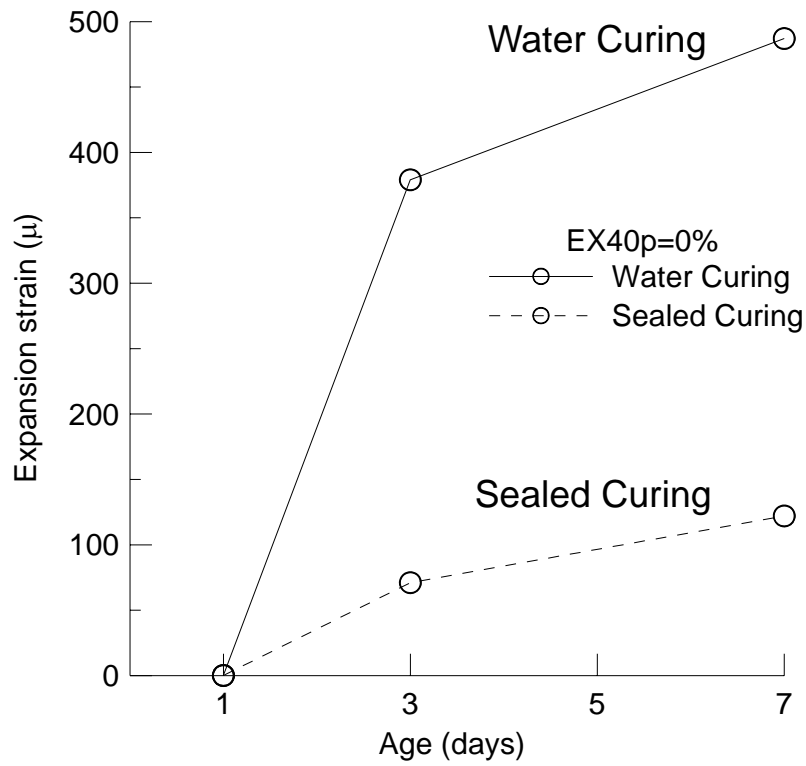


Fig.-3.10 Relationship between expansion strain and different curing method for EX40 (p=0%)

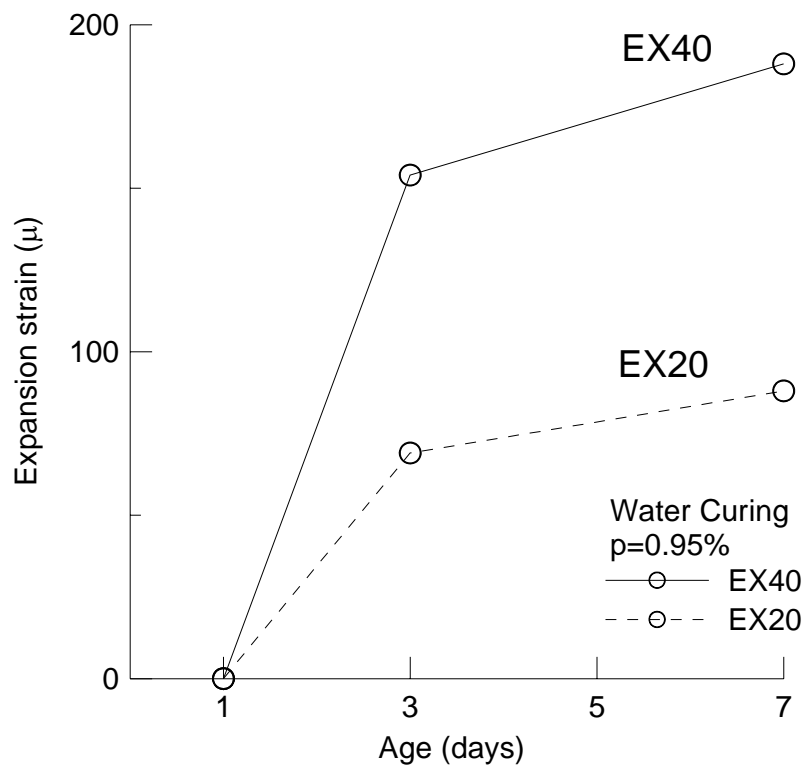


Fig.-3.11 Relationship between expansion strain and different dosage of expansive agent at p=0.95% (Water Curing)

From the above experimental results, for SCC, it was found that the difference on expansion under water- and sealed-curing was very clear for EX40. On the other hand, the influence of the drying-curing on the expansion was not so clear compared with the sealed curing. It was revealed that the necessity for water in SCC using expansive agent was higher than the conventional concrete with the same dosage of expansive agent. (Fig.-3.12)

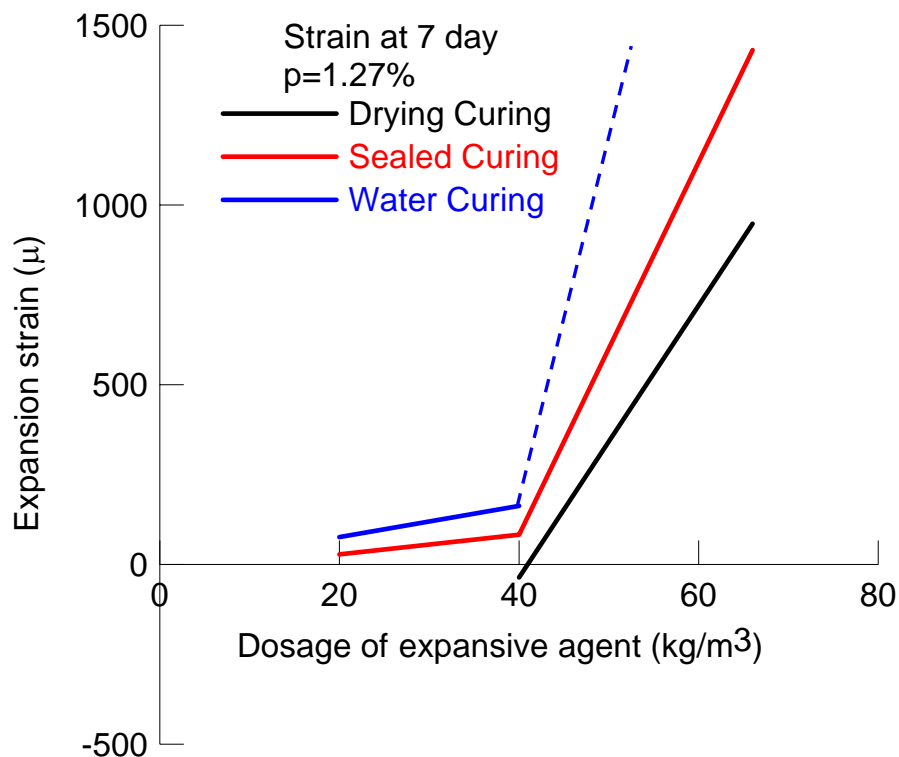


Fig.-3.12 Relationship between expansion strain and dosage of expansive agent under different curing methods

3.3.2 Cracking Occurrence Mechanism

Although crack occurred on both of specimen EX20 and EX66, the cracking occurrence mechanism and time of EX66 was different with the case of EX20. (Fig.-3.13)

Considering the expansion strain of EX20, EX40 and EX66 at the age of 3 day under sealed curing, it was 15 μ, 48 μ and 949 μ respectively. The expansion strain

increased substantially when the dosage of expansive agent was increased from 40 kg/m³ to 66 kg/m³. It was revealed that most of the water in the specimen under sealed curing was consumed by the hydration of expansive agent, since the hydration speed of expansive agent was much faster than cement. [13] (Fig.-3.14) Then due to the excessive expansion, crack was occurred in the very early age.

In the case of EX20, the insufficient expansion strain represented the shrinkage compensation of expansive concrete was not enough to compensate the shrinkage after the specimen was dried, even the specimen was cured in water for 7 days. After mold was removed, the expansion strain was changed to be shrinkage as the drying shrinkage increased. And the stress status of concrete was changed from compression to be tension as well. Then crack was occurred when the tensile stress of concrete over-passed concrete's tensile strength.

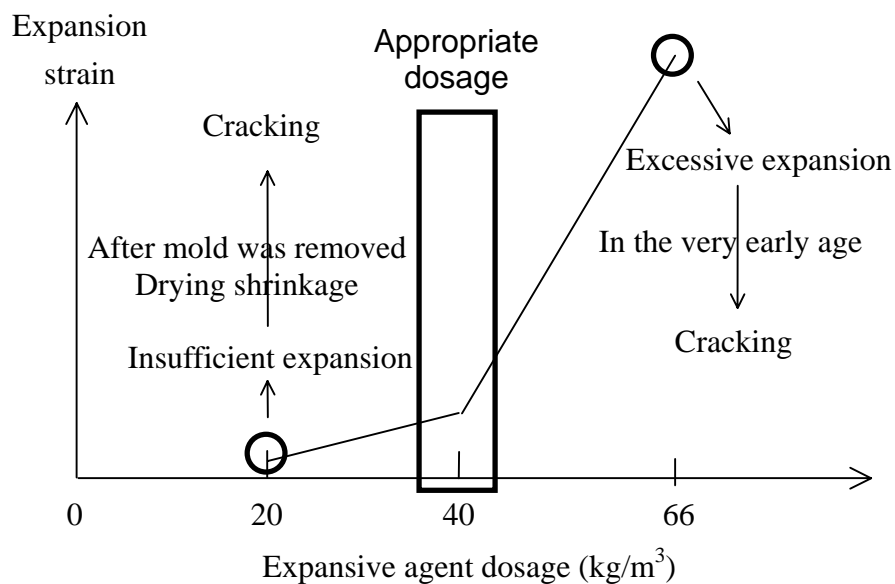


Fig.-3.13 Mechanism of cracking occurrence and appropriate dosage of expansive agent for SCC

Combining the experimental results in chapter 2 and chapter 3, 40kg/m³ of expansive agent could be the appropriate dosage for SCC. Since as the dosage of expansive agent was increased from 40kg/m³ to 66kg/m³, crack was occurred even under drying curing. 40kg/m³ was more than the recommended dosage 30kg/m³ in JSCE for shrinkage compensation. In comparison with conventional concrete, it was

found that the dosage of expansive agent has to increase when expansive agent is going to be employed in SCC. (Fig.-3.13)

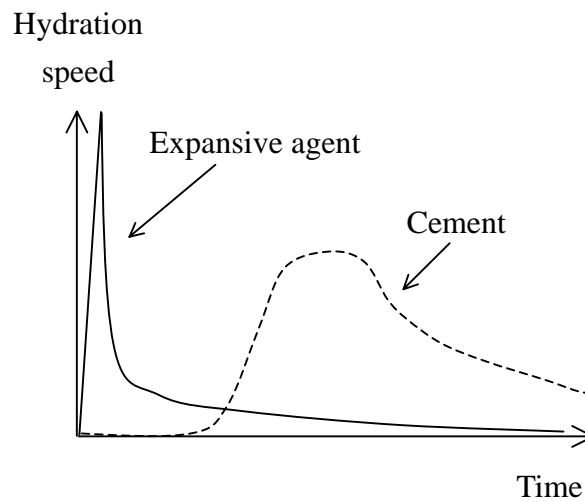


Fig.-3.14 Hydration speed of expansive agent and cement [13]

3.4 Summary

- ♦ The expansive characteristics greatly differ depending on curing method. From the experimental result, it was found that the necessity for water in SCC using expansive agent was much higher than the conventional concrete with the same dosage of expansive agent. The difference on expansion under water- and sealed-curing was very clear. On the other hand, the influence of the drying-curing on the expansion was not so clear compared with the sealed curing.
- ♦ 40kg/m^3 of expansive agent was proposed as the appropriate dosage for SCC that was higher than the regulation of JSCE. In addition, water curing was strongly recommended since water supplement was the most important factor for expansive agent. The excessive dosage of expansive agent resulted in crack at the very early age. Therefore, for the structure that water curing was available, water curing was strongly recommended, such as the big area plate that poor curing could be carried out. For the other structures that water curing was difficult to be carried out, the dosage of expansive agent had to be increased in order to achieve the enough expansion to prevent crack.



Photo-3.1 Crack occurred on the surface of drying-curing specimen due over-expansion (EX66)

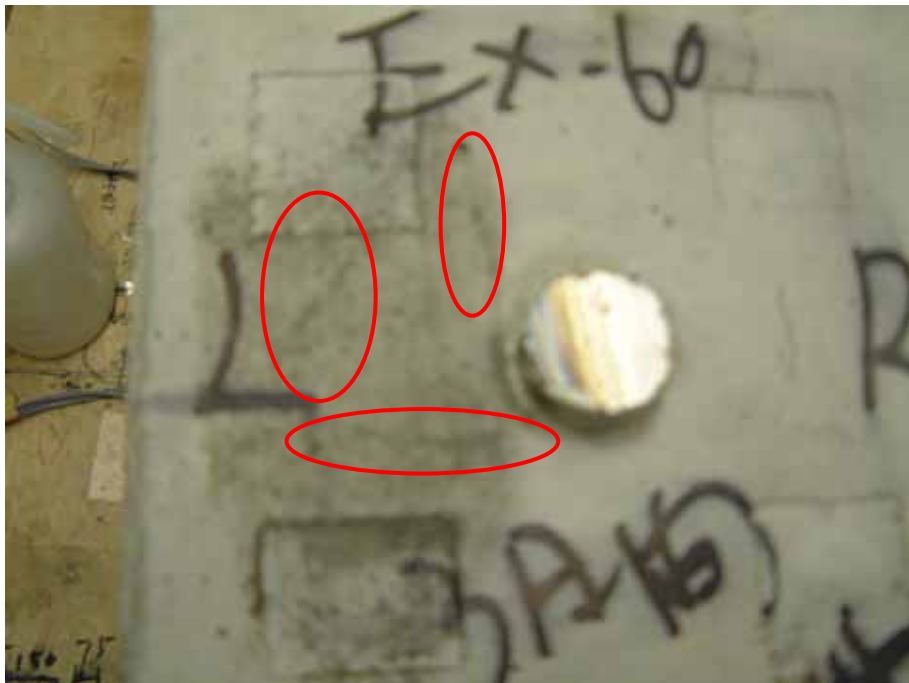


Photo-3.2 Crack occurred on the surface of sealed-curing specimen due over-expansion (EX66)

CHAPTER 4

INFLUENCE OF COARSE AGGREGATE ON SELF-COMPACTING CONCRETE USING EXPANSIVE AGENT

4.1 Introduction

As mentioned in previous chapters, in order to keep sufficient viscosity of SCC to avoid material segregation, a large amount of cement was employed in SCC. Therefore, most of the mix proportions of SCC were low water-to-cement ratio and high paste volume. Moreover, when concrete passed the complicated cross section or heavy reinforcement zone, good passing ability was indispensable to avoid block. Therefore the amount of coarse aggregate was limited to assure the passing ability. That was to say that the amount of powder was the key of the viscosity and the amount of coarse aggregate was related to passing ability.

In this chapter, the influence of coarse aggregate on expansion of SCC using expansive agent was investigated by experimental method.

4.2 Experimental Procedures

4.2.1 Materials and Mix Proportions

The materials in use and the mix proportions were shown in **Table-4.1** and **Table-4.2**. 40kg/m^3 of expansive agent was employed and the water-to-cement ratio and the ratio of sand to mortar in volume (V_s/V_m) were fixed at 30% and 45% for all mixing proportions. The only one varied parameter was the absolute volume of coarse aggregate. The mixing proportion of G0.29, G0.32 and G0.35 represented that the absolute volume of coarse aggregate was 0.29, 0.32 and $0.35\text{m}^3/\text{m}^3$ respectively. Besides, all mix proportions showed the good workability.

One-axial restraint specimen was prepared and deformed bar was installed in the center of the cross-section. Since contact chip could drop when the specimen was cured in water, mold gauge was set in the middle of specimen and connected to data logger. The outline of specimen was shown in **Fig.-4.1**.

Table-4.1 Materials used in experiment

Cement	C	Low Heat Cement: Specific gravity: 3.24
Expansive agent	E	CSA System: Specific gravity: 3.20
Admixture	SP	SP-S: Polycarboxylic acid-based AE HWRA
Fine aggregate	S	Crushed sand (C.S.): Specific gravity: 2.60 Sea sand (S.S.): Specific gravity: 2.58
Gravel	G	Specific gravity: 2.68
Steel		Es: 210 kN/mm ²

Table-4.2 Mix proportions of experiment

No.	W/(C+E)	Vs/Vm	Vw/Vp	E/(C+E)	W	C	E	S	G	SP
					Unit: kg/m ³					
G0.29	30%	45%	97%	6.59%	184	574	40	791	780	7.98
G0.32	30%	45%	97%	6.88%	176	548	40	757	858	7.64
G0.35	30%	45%	97%	7.21%	168	522	40	723	936	7.30

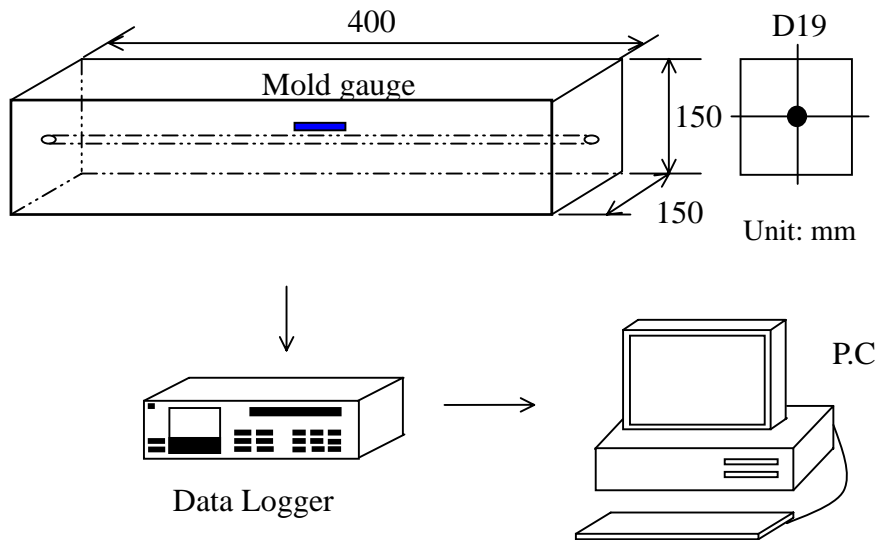


Fig.-4.1 Outline of specimen

4.2.2 Measurement and Curing

After the mold was removed at 1 day, all specimens were cured in the water until the age of 7 day. During this time, the expansion strain was measured from data logger connected to the mold gauge in the center of specimen.

4.3 Experimental Results and Discussion

As shown in **Fig.-4.2**, assuming the expansion of mortar specimen with expansive agent was A . When half volume of specimen was replaced by coarse aggregate, if the coarse aggregate was considered without expansion occurrence, the theoretical expansion of the specimen should be equal to half expansion of the pure mortar specimen, $0.5A$. However, since the coarse aggregate was uniformly distributed in the concrete specimen, mortar could not expand freely, like pure mortar specimen. Therefore, the expansion of the specimen was less than $0.5A$ and the role of coarse aggregate in expansive concrete was regarded as one kind of resistance force for expansion.

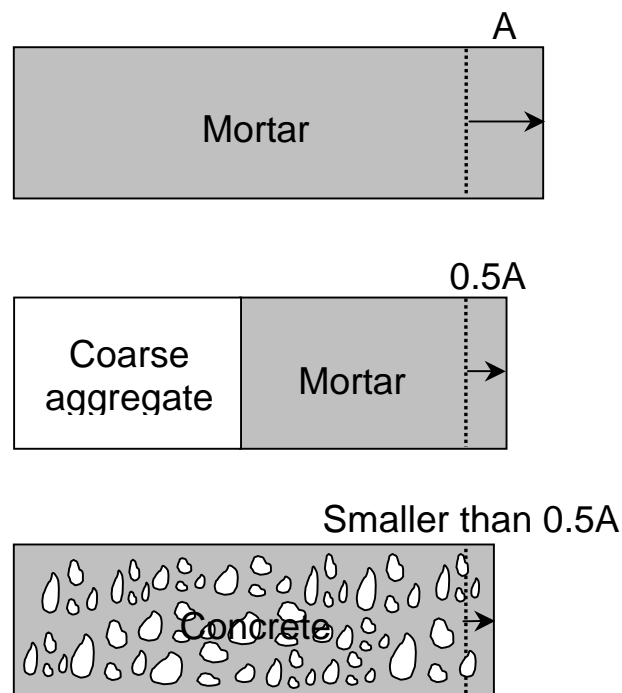


Fig.-4.2 The role of coarse aggregate in expansive concrete

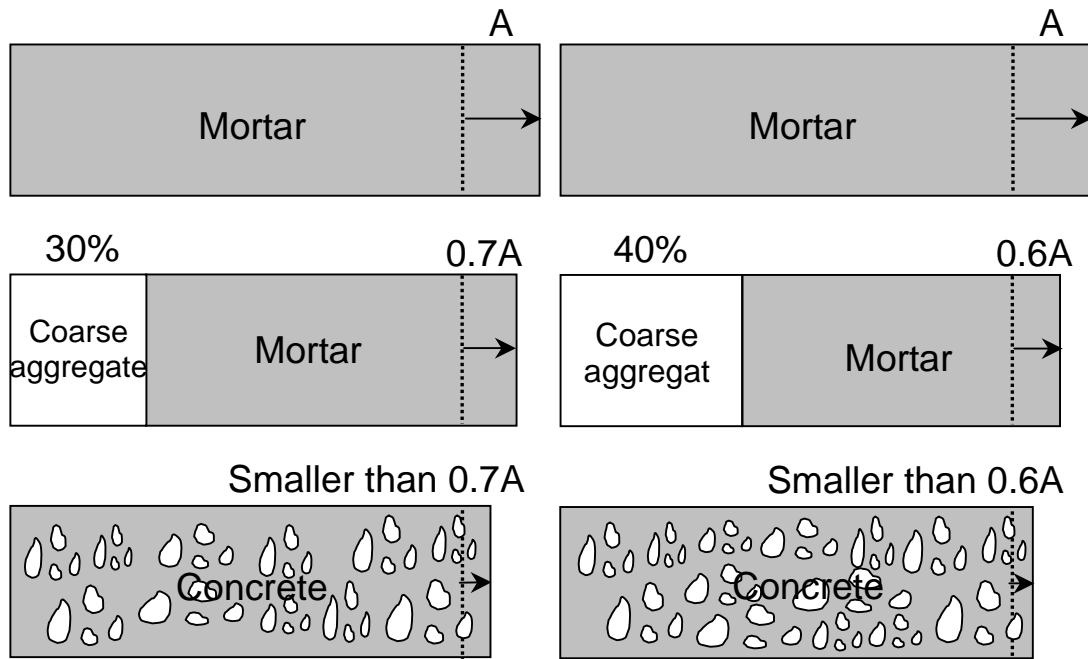


Fig.-4.3 Influence of coarse aggregate on expansion strain

Comparing two specimens in **Fig.-4.3**, the mortar was replaced 30% and 40% with coarse aggregate by volume respectively. Assuming the expansion of pure mortar specimen was A and same mortar was employed for two specimens. The theoretical expansion of specimen should be proportional to the mortar volume, $0.7A$ and $0.6A$. Therefore, the expansion of concrete specimen was less than $0.7A$ and $0.6A$ respectively. By this example, it was clear that the increase of coarse aggregate resulted in the decrease of expansion.

The experimental result was shown in **Fig.-4.4**. It was revealed that the expansion strain increased with the increase of coarse aggregate. As explained previously, the role of coarse aggregate in expansive concrete was regarded as the resistant force for expansion. That was to say that the increase of coarse aggregate represented the increase of resistant force to expansion. Therefore, the expansion strain of specimen should be decreased when the amount of coarse aggregate increased which was opposite with the experimental result.

Considering the control parameters in SCC mixing proportion design process, 50% of solid volume of coarse aggregate was set to be the volume of coarse aggregate. And depending on the used material, the ratio of sand to mortar in volume (V_s/V_m),

the ratio of water to powder in volume (V_w/V_p) and the dosage of SP were adjusted in order to achieve good self-compactability. In this experiment, sand volume in mortar and water volume in paste was fixed and amount of coarse aggregate was varied as 50%, 55% and 60% of the solid volume of coarse aggregate. Therefore, if without the employment of expansive agent, we can say the paste and mortar property in these three mix proportion was completely same. (Table-4.2) However, same weight of expansive agent, 40kg/m^3 , was employed for all mix proportions. Therefore, the paste's composition became different. That was to say that the increase of coarse aggregate's volume resulted in the decrease of the dispersion density of expansive agent in paste. ($E/(C+E)$)

To analyze the influence of $E/(C+E)$ on expansion strain, mortar expansion test with the same mortar under the same situation, curing method and steel restraint ratio, was carried out. And the amount of coarse aggregate was chosen to be the horizontal axis and the experiment result was re-drawn in Fig.-4.5. Besides, the experimental result under same design parameters from the other chapters was added in this Figure as well.

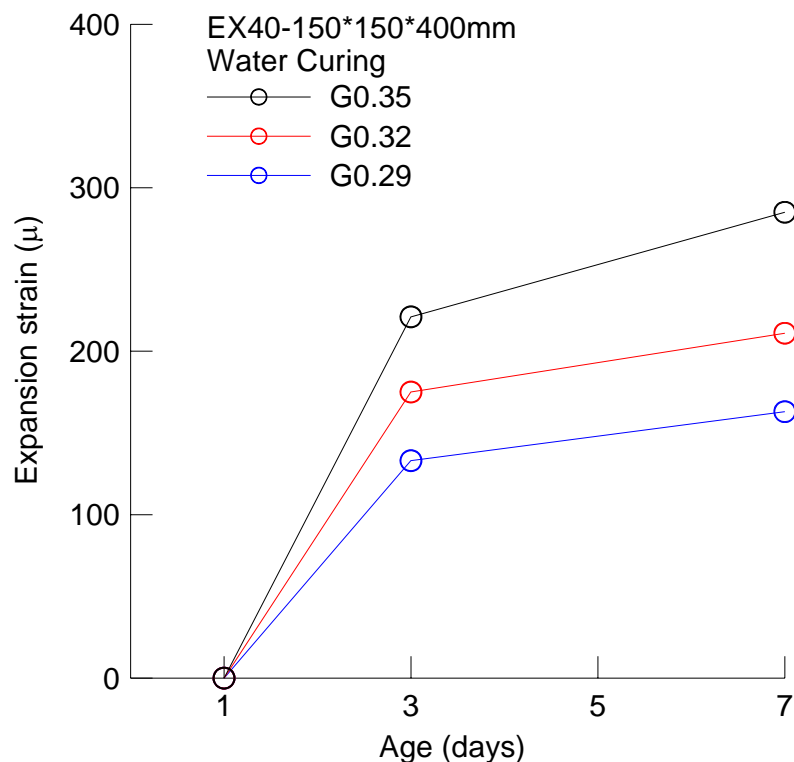


Fig.-4.4 Relationship of expansion strain and age for different amount of coarse aggregate (EX40)

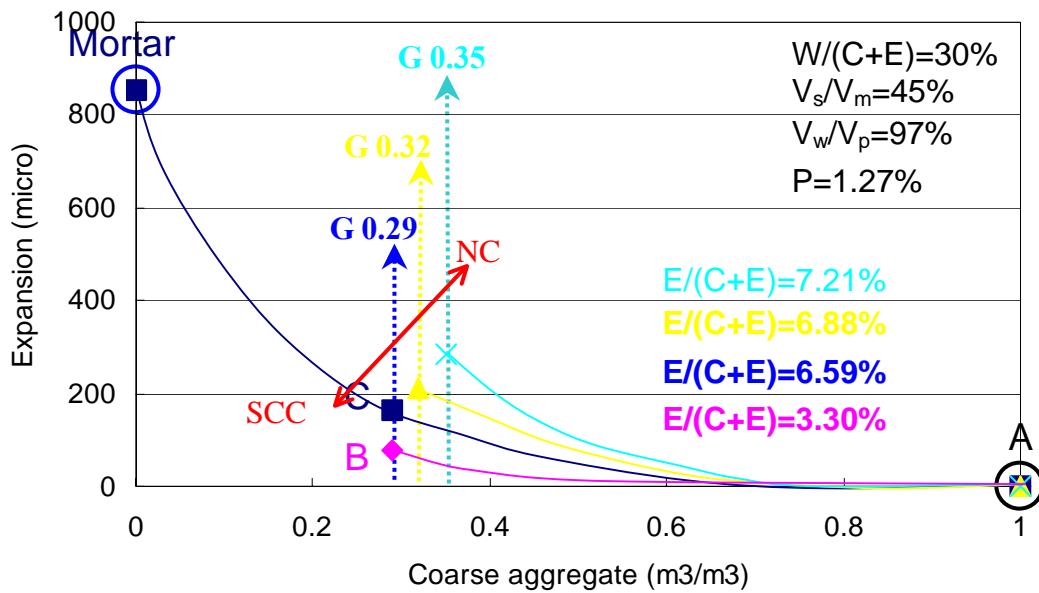


Fig.-4.5 Relationship of expansion strain and the amount of coarse aggregate

As shown in **Fig.-4.5**, when the volume of coarse aggregate was equal to 1.0 m^3/m^3 , the expansion strain was assumed to be zero (**A point**). In the case of $E/(C+E)$ equal to 6.59%, the relationship of expansion strain and coarse aggregate was revealed as the blue curve. Besides, according to the previous explanation, in the case of $E/(C+E)$ equal 6.59% (blue line), the theoretical expansion strain when coarse aggregate was equal to $0.29\text{m}^3/\text{m}^3$ should be 71% of the mortar expansion, about 603.5μ . ($850 \mu * 0.71 = 603.5 \mu$) However, the experimental result was only around 1/3 of the theoretical expansion which could prove that the existence of coarse aggregate in expansive concrete was one kind of resistant force to expansion.

Moreover, as the volume of coarse aggregate equal to $0.29 \text{ m}^3/\text{m}^3$, the expansion strain increased when $E/(C+E)$ increased from 3.30% to 6.59% (**B point** to **C point**). Comparing the mixing proportion of B and C point, the only one difference was $E/(C+E)$. That was to say that the increase of $E/(C+E)$ was the only reason to explain the increase of expansion strain. And it was revealed that the dispersion density of expansive agent to total powder ($E/(C+E)$) was positively proportional to expansion strain. From the experimental results, it was revealed that the expansion would be reduced on the design direction of SCC. Even if the amount of total aggregate was considered, it still revealed the same tendency. (**Fig.-4.6**) That is to say that the efficiency of expansive agent reduced on the application of SCC.

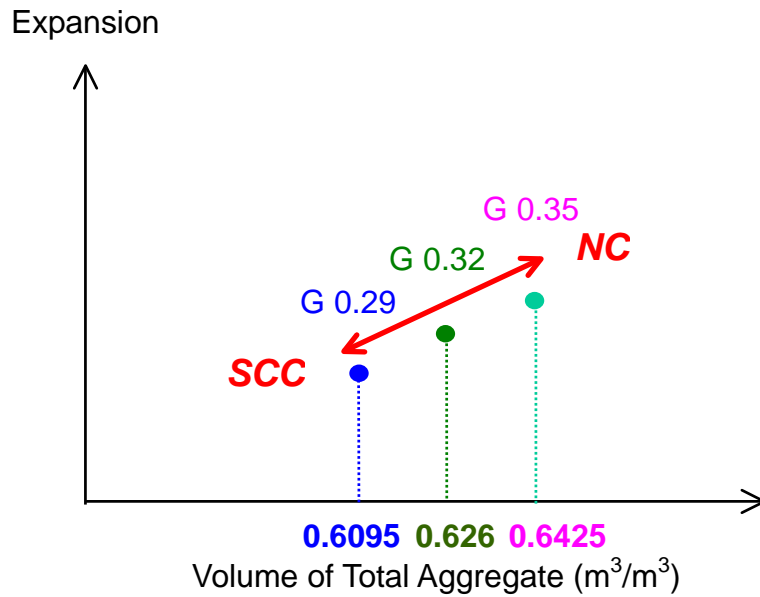


Fig.-4.6 Relationship of expansion strain and the amount of total aggregate

4.4 Summary

- ◆ According to the difference of theoretical expansion strain and experimental result, the role of coarse aggregate in expansive concrete was proved as one kind of resistant force on expansion. Therefore, if the value of $E/(C+E)$ were same, the expansion strain would decrease with the increase of coarse aggregate. And the relationship of expansion strain and coarse aggregate was curve depending on the value of $E/(C+E)$.
- ◆ As same weight of expansive agent was employed for SCC's mix proportions with different amount of coarse aggregate, the expansion strain reduced with the reduce of coarse aggregate. This phenomenon was explained by the ratio of expansive agent to total powder, $E/(C+E)$. Since as the volume of coarse aggregate reduced, the dispersion density of expansive agent in paste would be decreased as the same time. Therefore, though the amount of coarse aggregate reduced, the expansion strain still reduced. That is to say that the expansion of SCC using expansive agent was lesser than the case of conventional concrete. In another words, it was to say that the efficiency of expansive agent reduced on the application of SCC.

CHAPTER 5

EXPANSIVE CHARACTERISTICS OF SELF-COMPACTING CONCRETE USING LIMESTONE POWDER

5.1 Introduction

According to the result of Chapter 2, due to the low water-to-ratio character of SCC, water in the specimen was not enough for the hydration of expansive agent under sealed curing. Then crack occurred after the specimen was dried due to the insufficient expansion strain. It was revealed the efficiency of expansive agent was reduced on the application of SCC under sealed curing. However, practical curing condition in construction site is quite close to sealed curing situation. Therefore, how to increase the efficiency of expansive agent became the important issue.

With regard to SCC, sufficient viscosity was indispensable to avoid material segregation. Therefore, a large amount of cement was used in SCC. However, it resulted in the increase of the accompanied hydration heat and autogeneous shrinkage during hydration process. This is the defect of SCC. In order to solve this problem, low heat cement was used to reduce the hydration heat. In addition, limestone powder was often used to replace some part of cement as well.

In this chapter, limestone powder was employed to be the countermeasure to enhance the efficiency of expansive agent.

5.2 Experimental Procedures

5.2.1 Materials and Mix Proportions

The materials in use and the mix proportions were shown in **Table-5.1** and **Table-5.2**. The dosage of expansive agent was fixed at 20kg/m^3 and limestone powder was used to replace cement 20% and 40% by volume. In this experiment, the addition of expansive agent and limestone powder can't decrease the workability of SCC. It means the requirement of the mix proportions is all mix proportions have to possess good workability. By adjusting the dosage of SP, good workability could be achieved. And the dosage of SP was reduced as the replacement ratio of limestone powder increased. The result of flowability test was shown in **Table-5.3** and all mix

proportions showed the good workability.

Table-5.1 Materials used in experiment

Cement	C	Low Heat Cement: Specific gravity: 3.22
Limestone powder	LS	Specific gravity: 2.71
Expansive agent	E	CSA System: Specific gravity: 3.16
Admixture	SP	SP-M: Polycarboxylic acid-based AE HWRA
Fine aggregate	S	Crushed sand (C.S.): Specific gravity: 2.66 Sea sand (S.S.): Specific gravity: 2.60
Gravel	G	Specific gravity: 2.70
Steel		Es: 210 kN/mm ²

Table-5.2 Mix proportions of experiment

No.	W/P%	W/(C+E)%	W	C	LS	E	S	G	SP
			Unit: kg/m ³						
EX20LS0%	27.2	27.2	173	615	0	20	796	766	8.10
EX20LS20%	27.5	33.3	171	493	108	20	796	766	7.30
EX20LS40%	27.8	43.3	169	370	217	20	796	766	6.68

Table-5.3 Result of flowability test

	Slumpflow
EX20LS0%	600*610 mm
EX20LS20%	640*650 mm
EX20LS40%	630*640 mm

As showed in **Fig.-5.1**, one-axial restraint specimen was prepared. The deformed bar D19 was installed in the center of the cross-section and the restraint steel ratio was 1.27%.

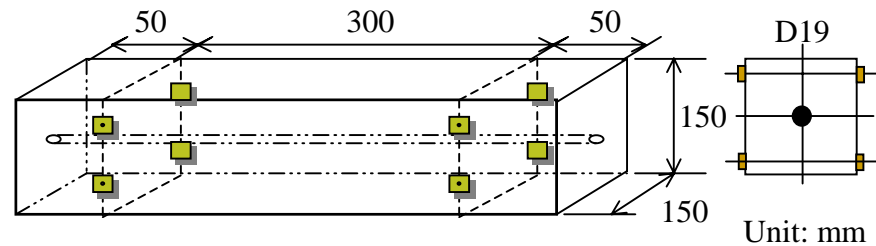


Fig.-5.1 Outline of specimen

5.2.2 Measurement and Curing

The mold was removed at the age of 1 day. Then, specimens were sealed with double layers of polyethylene. In the meantime, contact chips were attached at 50 mm away from the edge of the member. All sealed specimens were placed in the temperature-controlled room at 20°C and RH = 60% and measured from the spacing of contact chips regularly until 28 day. Then seal was removed and all specimens were put in the same environment to observe the crack.

5.3 Experimental Results and Discussion

5.3.1 Influence of Replacement of Limestone Powder on Expansion Strain

The experimental result was shown in **Fig.-5.2**. It was revealed that the expansion strain increased as the replacement ratio of limestone powder increased. In **Fig.-5.3** and **Fig.-5.4**, as the replacement ratio of limestone powder was 20%, the expansion strain was increased about 10%. As the replacement ratio of limestone powder was increased to 40%, the expansion strain was greatly increased above 50%.

In **Fig.-5.5**, the expansion strain was calculated from expansion energy method ($p=0.95\%$). It was very clear that the expansion strain was increased substantially when replacement ration of limestone powder was increased from 20% to 40%. Besides, when the replacement ratio was 40%, the expansion strain at 28 day was more than 150μ , the minimum recommended expansion strain of JSCE.

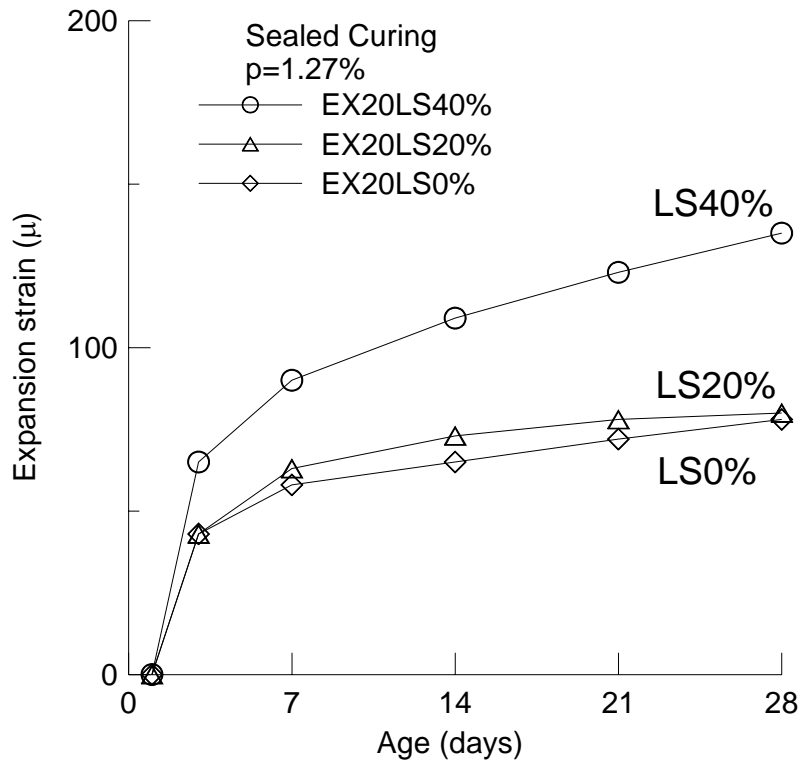


Fig.-5.2 Relationship between expansion strain and age for different replacement ratio of limestone powder at p=1.27% (Sealed Curing)

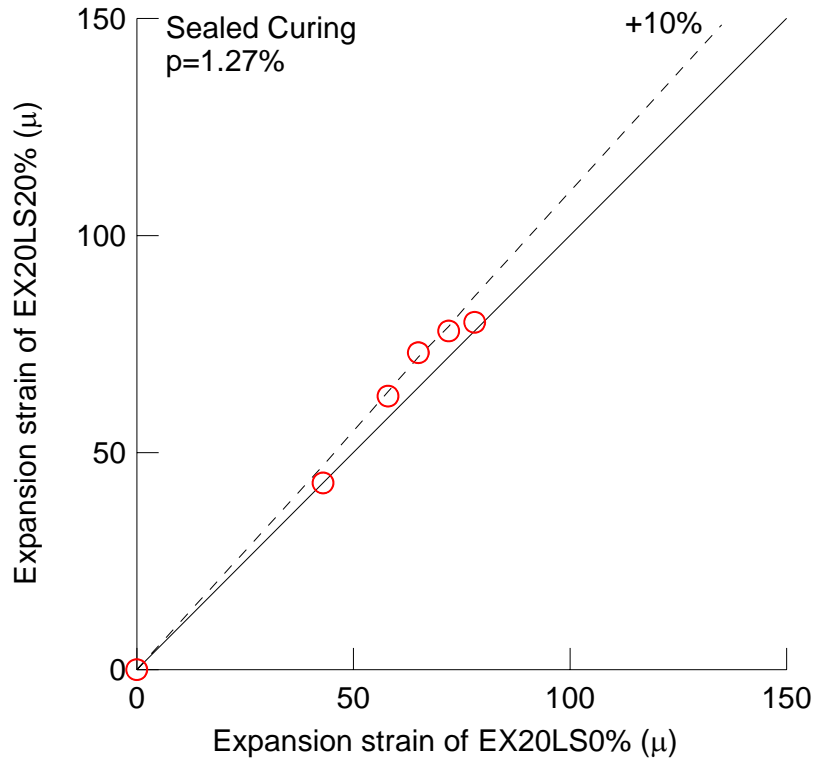


Fig.-5.3 Relationship of expansion strain between EX20LS0% and EX20LS20% at p=1.27% (Sealed Curing)

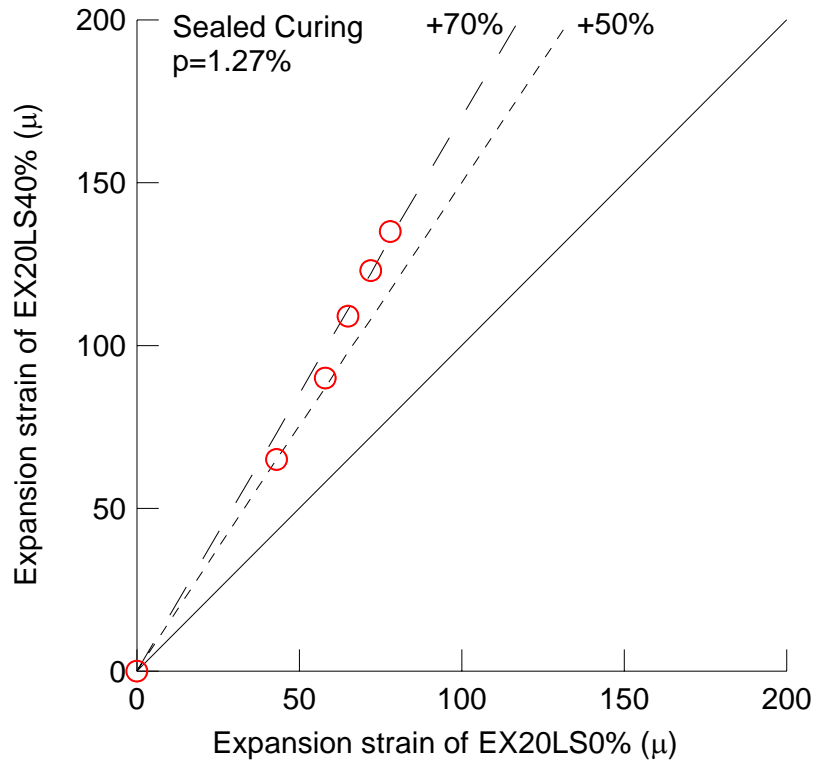


Fig.-5.4 Relationship of expansion strain between EX20LS0% and EX20LS40% at p=1.27% (Sealed Curing)

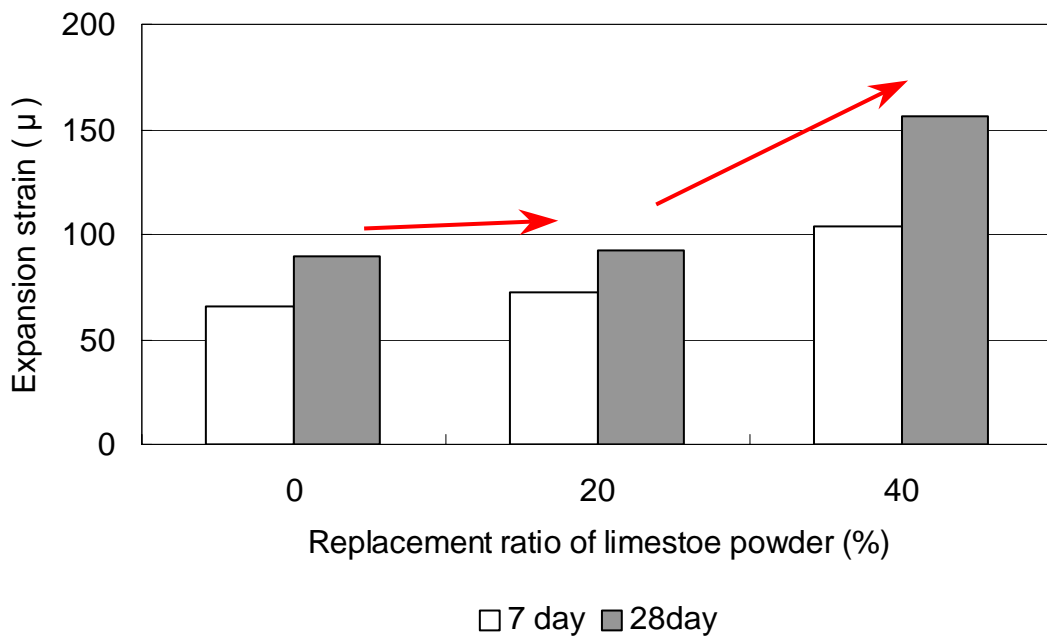


Fig.-5.5 Relationship between expansion strain and different replacement ratio of limestone powder at p=0.95%

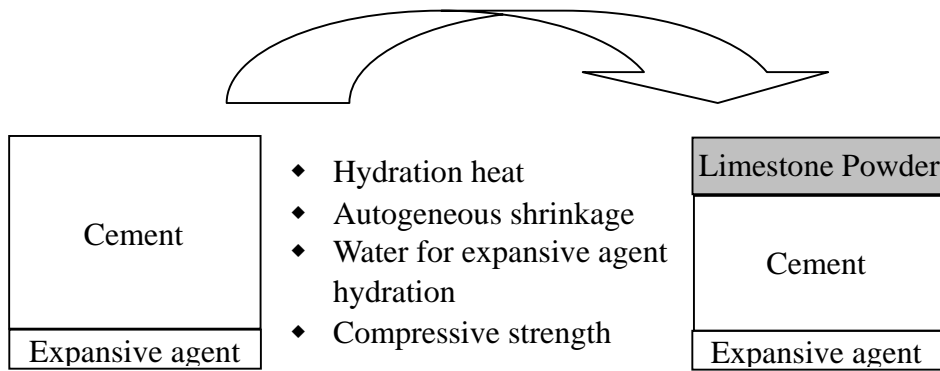


Fig.-5.6 Effect of utilization of limestone powder

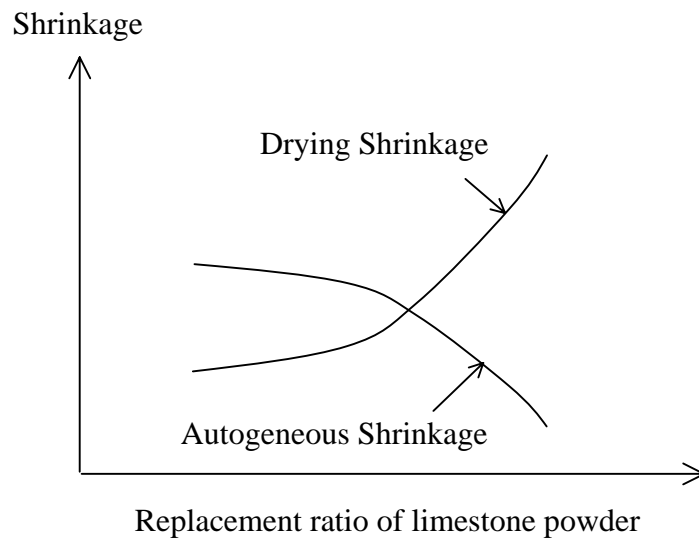


Fig.-5.7 Relationship between the variation of autogeneous and drying shrinkage as the replacement of limestone powder increased

The effects of utilization of limestone powder were represented by **Fig.-5.6**. To replace cement by limestone powder, the amount of cement was reduced. Therefore, not only the thermal shrinkage but also autogeneous shrinkage was reduced, although the drying shrinkage might be increased. (**Fig.-5.7**) In addition, water for the hydration of expansive agent was increased, especially under sealed curing situation. From the experimental result, in the case of 40% replacement ratio of limestone powder, expansion strain at 28 day under sealed curing could achieve about 150μ , especially only 20kg/m^3 of expansive agent was employed.

The expansion strain of EX20LS0% and EX20LS20% was only about 60μ at 7

day. Even at the age of 28 day, the expansion strain were still only about 80μ . Therefore, after the specimen was dried at 28 day, crack was occurred in both of the mix proportions due to the insufficient expansion. With regard to EX20LS40%, crack was not perceived after the specimen was dried, since the expansion strain at 28 day was close to 150μ . It was revealed the efficiency of expansive agent was greatly improved by the employment of limestone powder.

5.3.2 Influence of Replacement of Limestone Powder on Compressive Strength

Although the addition of limestone powder was favorable to shrinkage compensation and cracking resistance, there was still one defect. If large amount of cement was replaced by limestone powder, the compressive strength will decrease substantially. (Fig.-5.8) Therefore, compressive strength of mix proportion was necessary to check when the replacement ratio was decided. The compressive strength of three mix proportions in this experiment was shown in Fig.-5.9.

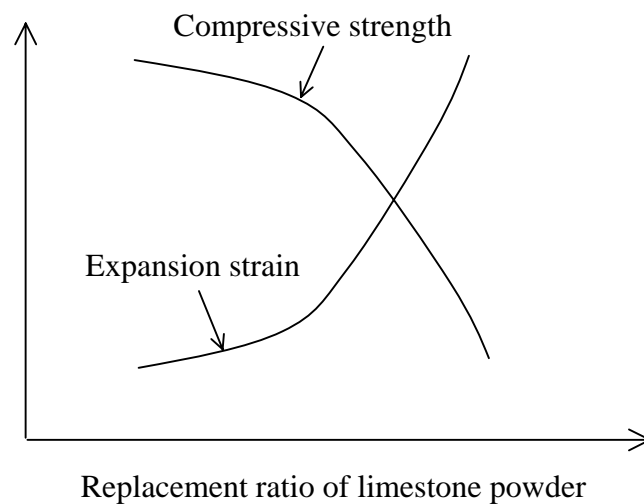


Fig.-5.8 Variation of expansion strain and compressive strength with the replacement of limestone powder

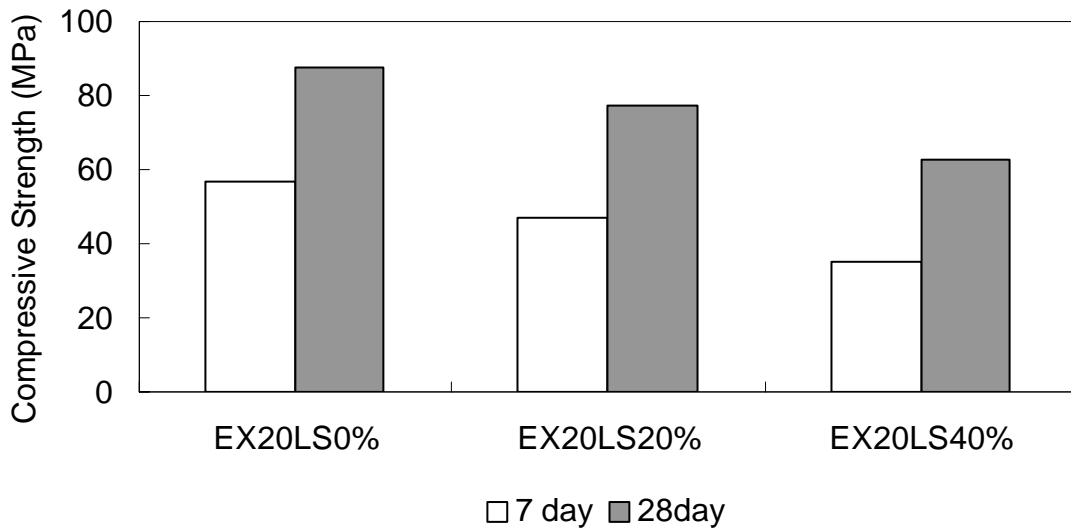


Fig.-5.9 Relationship between compressive strength and different replacement ratio of limestone powder at the different age

5.4 Summary

- ♦ Limestone powder was employed to be the countermeasure to enhance the efficiency of expansive agent. From the experimental result, to replace cement by limestone powder was proved to be contributive to the compensation for the shrinkage and crack was not occurred, although the drying shrinkage might be increased. In the case of the utilization of limestone powder, the expansion strain for the same dosage of expansive agent was increased due to the increase of the dispersion density of expansive agent in paste. And the dosage of expansive agent to achieve the same expansion with the conventional concrete was reduced as well. From the experimental result, when cement was replaced by limestone powder 40% by volume, the dosage of expansive agent could be reduced to 20kg/m^3 without crack under sealed curing. That is to say that the shortage of water in SCC using expansive agent can be solved by the utilization of limestone powder.
- ♦ Due to the replacement of limestone powder, the amount of cement was reduced. It resulted in the decrease of compressive strength. In addition, as the replacement ratio increased, the decrease of compressive strength was increased substantially. Therefore, special attention has to be paid to the compressive strength when limestone powder is used.

CHAPTER 6

EXPANSIVE CHARACTERISTICS OF SELF-COMPACTING CONCRETE USING EXPANSIVE AGENT UNDER MULTI-AXIAL RESTRAINT

6.1 Introduction

As mentioned in Chapter 1, the expansive characteristics of expansive concrete differ greatly depending on the mix proportion and the curing. In addition, the degree of the restraint has a significant influence as well. However, most of the past researches on expansive concrete were carried out for conventional concrete under one-dimensional restraint. In this chapter, the expansive characteristics of SCC with expansive agent under multi-axial restraint were investigated experimentally.

6.2 Experimental Procedures

6.2.1 Materials and Mix Proportions

The experiment was divided into two parts with the different size of specimen. In addition, the restraint steel ratio of two parts was different as well. One was used to be the “**seed experiment**” to calculate the friction coefficient of 3-dimensional composite model. The other one was used to compare with the estimation of 3-dimensional composite model. In the first part, the size of specimen was 150 × 150 × 400 mm and in the second part the size was 150 × 400 × 400 mm. The materials in use and mix proportions were as same as the materials and mix proportions in Chapter 2 shown in **Table-2.1** and **Table-2.2**. EX40 was the mix proportion of the first part and EX20 and EX40 were tested in the second part.

In the first part, four types of specimens shown in **Fig.-6.1** were prepared. The steel was installed in axial direction, lateral directions and both of axial and lateral directions of specimen, named r1, r2 and r3 specimen respectively. In addition, the concrete specimen without any restraint steel, named r0, was prepared as well. The axial and lateral steel were D19 and D13 respectively.

In the second part, three types of specimens shown in **Fig.-6.2** were prepared. The steel was installed in axial direction and both of axial and lateral directions of specimen, named R1 and R2 specimen respectively. In addition, the concrete

specimen without any restraint steel, named R0, was prepared as well. Both of axial and lateral steel were D16.

6.2.2 Measurement and Curing

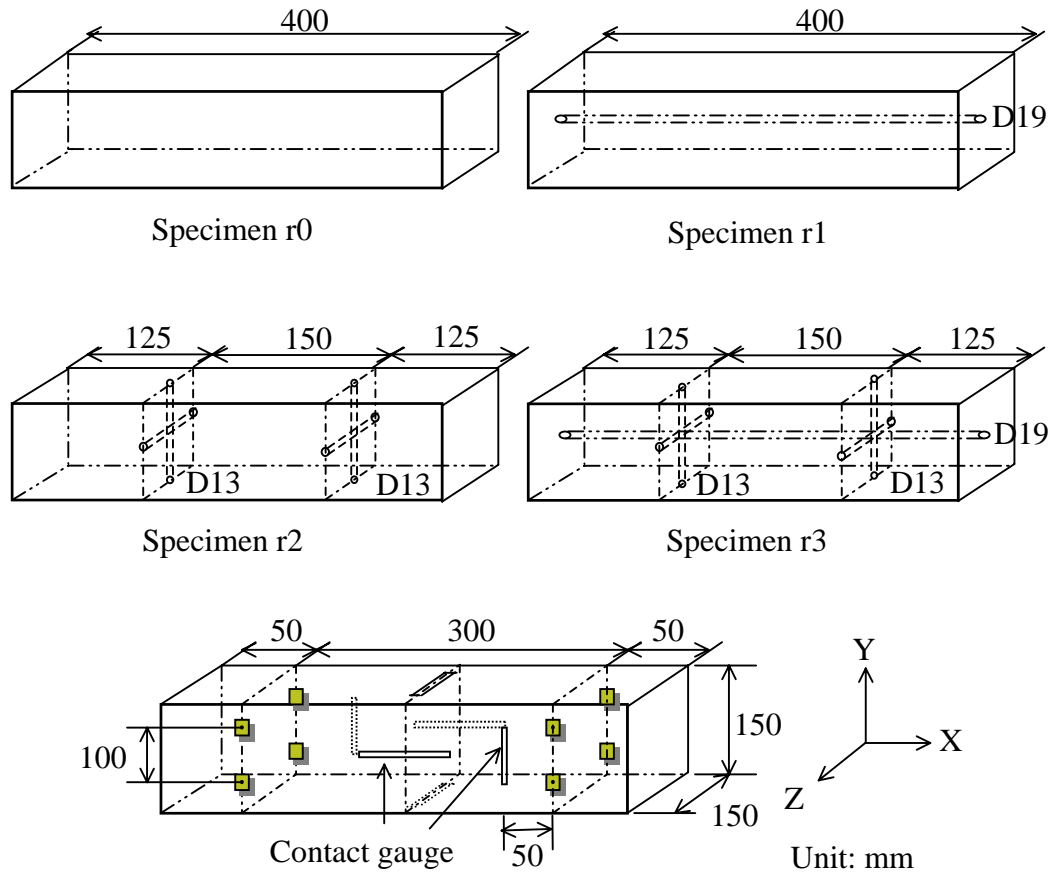


Fig.-6.1 Outline of specimen (the first part)

In the first part, the mold was removed at the age of 1 day. All the specimens were sealed with double layers of polyethylene. In the meantime, contact chips were attached at 50 mm away from the edge of the member. Since the lateral spacing of the contact chips was 100 mm only, considering the measurement accuracy, contact gauges were attached on the concrete surface to measure the strain in three directions as well. All the sealed specimens were placed in the temperature-controlled room at 20°C and RH = 60% and measured until the age of 28 day. Then seal was removed and all the specimens were put in the same environment to observe the crack. (Fig.-6.1)

In the second part, the mold was removed at the age of 1 day. Since both of water

curing and sealed curing were adapted, therefore, two specimens were prepared for each type of specimen. The seal of the sealed specimen was removed and the water-curing specimen was moved out of water at the age of 7 day. Then all specimens were placed in the temperature-controlled room to observe the crack. In addition, the mold gauge was installed before concrete was cast and the data was stored in the computer via data logger. (Fig.-6.2)

The list of specimen and curing was shown in Table-6.1.

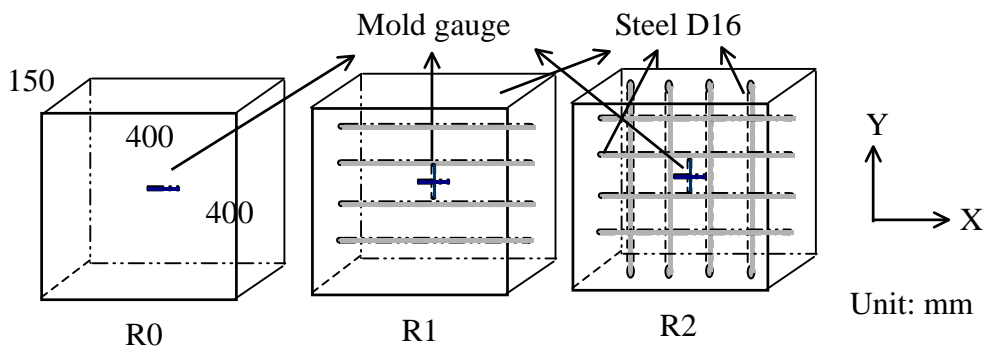


Fig.-6.2 Outline of specimen (the second part)

Table-6.1 List of the specimen and curing condition

	Restraint steel ratio			Curing
	p_x	p_y	p_z	
r0	0%	0%	0%	Sealed curing until 28 day
r1	1.27%	0%	0%	Sealed curing until 28 day
r2	0%	0.4223%	0.4223%	Sealed curing until 28 day
r3	1.27%	0.4223%	0.4223%	Sealed curing until 28 day
R0	0%	0%	0%	Sealed curing until 7 day Water curing until 7 day
R1	1.324%	0%	0%	Sealed curing until 7 day Water curing until 7 day
R2	1.324%	1.324%	0%	Sealed curing until 7 day Water curing until 7 day

6.3 Experimental Results and Discussion

6.3.1 Mutual Influence of the Restraint and the Expansion in the Perpendicular Direction

First Part

The experimental results of the first part were shown in **Fig.-6.3** and **Fig.-6.4**. Considering the effect of lateral restraint on the axial direction (X direction), the axial expansion strain of Specimen r0 was used to compare with Specimen r2 and Specimen r1 was used to compare with Specimen r3 respectively. In the both of cases, the axial expansion strain was reduced about 10% as lateral steel was installed. (**Fig.-6.5** and **Fig.-6.6**)

On the other hand, considering the effect of axial restraint on the lateral expansion (Y direction), the lateral expansion strain of Specimen r0 was used to compare with Specimen r1 and Specimen r2 was used to compare with Specimen r3. As same as the above case, in the both of cases, the lateral expansion strain was reduced about 10% as axial steel was installed. (**Fig.-6.7** and **Fig.-6.8**)

Second Part

The experimental results of the second part were shown from **Fig.-6.9** to **Fig.-6.12**. The expansion strain of R0-X (Specimen R0 in X direction) was used to compare with R1-Y and R1-X was used to compare with R2-X respectively. (The expansion strain of R0-Y was regarded as same as the expansion strain of R0-X) It was revealed the same tendency with the first part that expansion strain was reduced due to the installation of lateral restraint for EX40 and EX20 under both of the water and sealed curing. In the case of EX20 under sealed curing, the tendency was not so clear which might result from insufficient water supply.

Comparing R1 and R2 specimen of EX40 under water curing, the axial expansion strain (along X direction) was reduced about 10% as lateral steel was installed. (**Fig.-6.13**) Moreover, comparing R0 and R1 specimen, the expansion strain along Y direction was reduced about 40% as the installation of restraint steel in X direction. (**Fig.-6.14**) It was because there was no restraint in Y direction for specimen R0 and the expansion could be regarded as free expansion. Therefore, as restraint steel was installed in X direction, the expansion strain along Y direction was greatly reduced.

From the experimental results of two parts, it was clear that not only the axial expansion but also the expansion in the other two directions was reduced when the restraint was installed in the axial direction. In another word, the expansion was reduced in all the directions; even the restraint was only installed in one direction.

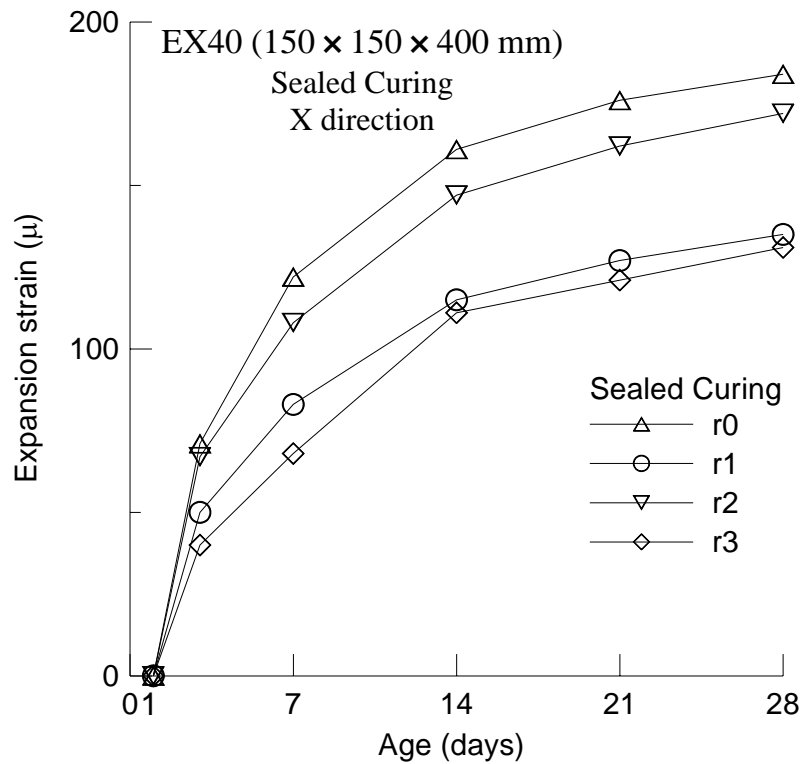


Fig.-6.3 Relationship between expansion strain and age under different restraint in axial (X) direction (EX40-Sealed Curing-150 × 150 × 400 mm)

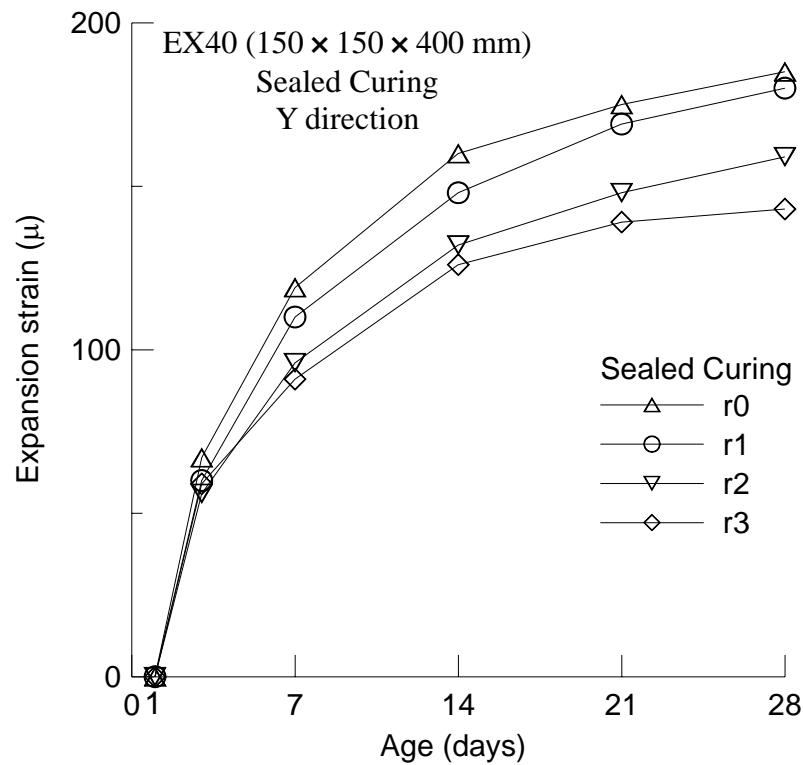


Fig.-6.4 Relationship between expansion strain and age under different restraint in lateral (Y) direction (EX40-Sealed Curing-150 × 150 × 400 mm)

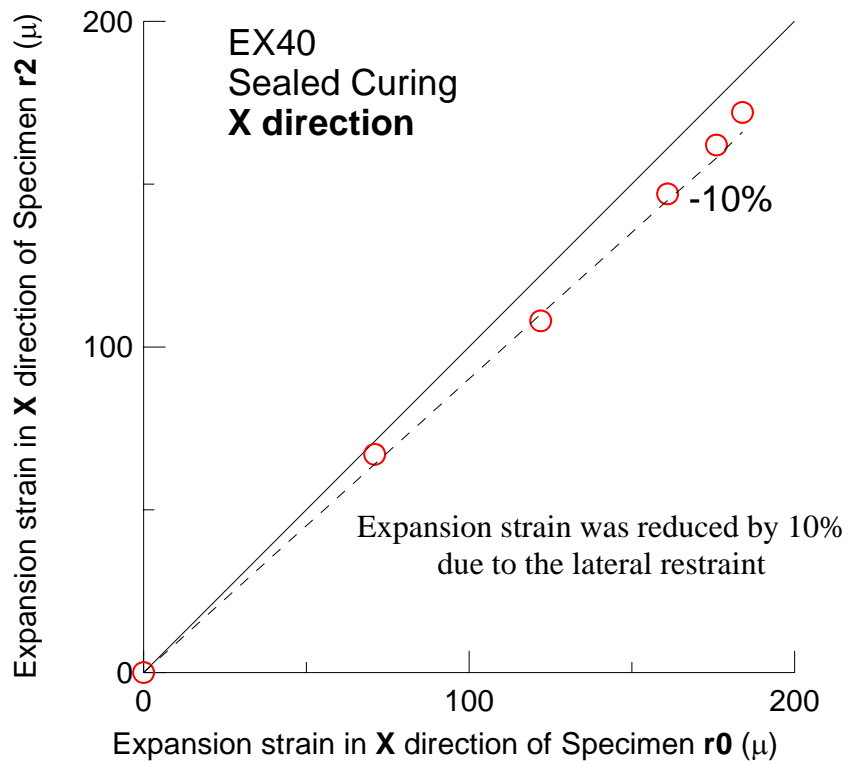


Fig.-6.5 Variation of expansion strain in the X direction between Specimen r0 and Specimen r2 (EX40-Sealed Curing-150 × 150 × 400 mm)

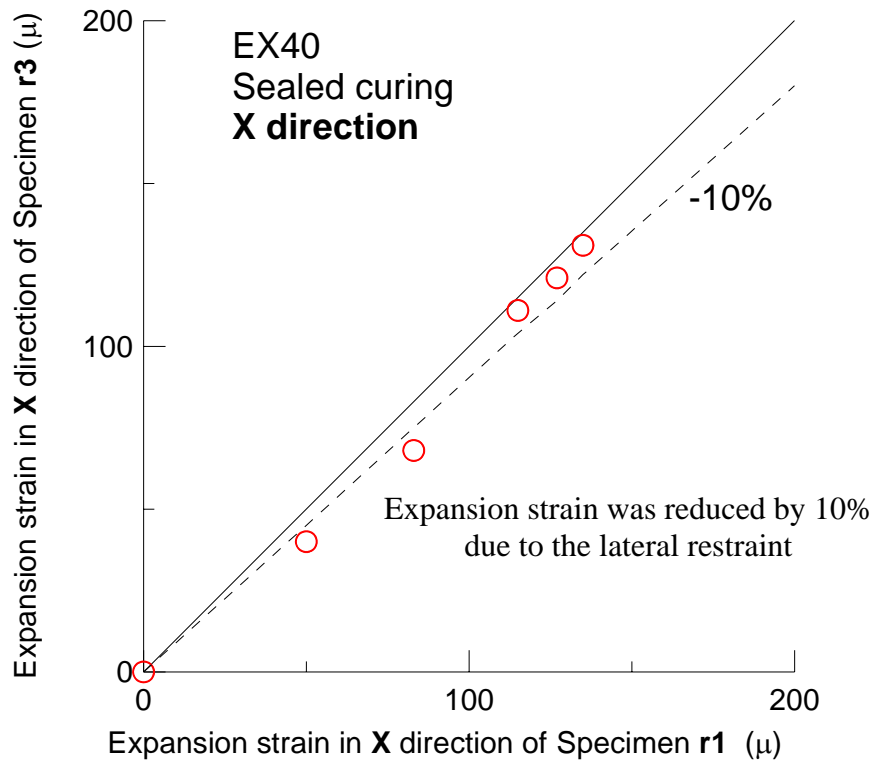


Fig.-6.6 Variation of expansion strain in the X direction between Specimen r1 and Specimen r3 (EX40-Sealed Curing-150 × 150 × 400 mm)

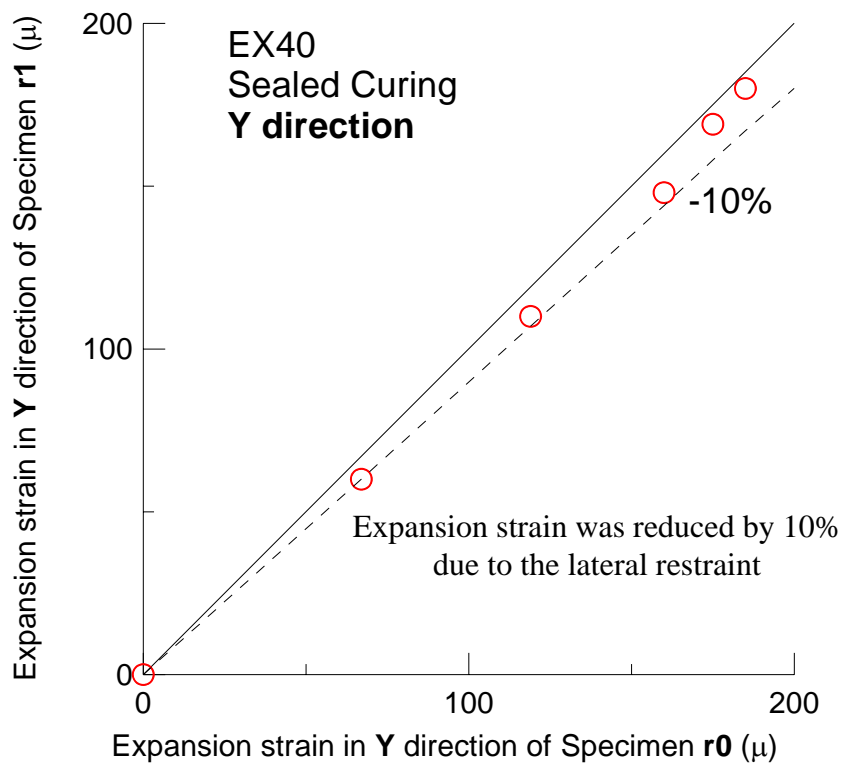


Fig.-6.7 Variation of expansion strain in the Y direction between Specimen r0 and Specimen r1 (EX40-Sealed Curing-150 × 150 × 400 mm)

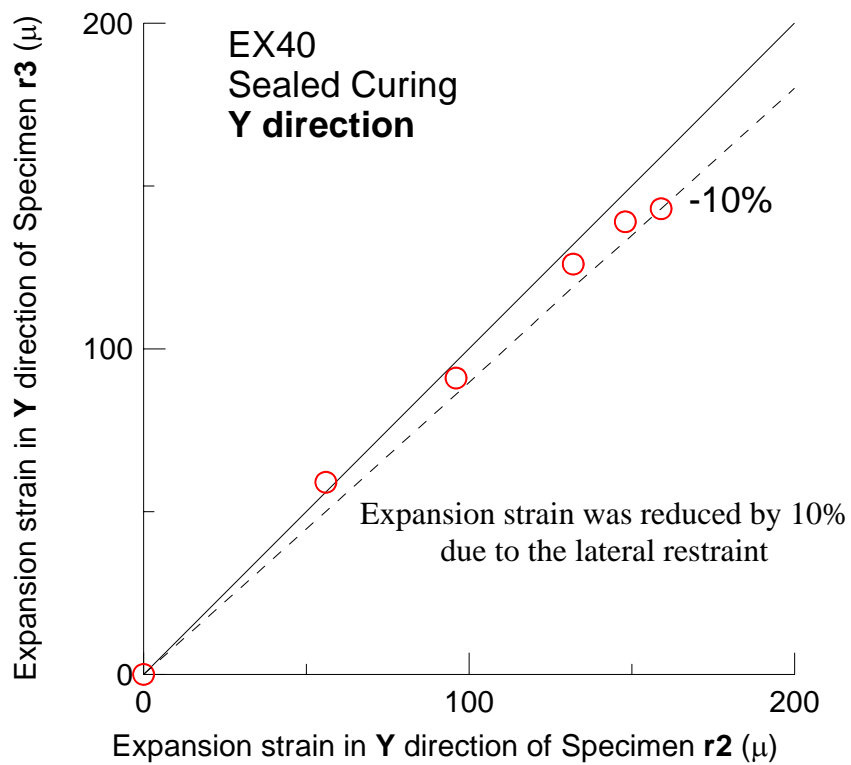


Fig.-6.8 Variation of expansion strain in the Y direction between Specimen r2 and Specimen r3 (EX40-Sealed Curing-150 × 150 × 400 mm)

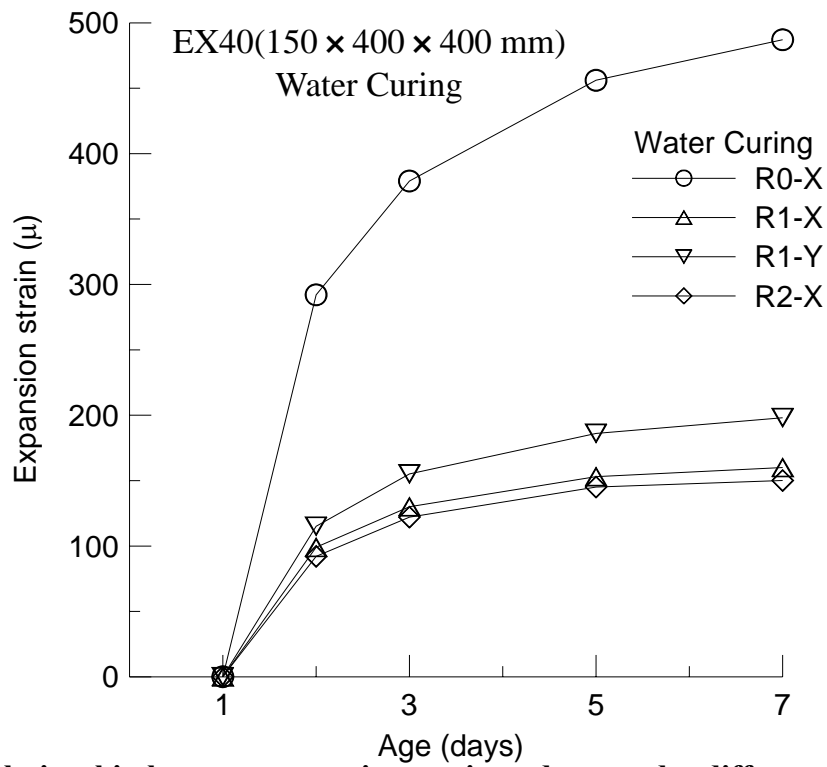


Fig.-6.9 Relationship between expansion strain and age under different restraint (EX40-Water Curing-150 × 400 × 400 mm)

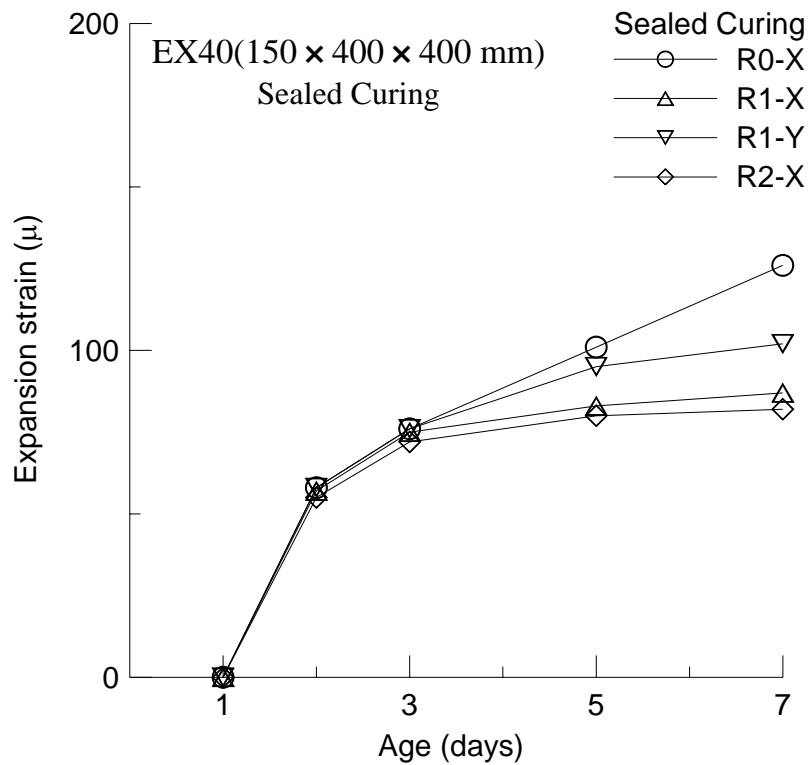


Fig.-6.10 Relationship between expansion strain and age under different restraint (EX40-Sealed Curing-150 × 400 × 400 mm)

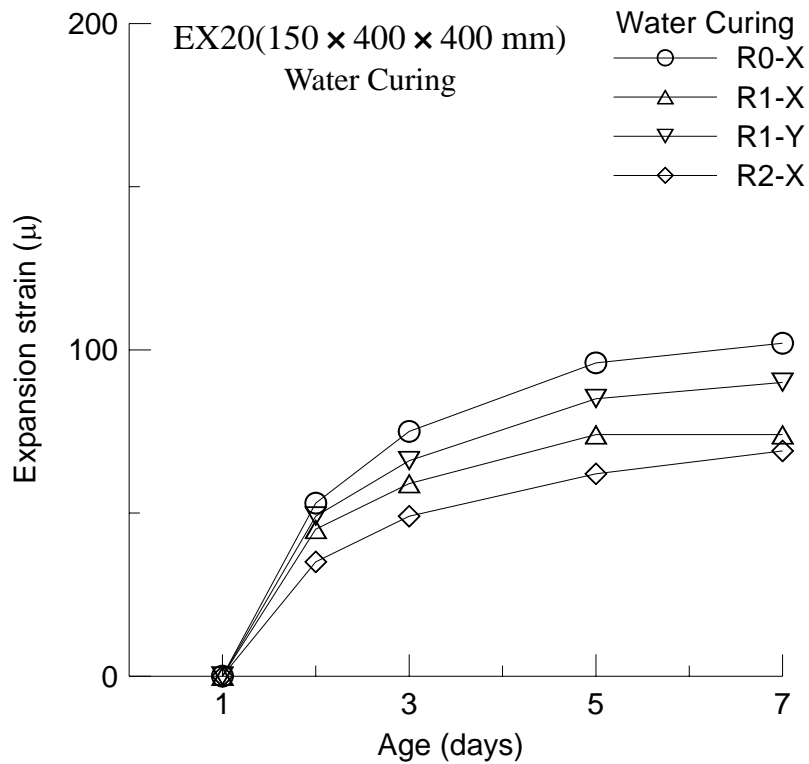


Fig.-6.11 Relationship between expansion strain and age under different restraint (EX20-Water Curing-150 × 400 × 400 mm)

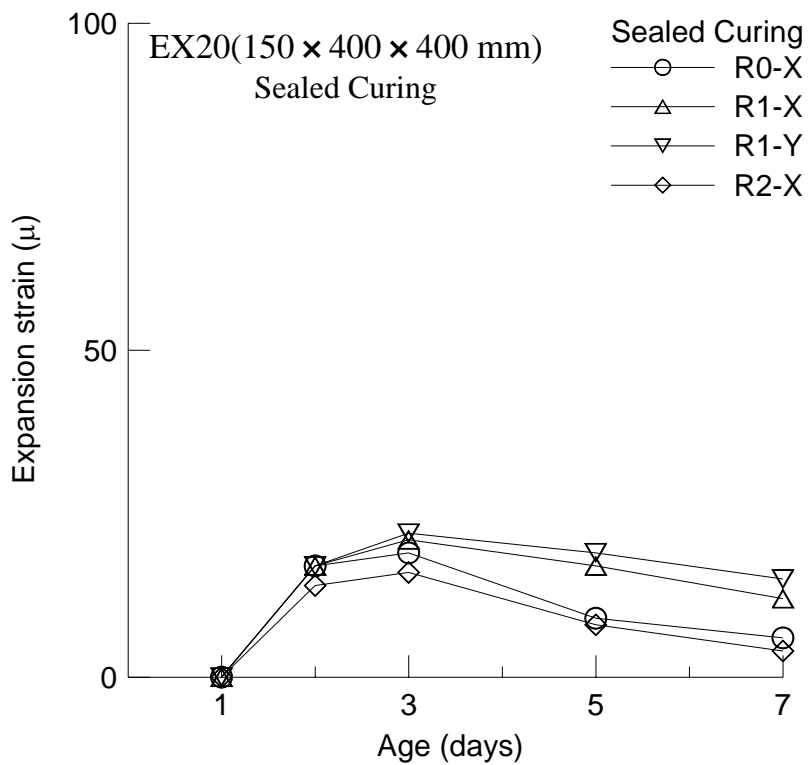


Fig.-6.12 Relationship between expansion strain and age under different restraint (EX20-Sealed Curing-150 × 400 × 400 mm)

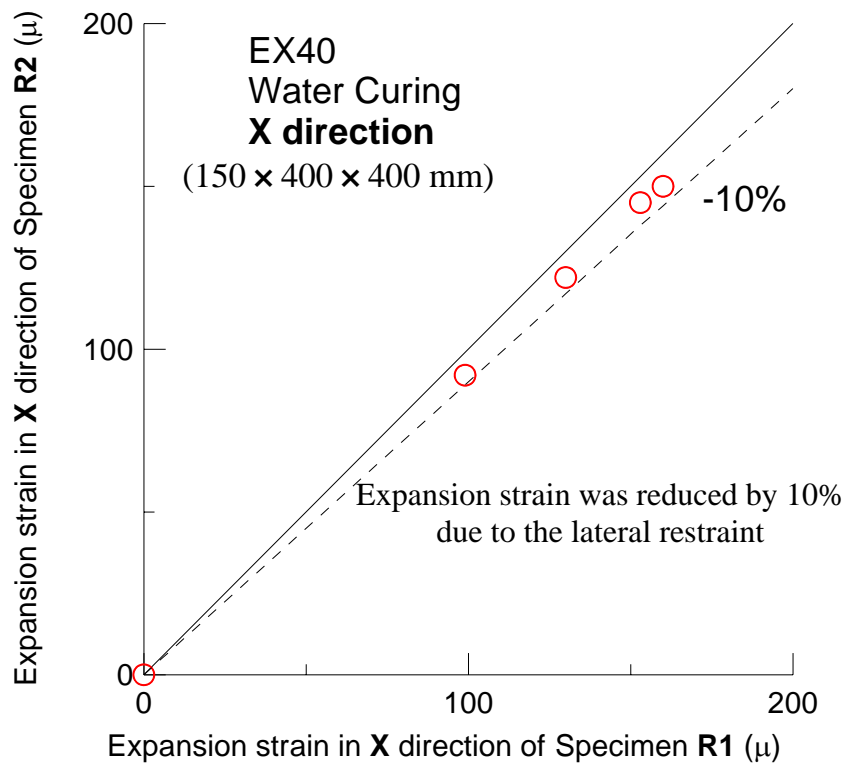


Fig.-6.13 Variation of expansion strain in the X direction between Specimen R1 and Specimen R2 (EX40-Water Curing-150 × 400 × 400 mm)

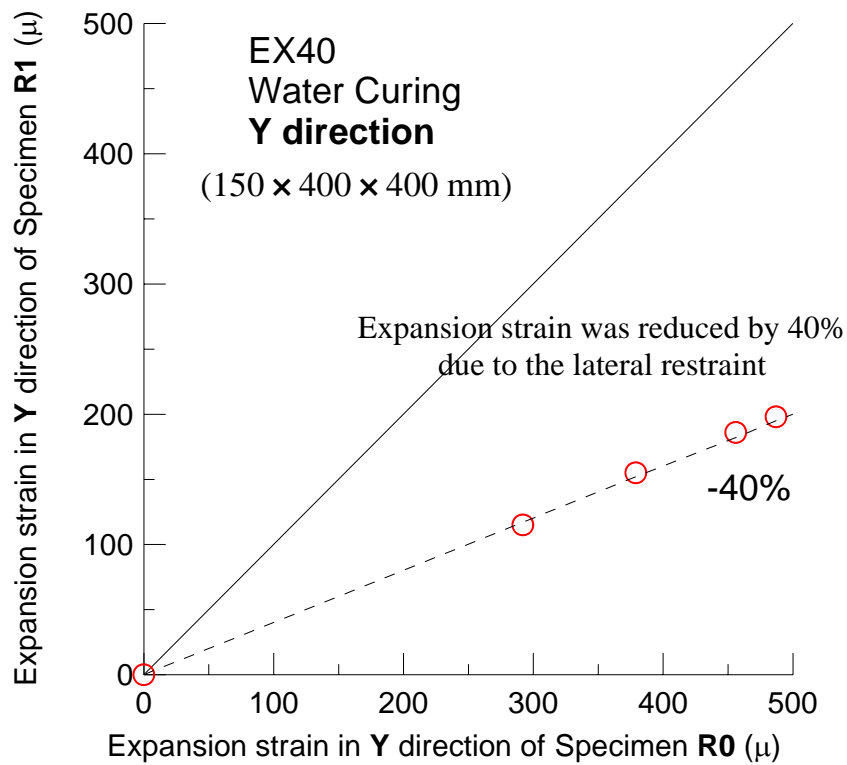


Fig.-6.14 Variation of expansion strain in the Y direction between Specimen R0 and Specimen R1 (EX40-Water Curing-150 × 400 × 400 mm)

6.3.2 Mechanism of the Lateral Restraint Effect on the Axial Expansion Strain

From the previous experimental result, it was revealed the expansion strain was reduced as the restraint was installed in the perpendicular direction. From the force viewpoint, there must generate some resistant force along the axial (X) direction. (Fig.-6.15) Since the restraint was installed in the perpendicular direction, friction was imagined to occur in concrete. Furthermore, considering in the early age, the hardness of coarse aggregate and mortar was different and therefore the weak interface was existed between coarse aggregate and mortar (Fig.-6.16) When the restraint was installed in lateral (Y) direction, the space of interface was compressed due to the chemical prestress and then friction occurred. Therefore, the expansion in X direction was reduced, since this friction was one kind of resistant force to the expansion in X expansion.

And this friction concept was reflected to the friction between expansion and compression elements in 3-dimension composite model. The friction was defined as the multiplication of the friction coefficient and normal stress on the interface of expansion and compression elements. And the friction coefficient was decided by the multi-axial restraint experimental result. (Fig.-6.17)

One-dimensional restraint along X direction



Two-dimensional restraint along X and Y direction

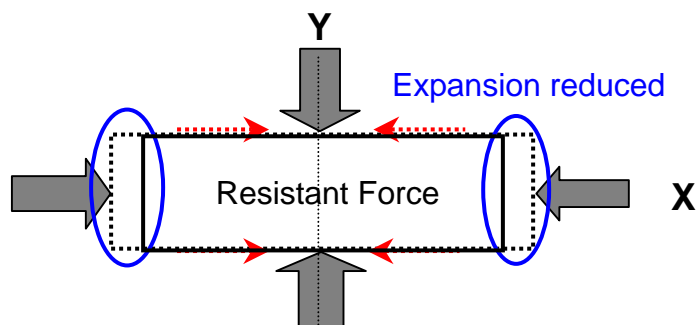


Fig.-6.15 Mechanism of the lateral restraint effect on the axial expansion strain-1

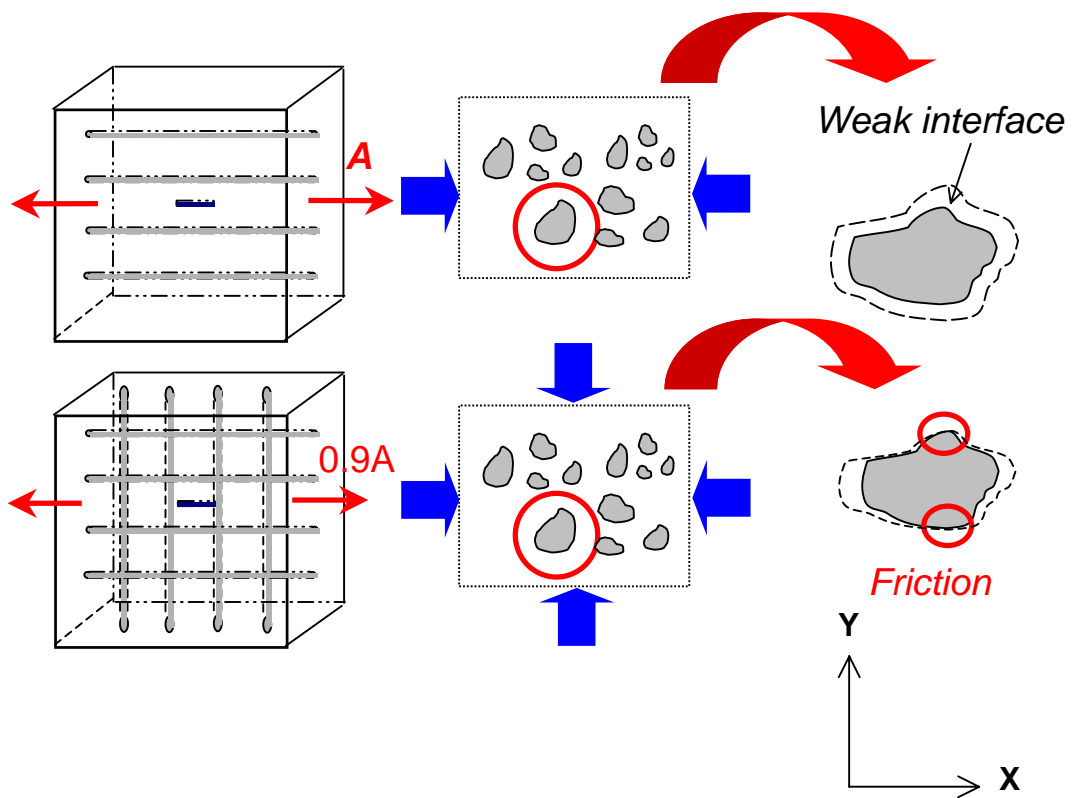


Fig.-6.16 Mechanism of the lateral restraint effect on the axial expansion strain-2

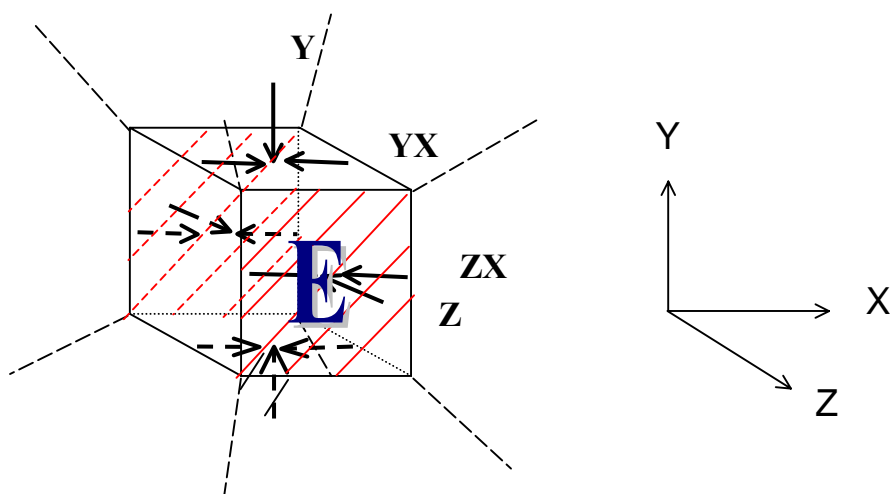


Fig.-6.17 Friction between expansion and tension element in three-dimensional composite model

6.3.3 Mortar Experiment to prove the Mechanism of the Lateral Restraint Effect on the Axial Expansion

As mentioned in 6.3.2, the friction occurred between coarse aggregate and mortar was assumed to be the reason of the decrease of axial expansion as the lateral restraint was installed. To prove this hypothesis, mortar experiment was carried out.

The materials in use and the mix proportions were shown in **Table-6.2** and **Table-6.3**. In order to prove the influence of coarse aggregate, the parameters of mortar were complete as same as the concrete mixing proportion, such as V_s/V_m and V_w/V_p . Moreover, the replacement ratio of expansive agent to total powder ($E/(C+E)$) was as same as the concrete mixing proportion as well. That was to say that the mortar in this experiment was completely as same as the mortar in the concrete experiment. Besides, paste experiment was carried out as well and the replacement ratio of expansive agent to total powder were set as 6.5% (as same as concrete and mortar experiment) and 1% respectively. As the dimension of specimen, steel restraint ratio and curing method (water curing until the age of 7 day) was set as same as the concrete experiment. (**Fig.-6.18**)

Table-6.2 Materials used in experiment

Cement	C	Low Heat Cement: Specific gravity: 3.24
Expansive agent	E	CSA System: Specific gravity: 3.20
Admixture	SP	SP-S: Polycarboxylic acid-based AE HWRA
Fine aggregate	S	Crushed sand (C.S.): Specific gravity: 2.60 Sea sand (S.S.): Specific gravity: 2.58
Steel		$E_s: 210 \text{ kN/mm}^2$

Table-6.3 Mix proportions of experiment

No.	W/(C+E)	V_s/V_m	V_w/V_p	$E/(C+E)$	W	C	E	S	SP
					Unit: kg/m^3				
Mortar	30%	45%	97%	6.5%	269	842	59	1166	11.7
Paste	30%	---	97%	6.5%	492	1537	107	0	3.3
Paste	30%	---	97%	1.0%	492	1628	16.4	0	3.3

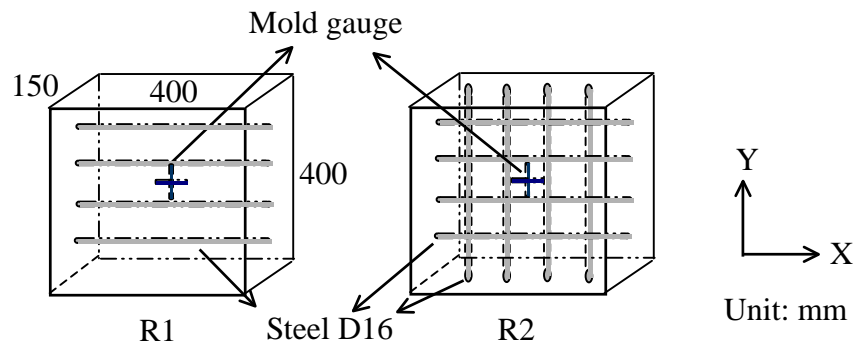


Fig.-6.18 Outline of specimen

The experimental results were shown in **Fig.-6.19** and **Fig.-6.20**. In the paste experiment, when replacement ratio of expansive agent ($E/(C+E)$) was 6.5%, the mold removed out automatically due to the excessive expansion. (**Photo-6.1** and **Photo-6.2**) And crack was observed to occur for both R1 and R2 specimen. (**Photo-6.3** and **Photo-6.3**) Therefore, the result of paste experiment in **Fig.-6.20** was the case of expansive agent replacement ratio equal to 1%.

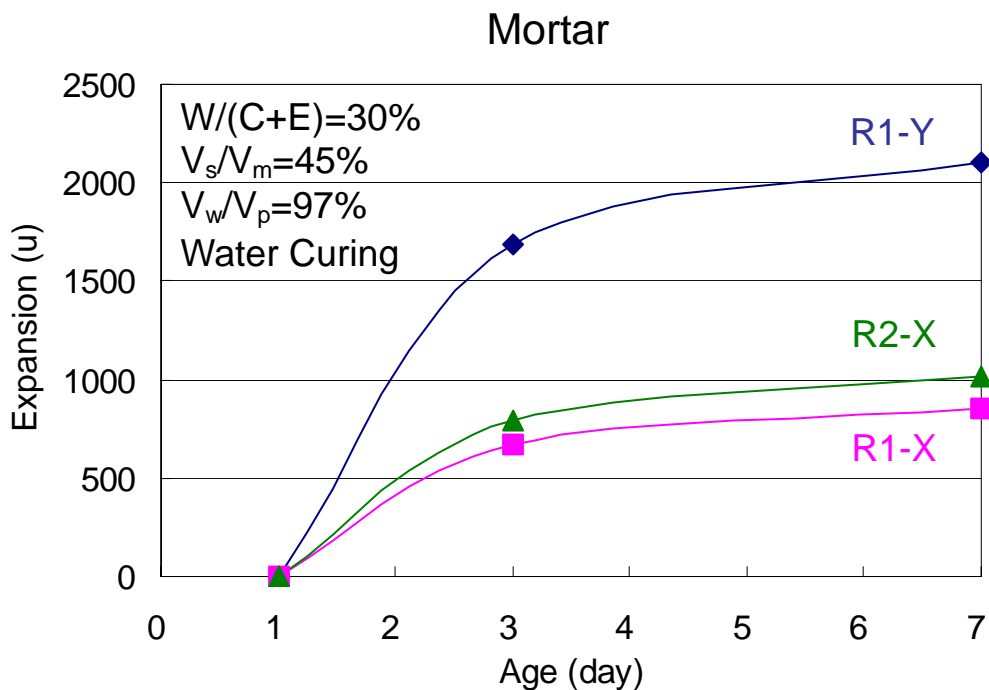


Fig.-6.19 Relationship between expansion strain and age under different restraint (Mortar experiment)

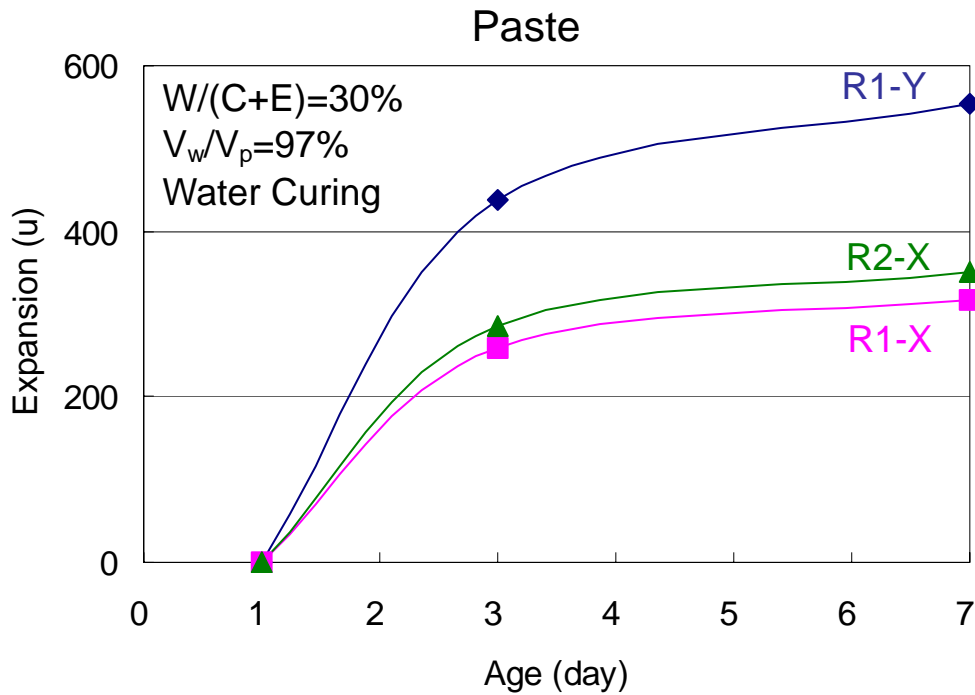
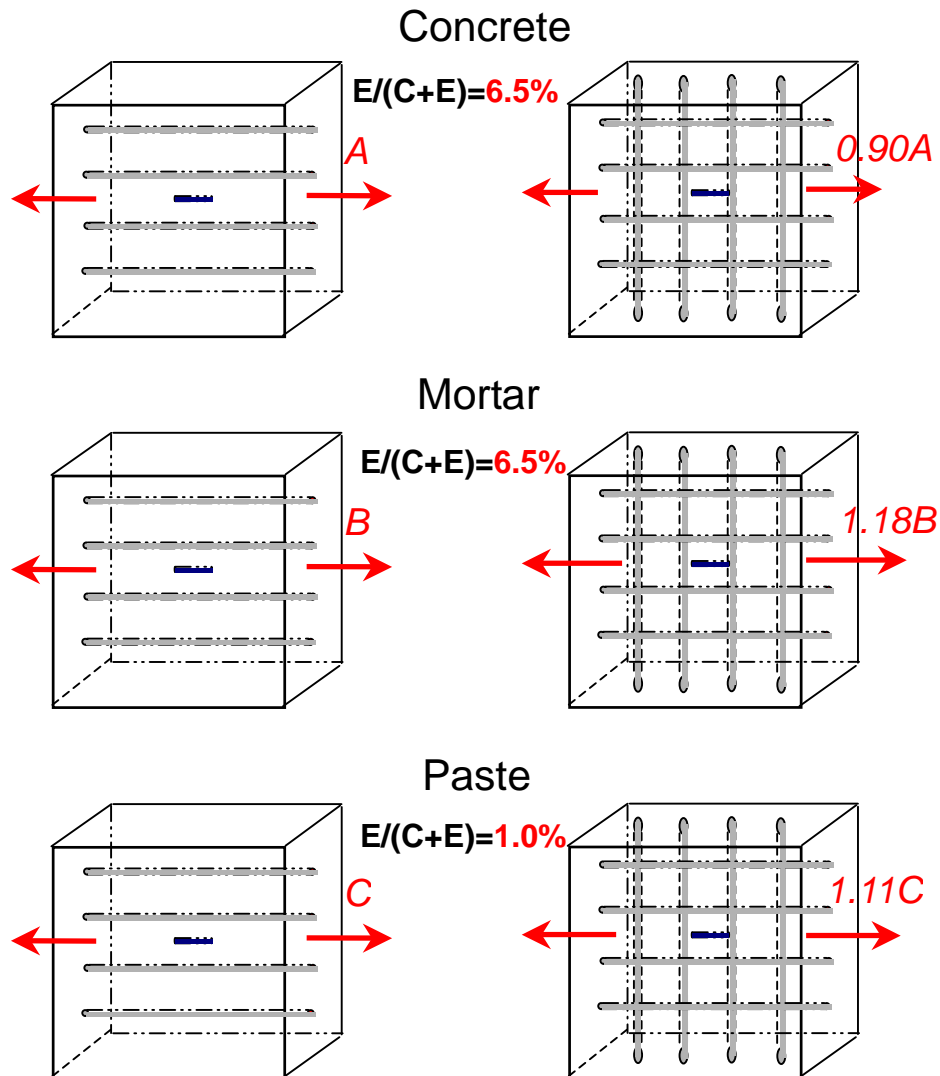


Fig.-6.20 Relationship between expansion strain and age under different restraint (Paste experiment)

Comparing concrete, mortar and paste experimental results, the influence of lateral restraint on axial expansion was redrawn in **Fig.-6.21**. Different with decrease tendency of concrete, the axial expansion increased 18% and 11% for mortar and paste respectively. According to the hypothesis, the existence of coarse aggregate was assumed one kind of resistant force to axial expansion. Therefore, the axial expansion of mortar should increase or the decrease level of expansion should reduce because the resistant force was not existed. And the experimental result coincided with the hypothesis.

Furthermore, special attention was put on the different increase percentage of axial expansion between mortar and paste experiment. At first, water-to-cement ratio in volume (V_w/V_p) and expansive agent replacement ratio ($E/(C+E)$) of paste mixing proportion was set as same as those in mortar experiment. The original purpose was to take out the same paste from the mortar experiment and tried to realize the influence of fine aggregate. However, due to the excessive expansion and crack, the expansion was unavailable. Therefore, the replacement ratio of expansive agent ($E/(C+E)$) was reduced to be 1% and it resulted in the low expansion strain. The low replacement ratio was inferred as the reason that the increase level of axial expansion in paste

experiment was smaller than the one in mortar experiment. However, it needs more experiments to prove this inference.



**Fig.-6.21 Influence of lateral restraint on axial expansion
from concrete, mortar and paste experiment**

6.4 Summary

- ♦ The expansive characteristics of SCC with expansive agent under multi-axial restraint were experimentally investigated. From the experimental results in this chapter, it was revealed that there was the mutual influence on restraint and expansion strain in perpendicular directions. Not only the axial expansion but also the expansion in the other two perpendicular directions was reduced when the

restraint was installed in the axial direction. In another word, the expansion was reduced in all the directions; even the restraint was only installed in one direction. From the experimental result, the axial expansion strain was reduced about 10% as the lateral restraint was installed.

- ◆ The friction occurred between coarse aggregate and mortar was inferred to be the reason of the decrease of axial expansion as the lateral restraint was installed. To prove this hypothesis, mortar and paste experiment were carried out. Different with decrease tendency of concrete, the axial expansion increased in both of mortar and paste experiment. That was to say that the resistant force in axial expansion direction disappeared without the existence of coarse aggregate and the hypothesis was clarified.
- ◆ The friction concept was reflected to the friction between expansion and compression elements in 3-dimension composite model. The friction was defined as the multiplication of the friction coefficient and normal stress on the interface of expansion and compression elements. And the friction coefficient was decided by the multi-axial restraint experimental result.



Photo-6.1 Paste specimen R1-E/(C+E) = 6.5% (before mold removed)



Photo-6.2 Paste specimen R2-E/(C+E) = 6.5% (before mold removed)



Photo-6.3 Paste specimen R1-E/(C+E) =6.5% (after mold removed)

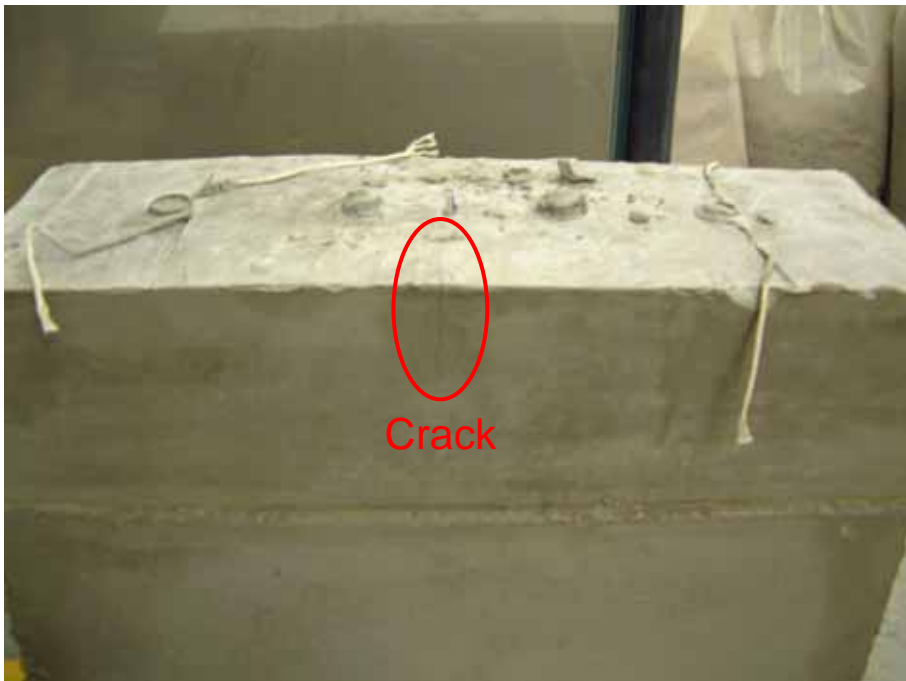


Photo-6.4 Paste specimen R2-E/(C+E) =6.5% (after mold removed)

CHAPTER 7

THREE-DIMENSIONAL COMPOSITE MODEL OF EXPANSIVE CONCRETE

7.1 Introduction

From the result of the previous chapters, it was revealed that crack was occurred after the formwork was removed if insufficient dosage of expansive agent was employed. On the contrary, if too much amount of expansive agent was employed, crack was occurred in the very early age as well. In Chapter 4, the appropriate dosage of expansive agent for SCC was proposed. However, in order to handle the characteristics of expansive concrete, the expansion estimation method was indispensable for the application of expansive agent.

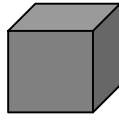
In this chapter, 3-dimensional composite model of expansive concrete was proposed to estimate the expansion of expansive concrete based on the existing one-dimensional composite model by taking the mix proportions, curing methods and degree of the restraints into accounted.

7.2 Three-Dimensional Composite Model

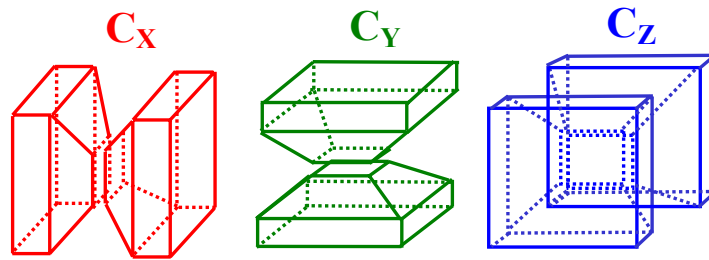
7.2.1 Geometric Shape of 3-Dimensional Composite Model

The geometric shape of 3-dimensional composite model was a cube with the side length equal to 1. In the model, concrete was regarded as a composite material and divided into eight elements, including one expansion element, six compression elements and one tension element. And the restraint of steel was expressed as the external restraint along three axial directions. The expansion element was a cube with the length equal to $\frac{1}{8}$ and arranged in the center. And three pairs of compression elements were symmetrically arranged along three axial directions. Tension element was a frame to cover six compression elements. (Fig.-7.1)

Expansion element×1



Compression element×6



Tension element×1

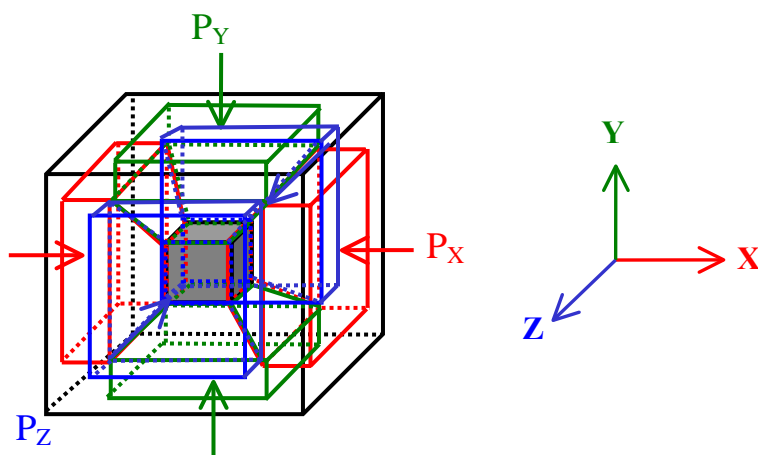
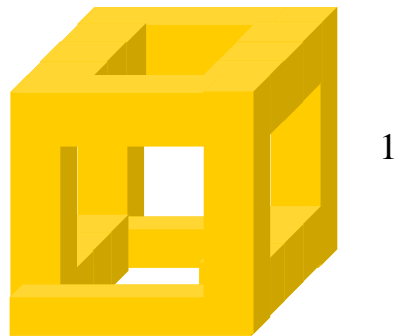


Fig.-7.1 Geometric shape of three-dimensional composite model

7.2.2 Friction between Expansion Element and Compression Element

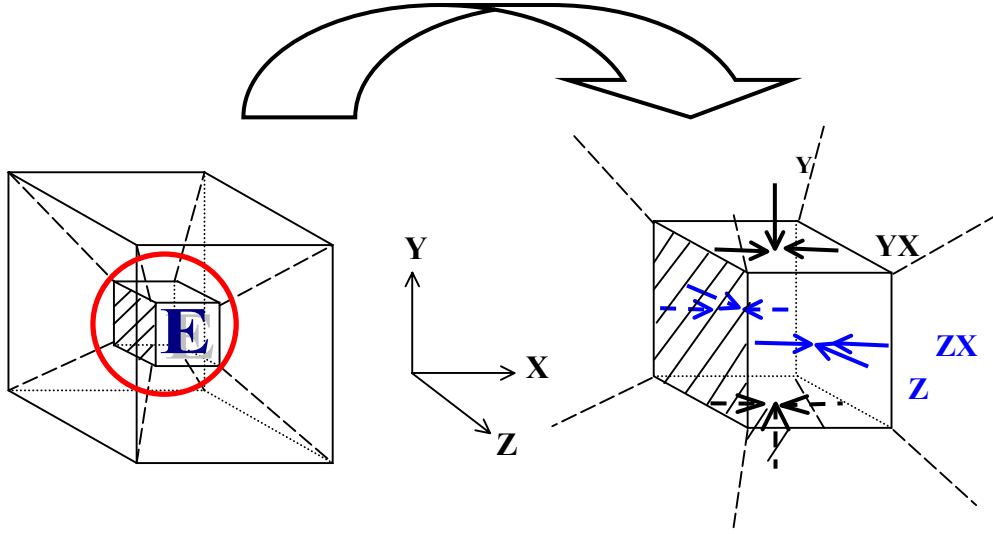


Fig.-7.2 Friction between expansion and compression element

To extend one-dimensional composite model to three-dimensional one, the influence of lateral restraint was simulated by the assumption of the friction between the expansion and the compression elements. (Fig.-7.2)

When the expansion strain in X direction was considered in the 1-dimensional composite model, the force equilibrium equation in the oblique surface, the interface between expansion and compression element, was set up. (Eq.7.1)

$$\Delta\varepsilon_{ee} \cdot E_e \cdot A_e = \Delta\varepsilon_c \cdot E_c \cdot A_c \quad (\text{Eq.7.1})$$

In the 3-dimensional composite model, when restraint was installed in another two lateral directions, friction between expansion and compression element was assumed to occur along Y and Z direction and regarded as one kind of resistant force in X direction. The friction was considered in the force equilibrium equation of the interface between expansion and compression element along X direction. (Fig.7-2) Therefore, the force equilibrium equation was rewritten as follows. (Eq.7.2)

$$(\Delta\varepsilon_{ee} \cdot E_e + 2\tau_{YX} + 2\tau_{ZX}) \cdot A_e = \Delta\varepsilon_c \cdot E_c \cdot A_c \quad (\text{Eq.7.2})$$

7.2.3 Determination of Friction Coefficient

The friction between expansion element and compression element was defined as

the multiplication of friction coefficient and the normal stress. (Eq.7.3) The friction coefficient was regarded as the interface character of expansion element and compression element. It was assumed to be constant and determined from the multi-axial restraint experiment.

$$\tau_{YX} = \mu \cdot \sigma_Y ; \tau_{ZX} = \mu \cdot \sigma_Z \quad (\text{Eq.7.3})$$

Here,

μ : Friction coefficient

σ_Y : Normal stress along Y direction

σ_Z : Normal stress along Z direction

7.2.4 Determination of Normal Stress

Normal stress was increased with the increase of restraint level in the normal direction. And it was defined to be proportional with the difference of free expansion and restraint expansion. [14] (Eq.7.4)

$$\sigma_n(t) = \{\Delta\varepsilon_{free}(t) - \Delta\varepsilon(t)\} \cdot E_s \cdot p \quad (\text{Eq.7.4})$$

Here,

$\Delta\varepsilon_{free}(t)$: Increment of free expansion strain at t day for same mix proportion

$\Delta\varepsilon(t)$: Increment of restraint expansion strain at t day for same mix proportion

E_s : Young's modulus of restraint steel

p : Restraint steel ratio

7.2.5 New Proposal to Determine the Length of Expansion Element “ ”

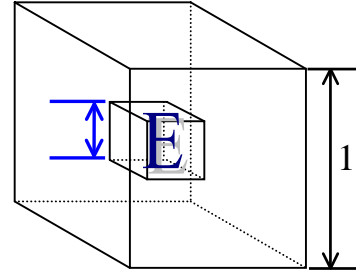
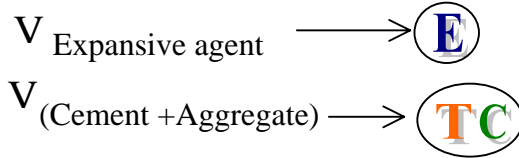
In 1-dimensional composite model, some parameters were difficult to assume and impossible to simulate from experiment, such as potential expansion (ε_o) and the length of expansion element (). Therefore, these two factors were determined by the trial calculation with the best accuracy of experimental result. However, there was the mutual influence between these two uncertain parameters. It means that different pairs of these two factors may have the same estimation result. Therefore, it was difficult to estimate the expansion of the other mix proportions with good accuracy.

In this research, new method was proposed by the author to determine the length of expansion element “ ”. By this new method, the length of expansion element was

estimated by the volume distribution of each component material from the mix proportion. In another words, after mix proportion was decided, the geometric shape of model was fixed as well.

Volume Distribution

First step



Second step

$$V_{\text{water in } \textcircled{E}} = V_{\text{water}} \times \left(\frac{V_{\text{Expansive agent}}}{V_{\text{Cement}}} \right)$$

$$V_{\text{air in } \textcircled{E}} = V_{\text{air}} \times \left(\frac{V_{\text{Expansive agent in } \textcircled{E}} + V_{\text{water in } \textcircled{E}}}{V_{\text{(Cement + Aggregate) in } \textcircled{TC}} + V_{\text{water in } \textcircled{TC}}} \right)$$

Third step

$$= (V_{\text{Expansive agent in } \textcircled{E}} + V_{\text{(water + air) in } \textcircled{E}})^{1/3}$$

“ ” is decided by mix proportion.

Fig.-7.3 New proposal to determine the length of expansion element “ α ”

The volume of each material was calculated from the mix proportion. Then each material was distributed to expansion element, compression element and tension element by following steps. At first, expansive agent was distributed to expansion element, and both of cement and aggregates were distributed to the other two elements. Then water was distributed proportionally into the expansion element and the other two elements by the volume ratio of expansive agent and cement. At last, air was distributed by the volume ratio of the previously distributed materials in expansion element and the other two elements. Therefore, expansive agent and some part of water and air existed in the expansion element and cement, aggregates and the other part of water and air existed in the tension and compression parts. Finally, the volume of expansion element could be calculated and then “ ” could be calculated as well. (Fig.-7.3)

7.2.6 Potential Expansion of Expansion Element “ ϵ_o ”

The strain of expansion element (ϵ_o) was divided into the chemical expansion (ϵ_{eo}) from the hydration reaction of expansive agent and the strain due to the restraint of compression element (ϵ_e). The chemical expansion was the strain of expansion element without any restraint. Accordingly, if the mix proportion, curing method (temperature, water supply) was fixed, the chemical expansion should be constant. Actually, it was the expansive origin and impossible to measure. Therefore, it was called as “Potential Expansion”. Comparatively, the whole strain of expansive concrete observed from the appearance was called “Apparent Expansion”. And it could be measured from the specimen.

The potential expansion of expansion element was determined by following equation. (Eq.7.5)

$$\epsilon_{eo}(t) = \left[e^{N_1 \cdot \left(\frac{E}{E+C} \% \right)} + N_2 \right] \cdot \left[A_0 + A_1 \left(1 - e^{-A_2(t-1)} \right) \right] \quad (\text{Eq.7.5})$$

Here, coefficients (N_1 and N_2) depend on the sort of expansive agent and coefficients (A_0 , A_1 and A_2) depend on curing method.

The potential expansion of expansion element was regarded as the source of expansion and impossible to simulate from experiment. In this research, it was divided as two parts. (Eq.7.5) The first part was related to the character of expansive agent and regarded as the function of the dispersion density of expansive agent in paste ($E/(E+C)$). And the second part was related to the curing method. In another word, the potential expansion was identical if expansive agent and curing method was same. Therefore, if the other parameters in composite model were determined, the potential expansion could be estimated by the experimental result.

7.2.7 Young’s Modulus

In the existing 1-dimensional composite model, Young’s modulus of three elements was determined by following equations. (Eq.7.6)

$$E = E_0 + E_1 \left(1 - e^{-E_2(t-1)} \right) \quad (\text{Eq.7.6})$$

Here, E_0 , E_1 and E_2 are constant and decided by the experimental results.

In 3-dimensional composite model, Sakata's proposal was adopted to determine Young's modulus of compression and tension element. [15] (Eq.7.7). And the Young's modulus of expansion element was assumed to be 45% of Young's modulus of compression and tension element.

$$E(t) = 15840 f'(t)^{0.5}$$

$$f'(t) = (0.469 f'(28) + 40.1) \log(t) + 0.32 f'(28) - 58.1 \quad (\text{Eq.7.7})$$

$$f'(28) = 1.52C - 39.6W + 552$$

Here,

$E(t)$: Young's Modulus at t day (kgf / cm^2)

$f'(t)$: Compressive Strength at t day (kgf / cm^2)

C, W : kg / m^3

Assuming $E_t(t) = E_c(t)$ and $E_e(t) = 0.45E_c(t) = 0.45E_t(t)$

7.2.8 Creep Coefficient

In the existing prediction methods, the creep coefficient was defined in two ways. Firstly, the ratio of creep at any age t , after application of load at the age t_0 , to the elastic strain at the age of 28 days was:

$$\phi_{28}(t, t_0) = C(t, t_0) \cdot E_{c28}$$

Here,

$\phi_{28}(t, t_0)$ = creep coefficient

$C(t, t_0)$ = creep per unit of stress, i.e. specific creep

E_{c28} = Modulus of elasticity at the age of 28 day

Secondly, the creep coefficient was the ratio of creep at any age t , after application of load at time t_0 , to the elastic strain at the age at application of load t_0 , so that:

$$\phi(t, t_0) = C(t, t_0) \cdot E_c(t_0)$$

Here,

$\phi(t, t_0)$ = creep coefficient

$C(t, t_0)$ = creep per unit of stress, i.e. specific creep

$E_c(t_0)$ = Modulus of elasticity at the age at application of load t_0

Therefore, $\phi(t, t_0)$ could be calculated by **Eq.7.8**.

$$\phi(t, t_0) = \frac{E_c(t_0)}{E_{c28}} \cdot \phi_{28}(t, t_0) \quad (\text{Eq.7.8})$$

In the existing 1-dimensional composite model, the creep coefficient of each element was determined by following equation. (**Eq.7.9**)

$$\phi_{in} = \left[t_n / (C_1 + C_2 \cdot t_n) - t_i / (C_1 + C_2 \cdot t_i) \right] + \left[(t_n - t_i) / (D_1 + D_2(t_n - t_i)) \right] \quad (\text{Eq.7.9})$$

Here, C_1 , C_2 , D_1 and D_2 are constants and decided by the experimental results.

In 3-dimensional composite model, the CEB-FIP Model Code 1978 was adopted to determine creep coefficient of compression and tension element. [16] And the creep coefficient of expansion element was decided by the relationship of free expansion and restraint expansion.

CEB-FIP Model Code 1978

In the CEB-FIP Model Code 1978, creep was divided into irreversible creep (plastic flow) and reversible flow (delayed elastic strain). In addition, the plastic flow was subdivided into a component representing flow for the first day under load (initial flow) and subsequent flow.

The creep coefficient $\phi_{28}(t, t_0)$ was estimated from the sum of initial flow, delayed elastic flow and delayed flow components (**Eq.7.10**), i.e.

$$\phi_{28}(t, t_0) = \beta_a(t_0) + \phi_d \beta_d(t - t_0) + \phi_f [\beta_f(t) - \beta_f(t_0)] \quad (\text{Eq.7.10})$$

In the above equations, β_a was the initial flow and obtained from following equation. (**Eq.7.11**)

$$\beta_a(t_0) = 0.8 \cdot \left[1 - \left(\frac{t_0}{t_0 + 47} \right)^{1/2.45} \right] \quad (\text{Eq.7.11})$$

The function, β_d , described the development of delayed elastic strain with time. And ϕ_d was the ratio of limiting delayed elastic strain to the initial elastic strain at the age of 28 days that was equal to 0.4. (Eq.7.12)

$$\phi_d \beta_d(t - t_0) = 0.4 \cdot \left[\frac{(t - t_0)}{(t - t_0 + 328)} \right]^{1/4.2} \quad (\text{Eq.7.12})$$

The last term ϕ_f was the flow coefficient. (Eq.7.13)

$$\phi_f = \phi_{f1} \times \phi_{f2} \quad (\text{Eq.7.13})$$

Here,

$$\phi_{f1} = 4.45 - 0.035 \times R.H.$$

$$\phi_{f2} = e^{[4.4 \cdot 10^{-5} \cdot h_0 - 0.357/h_0 - \ln(h_0^{0.1667}/2.6) + 0.34]}$$

$R.H. = \text{Relative Humidity } (\%)$

The term ϕ_{f2} was the notional thickness coefficient that takes into account the member size by the notional thickness h_0 that was given by Eq.7.14:

$$h_0 = \lambda \cdot \frac{2A_c}{u} \quad (\text{Eq.7.14})$$

Here,

$A_c = \text{cross - sectional area of the member } (mm^2)$
 $u = \text{perimeter exposed to drying } (mm)$
 $\lambda = \text{coefficient for ambient humidity } (\text{Table - 7.1})$

Table-7.1 Ambient humidity coefficient (λ)

Ambient environment	Relative humidity (%)	λ
Water	-----	30
Very damp	90	5
Outside in general	70	1.5
Very dry atmosphere	40	1.0

The plastic flow parameters $\beta_f(t)$ was a function describing the development of delayed plastic strain with time and depended on the notional thickness h_0 , and $\beta_f(t_0)$ which was a function to account for the age at application of load, i.e. when $t = t_0$. (Eq.7.15)

$$\beta_f(t) = \left(\frac{t}{t + H_f} \right)^{1/3} \quad \text{(Eq.7.15)}$$

Here, the time delay coefficient H_f was a function of h_0 . (Eq.7.16)

$$H_f(h_0) = 275 + 1.5 \cdot h_0 \quad \text{(Eq.7.16)}$$

Modification of CEB-FIP Model Code 1978

The CEB-FIP Model Code 1978 was a regression estimation method. Based on the database, the coefficients in this model were determined. In 1970's, the paste volume in different mix proportions was not so much different. That is to say that the variation of paste volume was not considered in this model. However, in the case of SCC, in order to maintain enough viscosity, the paste volume was greatly increased. Therefore, the estimation value of creep coefficient needs to be modified.

According to Neville's research, creep was assumed to be proportional to the volume of paste. (In the case of $a=0$, i.e. pure cement paste.)

$$C = C_p \cdot (1 - a) \quad \text{i.e. } C \propto (1 - a)$$

Here,

$C = \text{Creep of concrete}$

$C_p = \text{Creep of pure cement paste}$

$a = \text{fractional volume of aggregate (including coarse and fine aggregate)}$

Therefore, paste modification coefficient, $\frac{(1 - g)}{0.30}$, was added to Eq.7.8. (Eq.7.17)

$$\phi(t, t_0) = \frac{(1-g)}{0.30} \cdot \frac{E_c(t_0)}{E_{c28}} \cdot \phi_{28}(t, t_0) \quad (\text{Eq.7.17})$$

7.3 Calculation of Three-Dimensional Composite Model

7.3.1 Equations of the Increment of Apparent Expansion

Assuming the expansion strain in X direction was calculated when restraint was installed in X, Y and Z direction. Since the geometric shape of 3-dimensional composite model was as same as the 1-dimensional composite model, therefore the dimension of each element was as same as the dimension of 1-dimensional model defined as follows. Notice that the following equations from Eq.7.18 to Eq.7.26 were same in three directions since the geometric shape of composite model was symmetric.

$$V_e = \alpha^3 \quad (\text{Eq.7.18})$$

$$V_t = 2 \cdot (1 - \alpha^3) / 3 \quad (\text{Eq.7.19})$$

$$V_c = (1 - \alpha^3) / 3 \quad (\text{Eq.7.20})$$

$$l_e = \alpha \quad (\text{Eq.7.21})$$

$$l_t = 1 \quad (\text{Eq.7.22})$$

$$l_c = 1 - \alpha \quad (\text{Eq.7.23})$$

$$A_e = V_e / l_e \quad (\text{Eq.7.24})$$

$$A_t = V_t / l_t \quad (\text{Eq.7.25})$$

$$A_c = V_c / l_c \quad (\text{Eq.7.26})$$

Assuming the apparent expansion ϵ_x in X direction was occurred in a finite period due the increment of potential expansion ϵ_{eo} . The following equations (Eq.7.27~7.29) were set up based on the compatible conditions.

$$\Delta \epsilon_{Xe} = \Delta \epsilon_{eo} + \Delta \epsilon_{Xee} \quad (\text{Eq.7.27})$$

$$\Delta \epsilon_X \cdot l = \Delta \epsilon_X \cdot 1 = \Delta \epsilon_{Xt} \cdot l_t \quad (l=1) \quad (\text{Eq.7.28})$$

$$\Delta \epsilon_X \cdot l = \Delta \epsilon_{Xe} \cdot l_e + \Delta \epsilon_{Xc} \cdot l_c \quad (l=1) \quad (\text{Eq.7.29})$$

Here, ϵ_e , ϵ_t and ϵ_c are the average strain increment of expansion, tension and compression element in X direction.

Concerning the force equilibrium conditions, Eq.7.30 and Eq.7.31 were set up.

$$\begin{aligned} & \Delta \varepsilon_{Xt} \cdot E_t \cdot A_t / A_{concrete} + \Delta \varepsilon_{Xc} \cdot E_c \cdot A_c / A_{concrete} \\ & = \Delta \varepsilon_{Xt} \cdot E_t \cdot A_t + \Delta \varepsilon_{Xc} \cdot E_c \cdot A_c \end{aligned} \quad (\text{Eq.7.30})$$

$$\begin{aligned} & = -\Delta \varepsilon_X \cdot p_X \cdot E_s \quad (A_{concrete} = 1) \quad (p_X = A_{Xsteel} / A_{concrete}) \\ & (\Delta \varepsilon_{Xee} \cdot E_e + 2 \cdot \tau_{YX} + 2 \cdot \tau_{ZX}) \cdot A_e = \Delta \varepsilon_{Xc} \cdot E_c \cdot A_c \end{aligned} \quad (\text{Eq.7.31})$$

Here,

E_e, E_t, E_c and E_s are the Young's modulus of three elements and restraint steel.
 p_X is the restraint steel ratio in X direction defined as the ratio of steel area to the concrete cross-section area.

τ_{YX} and τ_{ZX} are the friction between expansion and compression element along Y and Z direction respectively.

Then, the relation of the increment of potential expansion and apparent expansion in X direction can be expressed as **Eq.7.32** derived from **Eq.7.27** to **Eq.7.31**.

$$\begin{aligned} \Delta \varepsilon_X & = \frac{\Delta \varepsilon_{eo} \cdot l_e - \left[\frac{(2\tau_{YX} + 2\tau_{ZX}) \cdot l_e}{E_e} \right]}{l + K} \\ & = \frac{\Delta \varepsilon_{eo} \cdot l_e - \left[\frac{(2\tau_{YX} + 2\tau_{ZX}) \cdot l_e}{E_e} \right]}{1 + K} \quad (l = 1) \end{aligned} \quad (\text{Eq.7.32})$$

$$\text{Here, } K = (K_t + p_X \cdot E_s) \times (1/K_e + 1/K_c) \quad (\text{Eq.7.33})$$

$$K_e = (E_e \cdot A_e) / (l_e \cdot A_{concrete}) = (E_e \cdot A_e) / l_e \quad (A_{concrete} = 1) \quad (\text{Eq.7.34})$$

$$K_t = (E_t \cdot A_t \cdot l) / (l_t \cdot A_{concrete}) = (E_t \cdot A_t) / l_t \quad (l = 1; A_{concrete} = 1) \quad (\text{Eq.7.35})$$

$$K_c = (E_c \cdot A_c) / (l_c \cdot A_{concrete}) = (E_c \cdot A_c) / l_c \quad (A_{concrete} = 1) \quad (\text{Eq.7.36})$$

7.3.2 Calculation Method of Apparent Expansion

With the potential strain occurred in a finite period t , there were strain and stress occurred in three elements to satisfy the compatible conditions of deformability and force. However, these strains and stresses changed due to the effect of creep, even potential expansion was constant. To simulate the above phenomenon, the following method was used.

Assuming the expansion strain in X direction was calculated when restraint was installed in X, Y and Z direction. According to the increment of potential strain ε_{eo}

from t_{i-1} to t_i , the increment of apparent expansion strain ε_{Xin} at t_n was defined (Fig.-7.4). Creep effect occurred from t_i to t_n was considered when ε_{Xin} was calculated. The elastic modulus E from Eq.7.34 to Eq.7.36 was replaced by E_{in} . And E_{in} was expressed by creep coefficient φ_{in} and the elastic modulus E_i at t_i . The relation of the increment of potential expansion ε_{eoi} at t_i and apparent expansion ε_{Xin} at t_n was rewritten as follows.

$$\begin{aligned}\Delta\varepsilon_{Xin} &= \frac{\Delta\varepsilon_{eoi} \cdot l_e - \left[\frac{(2\tau_{YXi} + 2\tau_{ZXi}) \cdot l_e}{E_{ein}} \right]}{l + K_{in}} \\ &= \frac{\Delta\varepsilon_{eoi} \cdot l_e - \left[\frac{(2\tau_{YXi} + 2\tau_{ZXi}) \cdot l_e}{E_{ein}} \right]}{1 + K_{in}} \quad (l=1)\end{aligned}\quad (\text{Eq.7.37})$$

$$\text{Here, } K_{in} = (K_{tin} + p \cdot E_s) \times (1/K_{ein} + 1/K_{cin}) \quad (\text{Eq.7.38})$$

$$K_{ein} = (E_{ein} \cdot A_e) / (l_e \cdot A_{concrete}) = (E_{ein} \cdot A_e) / l_e \quad (A_{concrete} = 1)$$

$$E_{ein} = E_{ei} / (1 + \varphi_{ein})$$

$$(\text{Eq.7.39})$$

$$K_{tin} = (E_{tin} \cdot A_t \cdot l) / (l_t \cdot A_{concrete}) = (E_{tin} \cdot A_t) / l_t \quad (l=1; A_{concrete} = 1)$$

$$E_{tin} = E_{ti} / (1 + \varphi_{tin})$$

$$(\text{Eq.7.40})$$

$$K_{cin} = (E_{cin} \cdot A_c) / (l_c \cdot A_{concrete}) = (E_{cin} \cdot A_c) / l_c \quad (A_{concrete} = 1)$$

$$E_{cin} = E_{ci} / (1 + \varphi_{cin})$$

$$(\text{Eq.7.41})$$

$$\tau_{YXi} = u \cdot \{ \Delta\varepsilon_{Yfree}(i) - \Delta\varepsilon_Y(i) \} \cdot E_s \cdot p_Y$$

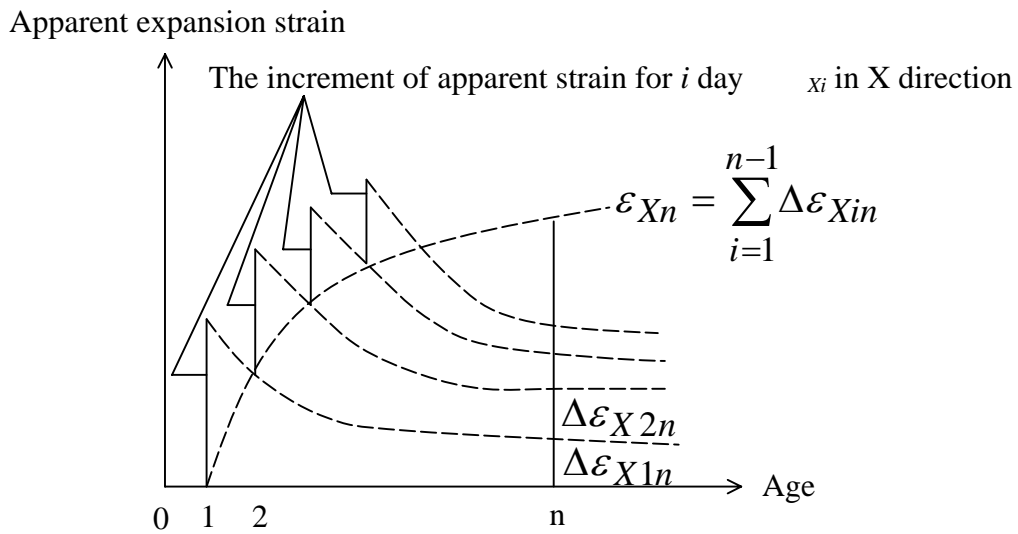
$$(\text{Eq.7.42})$$

$$\tau_{ZXi} = u \cdot \{ \Delta\varepsilon_{Zfree}(i) - \Delta\varepsilon_Z(i) \} \cdot E_s \cdot p_Z$$

$$(\text{Eq.7.43})$$

Then the apparent strain ε_{Xn} at t_n can be calculated by the summation of ε_{Xin} from t_1 to t_n . (Eq.7.44)

$$\varepsilon_{Xn} = \sum_{i=1}^n \Delta\varepsilon_{Xin} \quad (\text{Eq.7.44})$$



$\Delta \epsilon_{Xin}$: Apparent expansion increment of i day in X direction for n day

Fig.-7.4 Calculation of apparent expansion in X direction

7.3.3 Calculation Flow Chart of 3-dimensional Composite Model

Assuming the expansion strain in X direction was calculated when restraint was installed in X, Y and Z direction. The input parameters in 3-dimensional composite model were the length of expansion element, Young's modulus and creep coefficient of three elements and restraint steel ratio in three directions. And all of the input parameters were decided by mix proportion and curing condition. Then potential expansion could be estimated from one-axial restraint experimental result. Up to now, one-dimensional composite model was achieved. The expansion strain when p was 0%, p_Y and p_Z were calculated by the achieved one-dimensional composite model respectively. Then, the normal stress in lateral direction, Y and Z direction, was estimated by Eq.7.4. Finally, comparing with the multi-axial restraint experimental result, the friction coefficient μ was estimated. (Fig.-7.5)

After potential expansion and friction coefficient was known, the expansion with the same expansive agent for the different mix proportion under multi-axial restraint condition could be predicted.

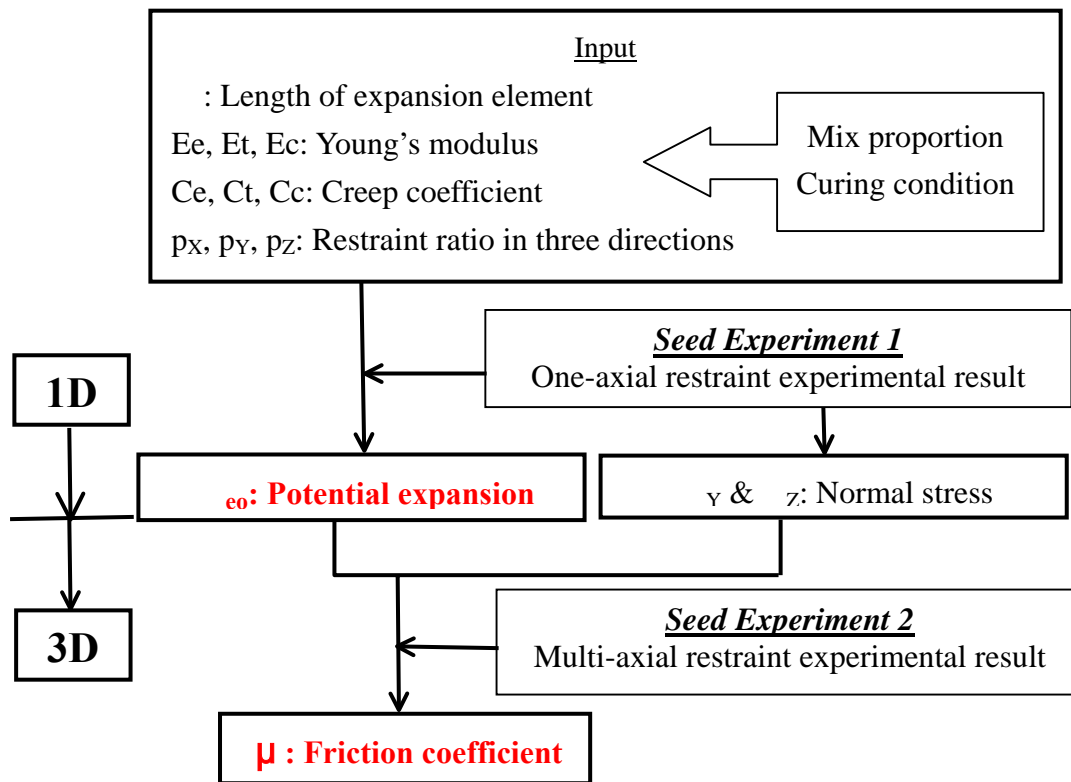


Fig.-7.5 Calculation flowchart of 3-dimensional Composite Model

7.4 Comparison of Estimation by Three-Dimensional Composite Model and Experimental Result

As mentioned in 7.3.3, two experimental results were necessary to achieve 3-dimensional composite model. One was the one-axial restraint experimental result to decide potential expansion “ e_o ” and the other was the multi-axial restraint experimental result to decide the friction coefficient “ μ ”. Both of experiments were regarded as the “seed experiment”. (Fig.-7.5)

From the experimental results in the previous chapters, the one-axial restraint experiment result of EX40 with $p=1.324\%$ was chose to be “seed experiment 1”. Since potential expansion was different depending on curing method, therefore, both of the experimental results under sealed and water curing were employed. Then, the potential expansion of expansion element under sealed and water curing was obtained. (Fig.-7.6) And the input data and estimation result was showed from Fig.-7.7 to Fig.-7.10. Up to here, one-dimensional composite model was achieved. And the estimation of the other mix proportion with different restraint steel ratio under sealed

and water curing could be made. The comparison of estimation and experimental result was shown from **Fig.-7.11** to **Fig.-7.13**. And all of the estimation showed the good accuracy with the experimental result.

Next, one-dimensional composite model was extended to three-dimensional composite model by the multi-axial restraint experimental result. The two-axial restraint experimental result of EX40 with $p_x=1.324\%$ and $p_y=1.324\%$ in Chapter 5 was chose to be “**seed experiment 2**”. The normal stress in Y direction was calculated by the achieved one-dimensional composite model. (**Fig.-7.14**) Then friction coefficient was estimated by the 2-dimensional restraint experimental result. (**Fig.-7.15**) Up to now, the 3-dimensional composite model was achieved.

The expansion strain in axial direction of the Specimen r3 of EX40 was estimated by the achieved 3-dimensional composite model. The estimation result was shown in with good accuracy with the experimental result. (**Fig.-7.16**)

7.5 Evaluation of Three-dimensional Composite Model

Based on this research, the “prototype” of 3-dimensional composite model of expansive concrete was achieved.

In comparison with the past research, the determination method of potential expansion of expansion element ” ” was solved by the author’s proposal. Based on the concept of volume distribution, ” ” could be simply decided by the mix proportion.

In the past research, the Young’s modulus and creep coefficient were decided by trial calculation with the best accuracy of experimental result. In this research, Sakata’s equation was adopted to determine the Young’s modulus of compression and tension element. By Sakata’s equation, Young’s modulus of compression and tension element could be easily decided by mixing proportion. And the Young’ modulus of expansion element was simply assumed as the 45% of compression and tension element. As to the creep coefficient, the CEB-FIP Model Code 1978 was adopted to determine creep coefficient of compression and tension element. By CEB-FIP Model Code 1978, creep coefficient of compression and tension element could be easily decided by mixing proportion, specimen dimension and curing method. Besides, modification factor was added to modify the creep coefficient with the consideration of the variation of paste volume. Then the creep coefficient of expansion element was

decided by the relationship of free expansion and restraint expansion. For example, the creep coefficient of expansion element was set to be 6 and 1.5 times of the tension and compression element for water and sealed curing respectively. (**Fig.-7.8** and **Fig.-7.9**)

Finally, the only one unknown parameter, potential expansion, could be decided by trial calculation with best accuracy of the one-axial restraint experimental result (**Seed experiment 1**). The potential expansion of expansion element was regarded as the source of expansion and impossible to simulate from experiment. In this research, it was divided as two parts. The first part was related to the character of expansive agent and regarded as the function of the dispersion density of expansive agent in paste ($E/(E+C)$). And the second part was related to the curing method. In another word, the potential expansion was identical if expansive agent and curing method was same. In **Fig.-7.6**, it was revealed the reasonable phenomenon that the potential expansion was larger and the hydration speed was faster under water curing than sealed curing.

The mutual effect of restraint and expansion in perpendicular directions was assumed to be due to the friction between expansion and compression elements. By using the multi-axial restraint experimental result and the friction concept, 1-dimensional composite model was expanded to 3-dimensional one. And the friction between expansion and compression elements was calculated by the multiplication of friction coefficient and normal stress. The friction coefficient was defined as the character of the interface of expansion and compression elements and assumed to be constant. And then friction coefficient could be estimated by the multi-axial restraint experimental result (**Seed experiment 2**). After the above parameters were decided, the 3-dimensional composite model of expansive concrete was achieved. By the input of the parameters decided above: friction coefficient, the potential expansion, the expansion with the same expansive agent for the different mix proportion under multi-axial restraint condition could be predicted.

More research has to be carried out on the issue of Young's modulus and creep coefficient of expansion element. That is to say that there is still a lot of space to improve the rationality of this model.

7.6 Summary

Three-dimensional composite model of expansive concrete was proposed to

estimate the expansion of expansive concrete based on the existing 1-dimensional composite model by taking the mix proportions, curing methods and degree of the restraints into account.

In the existing 1-dimensional composite model, there was no method to decide some parameters, such as the length of expansion, potential expansion, Young's modulus and creep coefficient. And most of the parameters were decided by the trial calculation with the best accuracy of the experimental result. However, due to the mutual effect, different combination pairs of parameters could have the same estimation result. Therefore, when mixing proportion changed, it could not be applied to estimate the expansion with good accuracy.

In this research, the new determination method for the length of expansion element was proposed. The length of expansion element was defined by the volume distribution of each component material by the mix proportion. And Young's modulus and creep coefficient were decided by Sakata's equation and CEB-FIP Model Code 1978 respectively. As to the left only one parameter, potential expansion of expansion element was assumed as the character of expansive agent under the specific curing method and it was decided by one one-axial restraint experimental result. After potential expansion was decided, 1-dimensional composite model was achieved and it was able to predict the expansion for the other mixing proportions under one-axial restraint.

By using the multi-axial restraint experimental result and the friction concept, one-dimensional composite model was expanded to three-dimensional one. The friction between the expansion and the compression elements was calculated by the multiplication of friction coefficient and the normal stress of lateral direction. The friction coefficient was defined as the character of the interface of expansion and the compression elements and assumed to be constant. And then friction coefficient was estimated by one multi-axial restraint experimental result. After the friction coefficient was determined, by the input of the parameters decided above: friction coefficient, the potential expansion, the expansion with the same expansive agent for the different mix proportion under multi-axial restraint condition could be predicted.

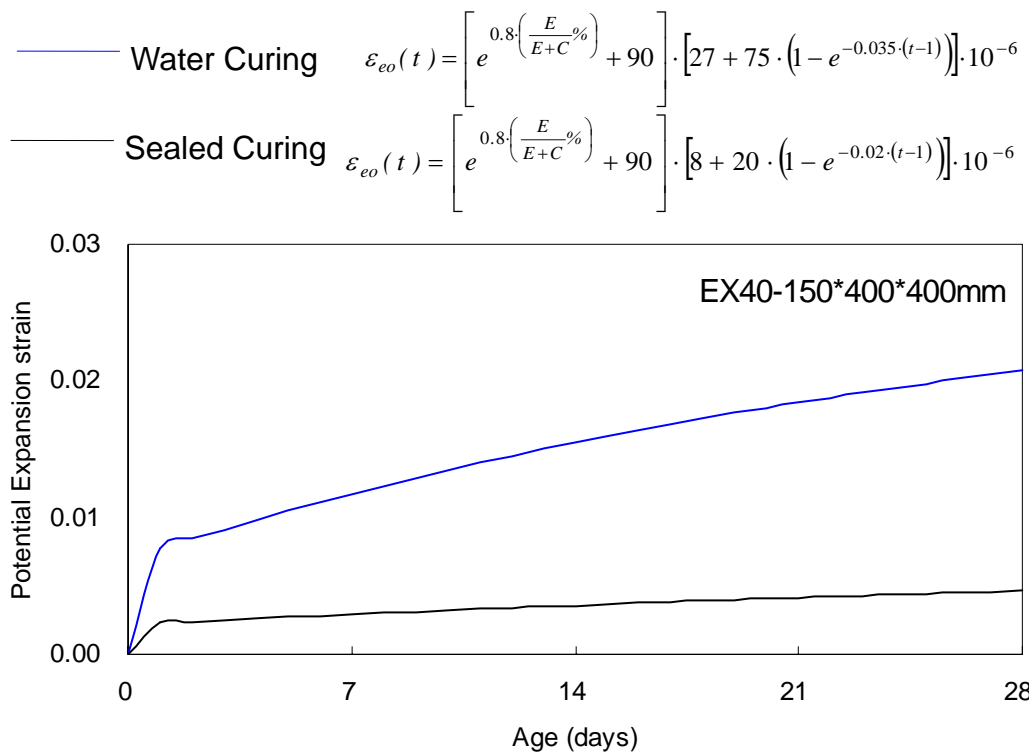


Fig.-7.6 Estimated potential expansion of EX40 under water and sealed curing

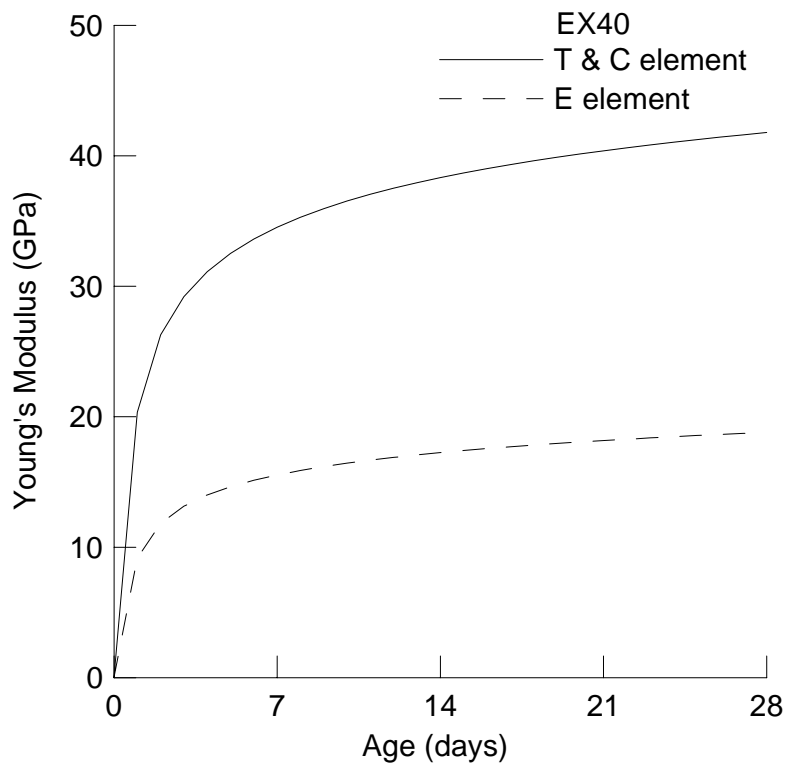


Fig.-7.7 Input Young's Modulus of EX40

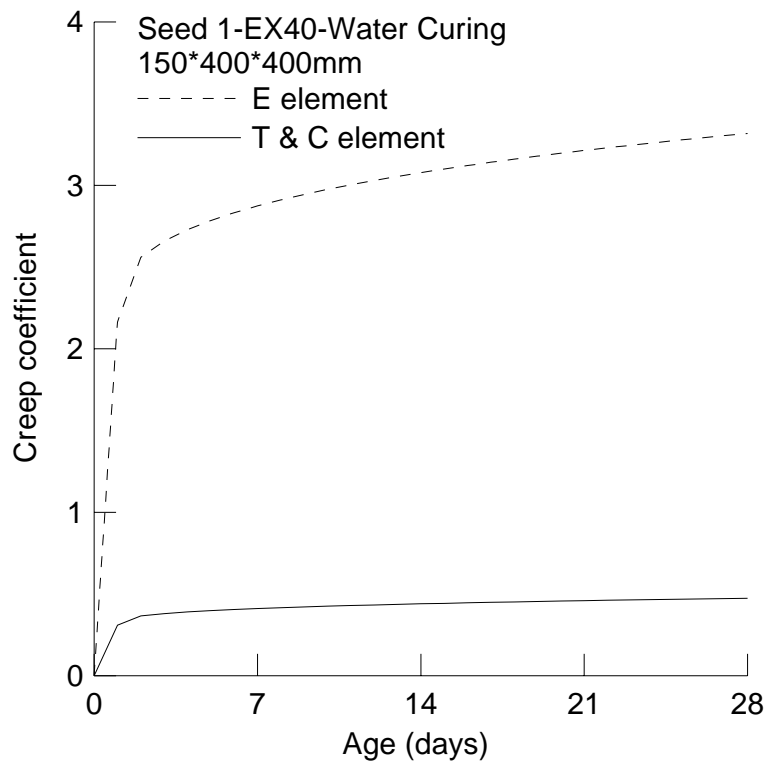


Fig.-7.8 Input creep coefficient of EX40 under water curing

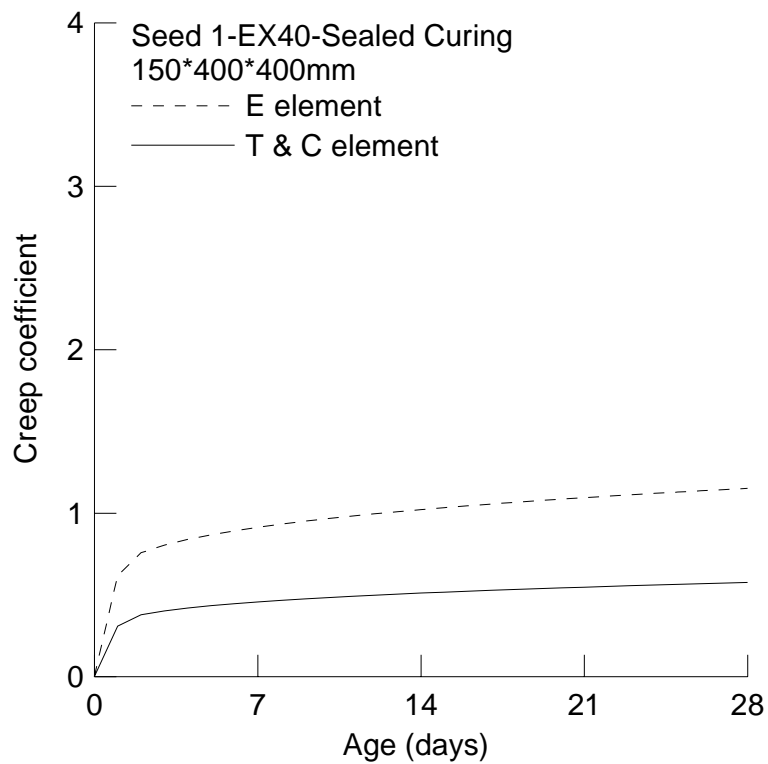


Fig.-7.9 Input creep coefficient of EX40 under sealed curing

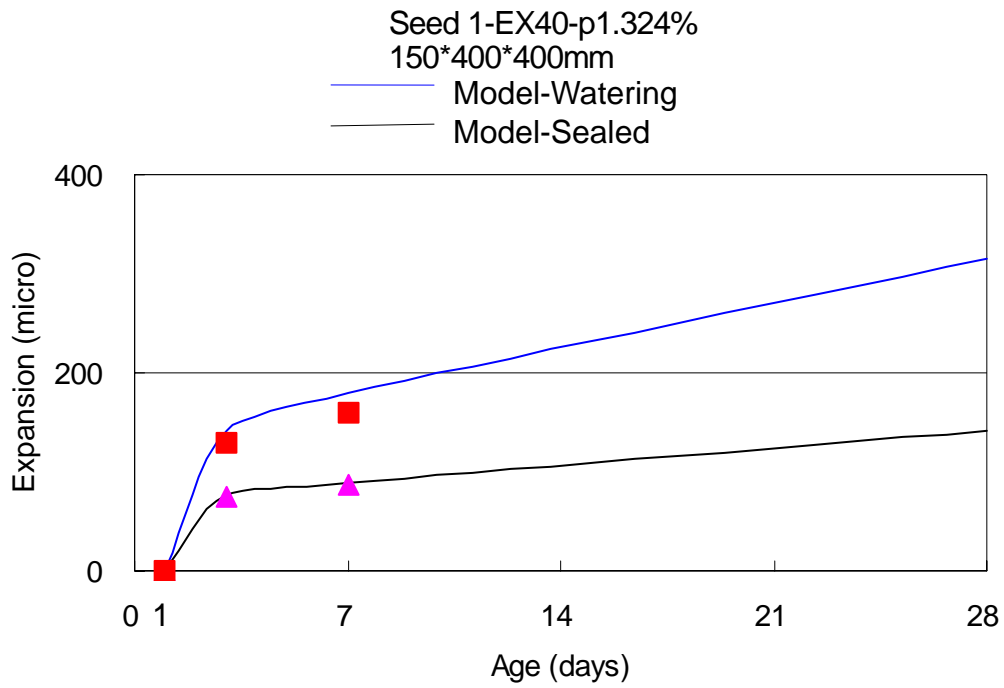


Fig.-7.10 One-axial restraint estimation result of EX40 under water and sealed curing

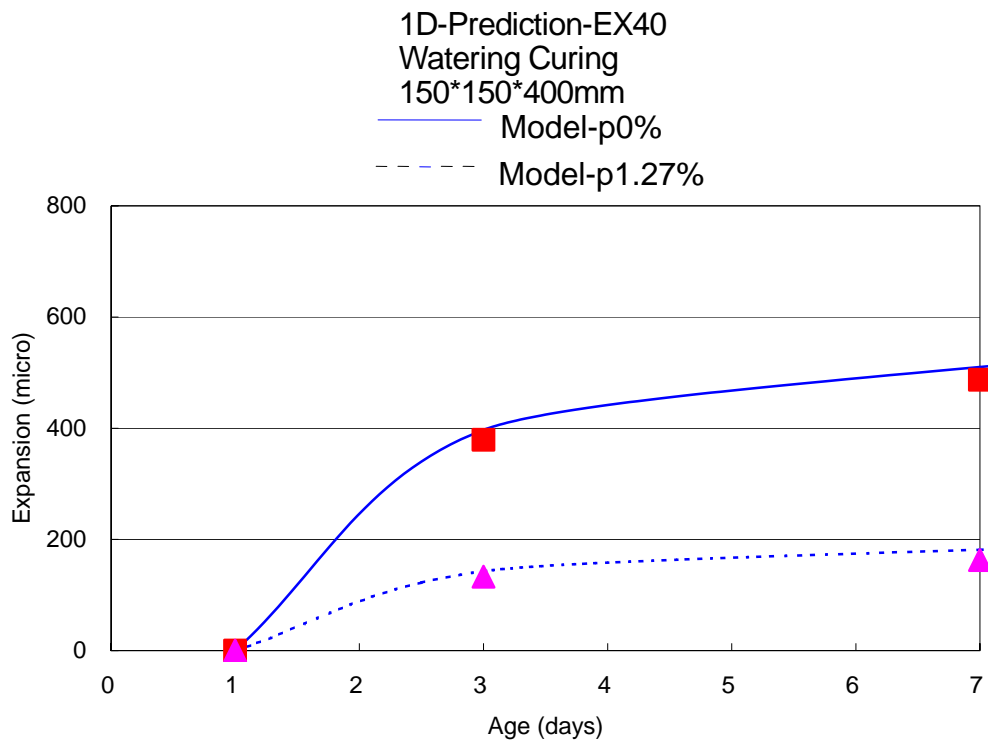


Fig.-7.11 Comparison of estimation and experimental result of EX40 under water curing

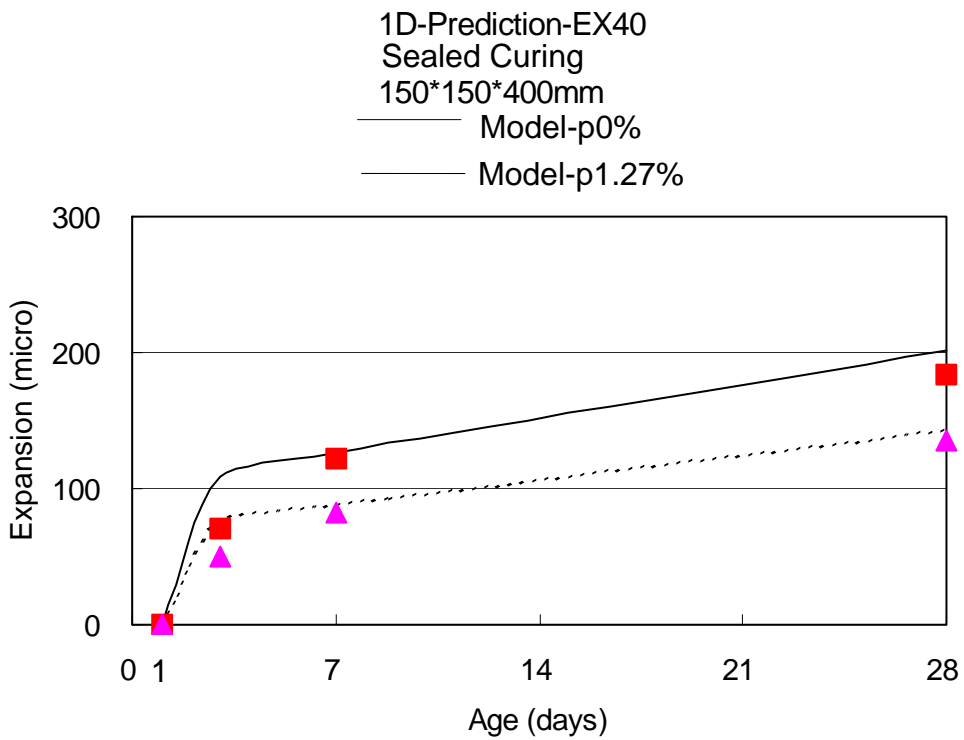


Fig.-7.12 Comparison of estimation and experimental result of EX40 under sealed curing

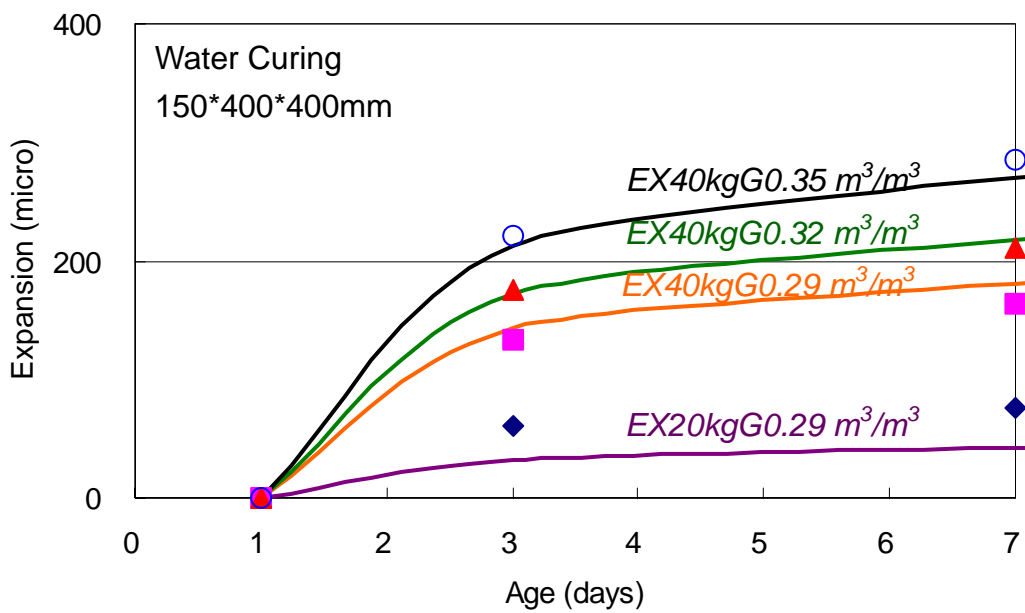


Fig.-7.13 Comparison of estimation and experimental result of different mix proportion with the variation of coarse aggregate

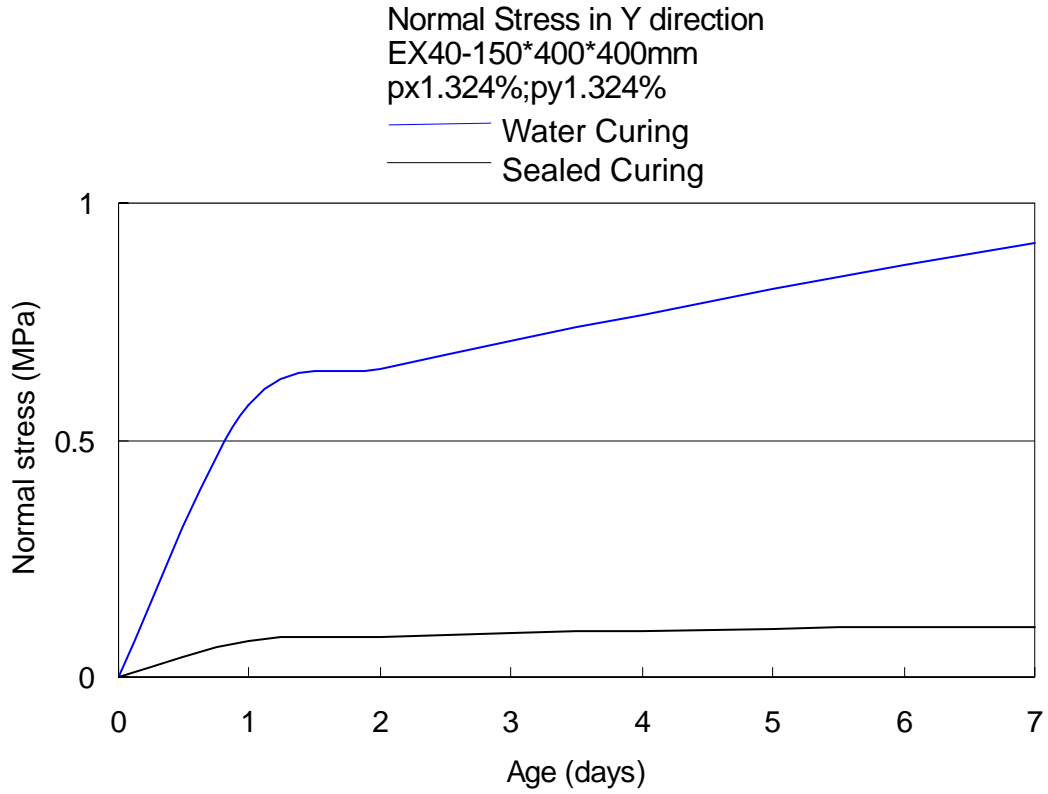


Fig.-7.14 Normal stress of EX40 in Lateral direction (Y direction)

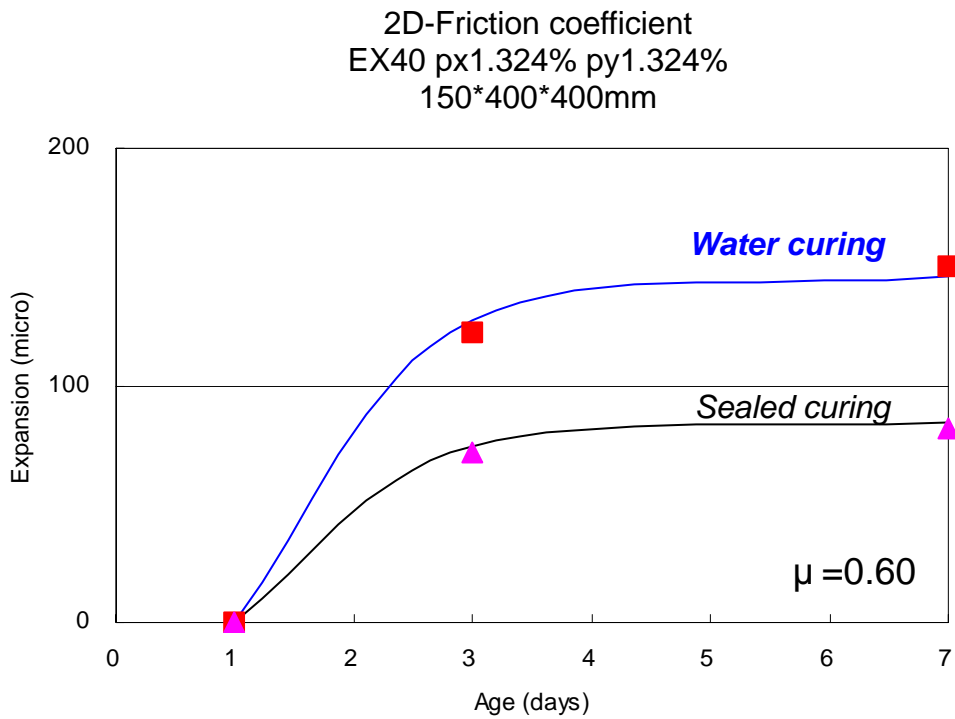


Fig.-7.15 Two-axial restraint estimation result of EX40 under water and sealed curing

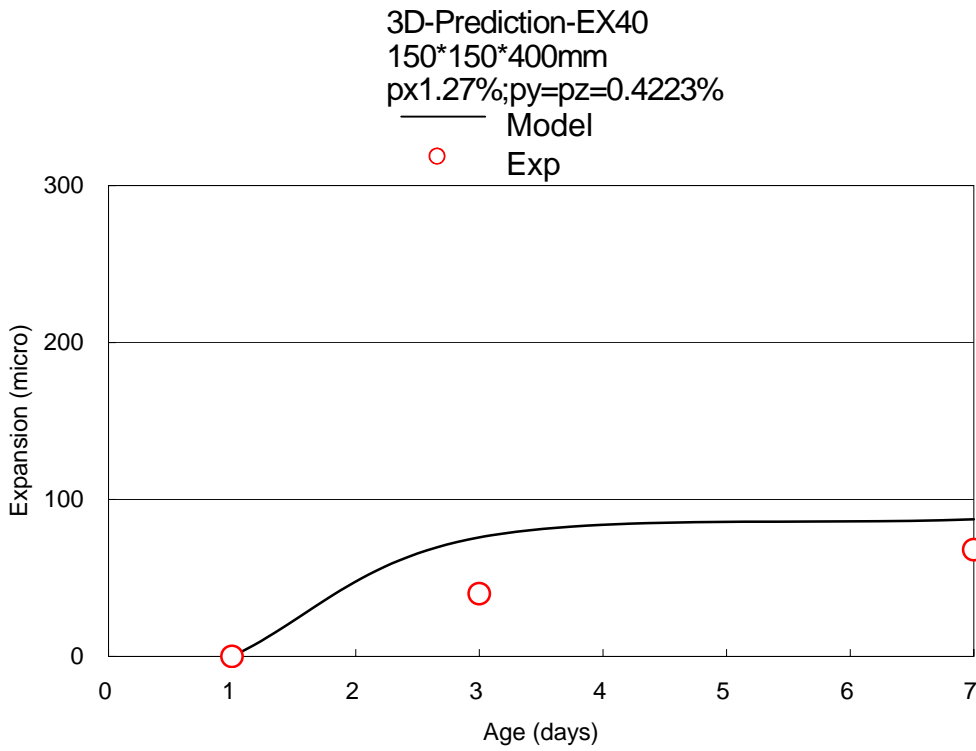


Fig.-7.16 Comparison of 3-D estimation and experimental result of EX40 under sealed curing

CHAPTER 8

CONCLUSIONS

8.1 Summary and Conclusions

According to this research, the characteristics of SCC using expansive agent was verified. The maximum expansion strain of SCC using expansive agent was less than that of conventional concrete with high water-to-cement ratio for the same dosage of expansive agent. And the insufficient expansion resulted in crack after the specimen was dried. It seemed that the efficiency of expansive agent was reduced on the application of SCC, due to the very low water-to-cement ratio. It was also found that the expansive characteristics greatly differ depending on curing method. The difference in the influence on expansion under water- and sealed-curing was very clear. On the other hand, the influence of the drying-curing on the expansion was not so clear compared with the sealed curing. It was revealed that the necessity for water in SCC using expansive agent was higher than the conventional concrete. Besides, the dosage of expansive agent for SCC under sealed curing condition had to be increased in order to achieve the enough expansion to prevent crack.

As the influence of the variation of coarse aggregate, when same amount of expansive agent was employed, the expansion strain reduced as the amount of coarse aggregate decreased, though coarse aggregate was regarded as the resistant force to expansion. It was explained by the decrease of the ratio of expansive agent to total powder ($E/(C+E)$). Since the dispersion density of expansive agent in paste reduced when the amount of coarse aggregate reduced, therefore, the expansion reduced. That is to say that the efficiency of expansive agent reduced on the application of SCC.

Limestone powder was employed to be the countermeasure to enhance the efficiency of expansive agent. Replacing cement by limestone powder was proved to be contributive to the compensation for the shrinkage and crack was not occurred, although the drying shrinkage might be increased. In the case of the utilization of limestone powder, the expansion strain for the same dosage of expansive agent was increased due to the increase of the dispersion density of expansive agent in paste. And the dosage of expansive agent to achieve the same expansion with the conventional concrete was reduced as well. That was to say that the shortage of water in SCC using expansive agent could be solved by the utilization of limestone powder.

On the other hand, the compressive strength was reduced as the replacement ratio of limestone powder increased.

The expansive characteristics of SCC using expansive agent under multi-axial restraint were experimentally investigated. The mutual effect of restraint and expansion in perpendicular directions was clarified. Not only the axial expansion but also the expansion in the other two directions was reduced when the restraint was installed in the axial direction. In another word, the expansion was reduced in all the directions; even the restraint was only installed in one direction. The friction occurred between coarse aggregate and mortar was set to be the hypothesis to explain the mechanism and proved by mortar and paste experiment. Moreover, the friction concept was reflected to the friction between expansion and compression elements in 3-dimension composite model. And the experimental results were employed to decide the friction coefficient, the ratio of the friction to normal stress on the interface of expansion and tension elements.

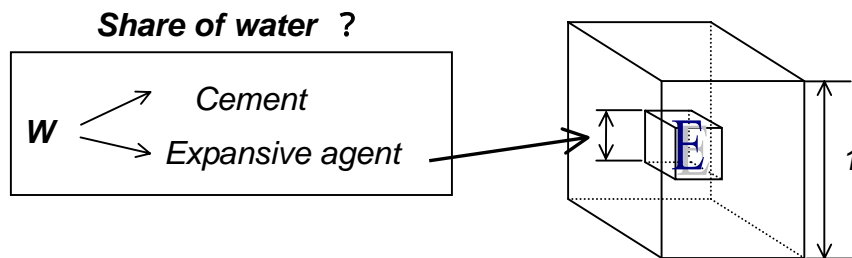
3-dimensional composite model of expansive concrete was proposed to estimate the expansion of expansive concrete based on the existing 1-dimensional composite model by taking the mix proportions, curing methods and degree of the restraints into accounted. In the 3-dimensional composite model, concrete was regarded as a composite material of three types of elements: expansion element, tension element and compression element. The concrete was divided into eight elements and the restraint of steel was expressed as the external restraint. By using the multi-axial restraint experimental result and the friction concept, 1-dimensional composite model was extended to be 3-dimensional one. And the friction between expansion and compression elements was calculated by the multiplication of friction coefficient and the normal stress. The friction coefficient was defined as the character of the interface of expansion and compression elements and assumed to be constant. In addition, based on the volume distribution concept of each component material from mix proportion, new determination method for the length of expansion element was proposed. And the potential expansion was assumed as the character of expansive agent under the specific curing method and divided into two parts related to the type of expansive agent and curing method respectively. By using the parameters decided above, the potential expansion could be estimated from the one-axial restraint experimental result. And then friction coefficient could be estimated by the multi-axial restraint experimental result. By the input of the parameters decided above: friction coefficient, the potential expansion, the length of expansion element, restraint steel ratio, Young's modulus and creep coefficient, the expansion with the same

expansive agent for the different mix proportion under multi-axial restraint condition could be predicted.

8.2 Recommendations for the Future Work

- ♦ Water in specimen was offered to the hydration of cement and expansive agent. However, the water distribution ratio in expansive concrete was unknown. And this will directly relate to the value of ϵ_{eo} . Therefore, more study should be made on the issue of the necessary water for the fully hydration of expansive agent.

Water distribution ratio



- ♦ In this research, the equation of potential expansion was divided into two parts. First part is related to the type of expansive agent and it is regarded as the function of $(E/(C+E))$. As to the second part, it is related to the curing method and inferred to be the function of water or water to powder ratio. However, the influence of water consumption on potential expansion was not clear yet. So it needs to study more about this issue as well.

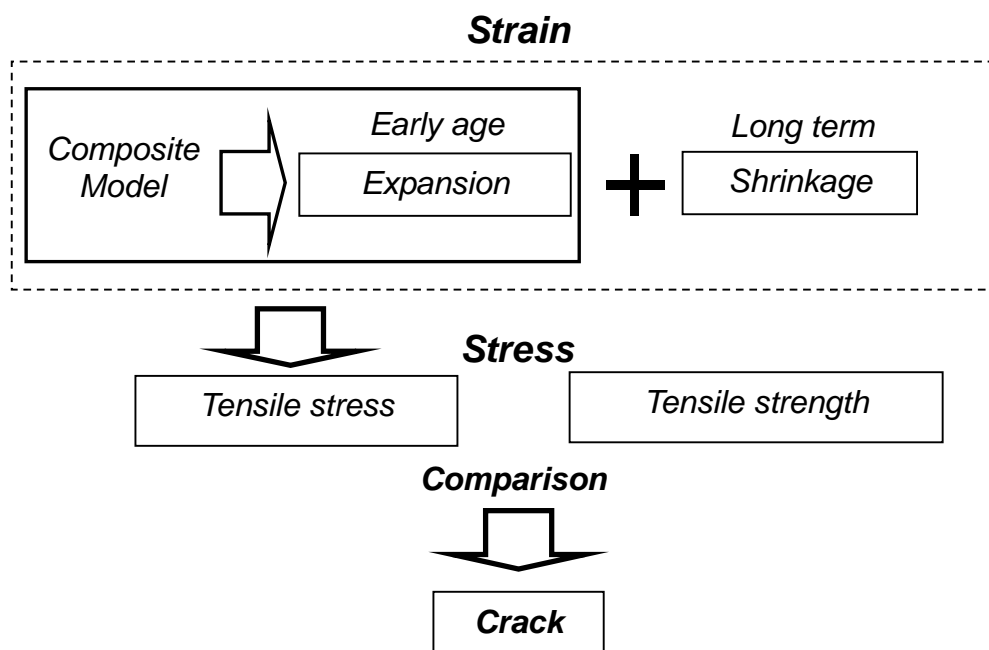
ϵ_{eo} : **Potential expansion of Expansion element**

$$\epsilon_{eo} = \left[e^{N_1 \cdot \left(\frac{E}{E+C} \right)} + N_2 \right] \cdot \left[A_0 + A_1 \cdot \left(1 - e^{-A_2(t-1)} \right) \right]$$

Type of expansive agent
Curing Condition

Function $(E/(C+E))$
Function $(W ; W/(C+E))$?

- ◆ More research has to be carried out on the issue of Young's modulus and creep coefficient of expansion element. In addition, more databases should be established for potential expansion as well.
- ◆ Considering the feasibility of cracking resistance on SCC using expansive agent. By this research, composite model was achieved to estimate the expansion at the early age. So the following job is to combine the influence of shrinkage, then, the strain behavior of expansive concrete could be clarified. And next is go to the stress field. By the comparison of tensile stress and strength, crack resistance of expansive concrete could be judged.



REFERENCES

1. Ouchi, M., “History of Development and Applications of Self-Compacting Concrete in Japan”, Proceedings of the International Workshop on Self-Compacting Concrete, pp.1-10, August 1998
2. OZAWA, K., “Utilization of New Concrete Technology in Construction Project ~Future Prospects of Self-Compacting Concrete~”, Proceedings of the Second International Symposium on Self-Compacting Concrete, pp.57-62, October 2001
3. Okamura, H., Tsuji, Y. and Maruyama, K., “Application of Expansive Concrete in Structural Elements”, Reprinted from Journal of the faculty of Engineering, the University of Tokyo (B) Vol.XXXIV, No.3, 1978
4. Japan Concrete Institute, Proceedings of JCI Symposium on Expansive Concrete for High Performance Durable Structures, pp. 1-3, September 2003 (in Japanese)
5. Japan Concrete Institute, Proceedings of JCI Symposium on Expansive Concrete for High Performance Durable Structures, pp. 101, September 2003 (in Japanese)
6. TSUJI, Y., “Estimation of Expansive Energy in Concrete Engineering”, Concrete Journal, Vol.26, No.10, pp.5-13, October 1988 (in Japanese)
7. Tsuji, Y., “Method of Predicting Chemical Prestress”, Annual Report of Cement Association of Japan, Vol. 27, 1973, pp.340-344 (in Japanese)
8. Okamura, H., Murakami, A. and Higuchi, Y., “Composite model for expansive concrete”, Proceedings of the Symposium on Composite Material, pp.115-124, 1976 (in Japanese)
9. Okamura, H. and Kunishima, M., “Composite Modelling on expansive concrete”, Annual Report of Cement Association of Japan, No. 27, pp.303-305, 1973 (in Japanese)
10. Hori, A., Kida, T., Tamaki, T. and Hagiwara, H., “ Study on Self-Compacting concrete with Expansive Additives”, Proceedings of International Workshop on Self-Compacting Concrete, Kochi, Japan, Aug-1998, Japan society of civil

engineers, pp.218-227, 1998

11. Japan Society of Civil Engineers, “Guideline of Design and Construction of Expansive Concrete”, Concrete Library 75, 1993 (in Japanese)
12. Architecture Institute of Japan, “Shrinkage Cracking in Reinforced Concrete Structures-Mechanisms and Practice of Crack Control”, April 2003 (in Japanese)
13. Hosoda, A., “Crack Resistance and Post Cracking Behavior of Expansive Concrete Based on Microscopic Mechanism and Application to RC Members”, University of Tokyo, March 2001 (in Japanese)
14. SAKIMURA, R., MARUYAMA, K., HASHIMOTO, C. and TSUJI, Y., “Modelling of Expansive Concrete Restrained in Multi-Axial Directions on a Composite Material”, JCI Annual Conference, Vol. 8, pp.369-372, 1986 (in Japanese)
15. SAKATA, K. and IKEDA, K., “Study on Prediction of Creep of Concrete”, Transactions, JSCE, No.340, pp. 185-191, December 1983 (in Japanese)
16. Neville A.M., Dilger W.H. and Brooks J.J., “Creep of Plain and Structural Concrete”